Climate change science and Victoria

Bertrand Timbal, Marie Ekström, Sonya Fiddes, Michael Grose, Dewi Kirono, Eun-Pa Lim, Chris Lucas and Louise Wilson

May 2016

Climate change science and Victoria

Bertrand Timbal, Marie Ekström, Sonya Fiddes, Michael Grose, Dewi Kirono, Eun-Pa Lim, Chris Lucas and Louise Wilson

Bureau Research Report No. 014

May 2016

Enquiries should be addressed to:

Contact Name: Bertrand Timbal

Bureau of Meteorology
GPO Box 1289, Melbourne
Victoria 3001, Australia

Contact Email: B.Timbal@bom.gov.au

Copyright and Disclaimer

Acknowledgments

Contents

List of Tables

List of Figures

FOREWARD

This report summarises the state of the science regarding the climate of Victoria, its variability, ongoing trends and projected future changes in response to continued anthropogenic forcings. It is based primarily on the recently released national climate change projections for Australia's Natural Resource Management (NRM) regions: http://www.climatechangeinaustralia.gov.au/en/

As part of the national climate change projections for the NRM program, a technical report was released to describe the science behind the projections (CSIRO and BoM 2015); this is an important source of information to gain further understanding about the projections being presented here and is often referred to in this report.

Also, as part of the release of the national climate change projections, reports were released for eight clusters of NRM regions. Two of these reports are relevant to Victoria but include areas outside the State boundaries: a report for the Murray Basin cluster covering part of Victoria, New South Wales and South Australia (Timbal et al. 2015) and one for the Southern Slopes cluster covering parts of Victoria and New South Wales and all of Tasmania (Grose et al. 2015).

For many climate variables, results from the NRM cluster reports relevant to the regions within Victoria are presented here. For future projections of rainfall and temperature, additional results were computed specifically for defined regions within the State of Victoria. These and the national climate change projections are based on the international collaborative effort coordinating and collecting a very large number of existing global model simulations of the future climate: the Coupled Model Intercomparison Project Phase 5 (CMIP5, Taylor et al. 2012). CMIP5 results also underpin the science of the Fifth Assessment Report of the Intergovernmental Panel on Climate Change (IPCC, 2013).

Important secondary sources of information for this report are the findings from a decade of climate research programs dedicated to understanding the climate of the region: the South-Eastern Australia Climate Initiative (SEACI, CSIRO 2010 and 2012) and the ongoing Victorian Climate Initiative (VicCI, Murphy et al. 2014; Hope et al. 2015). These programs underpin the additional work presented here regarding the understanding of climate variability and ongoing changes. A focus of these climate initiatives has been to link climate science with hydrology in order to deliver improved understanding of water availability. As such, these programs have been able to deliver estimates of the impact of climate change on future streamflow—these will be presented in a subsequent report.

Climate change analysis for Victoria is an ongoing activity. More information will be made available in the future through the VicCI website: http://www.cawcr.gov.au/projects/vicci/

Climate change projections for Victoria based on data released by CSIRO and the Bureau of Meteorology have also been included in the Victorian Government's Climate-Ready publications, released in 2015. Climatic trends have been used to highlight the impacts climate change will have on Victoria's regions and provides examples of how people are already becoming climate-ready, with links to more detailed information. The Climate-Ready publications are available at http://www.climatechange.vic.gov.au/understand

EXECUTIVE SUMMARY

This report compiles all existing climate research findings of relevance to the State of Victoria; it describes what is understood about the climate of the State and how it will likely evolve in the future in response to ongoing anthropogenic forcings. For the purposes of this report the State of Victoria was divided—by grouping the ten existing Catchment Management Authority (CMA) areas—into three regions which are meaningful from a climatic, vegetative and hydrological perspective: the Murray Basin, the South-West and South-East regions.

Victoria experiences a temperate climate: mean temperature ranges from 10 °C in winter to 20 °C in summer (with geographical differences); and rainfall, which is more abundant in the southern regions, occurs predominantly in the cool season (April–October). The climate is highly variable from year to year, particularly in summer. Victoria has experienced a warming trend over the last century averaging 0.06 °C per decade (1911 to 2014), in line with global warming. This warming trend is accompanied by natural climate variability on year-to-year and decadal timescales. There has been no long-term trend in annual total rainfall over the historical instrumental record, and this record exhibits marked decadal variability. But, split into two seasons, warm season rainfall has increased and cool season rainfall has decreased. The cool season rainfall deficit in relation to the long-term mean has accelerated in the second half of the 20th century and became statistically significant. This was particularly evident during the Millennium Drought from 1997 to 2009. The Millennium Drought was the most severe protracted drought of the instrumental record and was predominantly due to a cool season rainfall deficit. Along with the declining trend in cool season rainfall, the State has also experienced declining streamflows and increasing bushfire risk.

Ongoing climate change means the climate is non-stationary. Together with the high natural variability that characterises Victoria's climate, this makes it difficult to define a baseline that adequately characterises current climate. The last 30 years are a significant departure from the long-term historical record, being warmer than any previous 30-year period and with lower cool season rainfall. It is important that users of climate change projections understand which period has been used as the reference (or baseline) from which to measure future changes. The latest CMIP5 climate change projections use 1986–2005 as the baseline. Some climate change signal is present in this period. However, the warming anomalies are less for 1986–2005 than for the last 30 years and the rainfall anomalies also differ due to decadal variability.

Victorian mean climate experiences natural variability on interannual and longer timescales in response to a complex interplay of large-scale climatic phenomena. An understanding of these phenomena and how they influence the climate of Victoria now and into the future, is required to both appreciate local climate and also to predict its future evolution over a range of timescales (e.g. seasonal and long-term changes). The transfer of excess energy from the tropics to the pole(s) takes place via the mean meridional circulation, which controls the mean climate of Victoria, the position of the band of high pressure systems (the subtropical ridge) and the passage of rain-bearing weather systems. There are multiple lines of evidence showing that the characteristics of this particular global circulation has been changing over the last 50 years, in part due to anthropogenic forcings as well as natural fluctuations. These changes can be related to some of the observed changes in rainfall across Victoria. On interannual timescales the variability is often driven by remote large-scale mechanisms in the tropical oceans, in particular

the Pacific Ocean where ENSO variability (El Niños and La Niñas) has a strong influence. In addition to ENSO, the behaviour of the Indian Ocean, either in response to ENSO or independently, plays an important role. Besides tropical modes of variability, the trajectories of weather systems delivering rainfall across Victoria are affected by a hemispheric see-saw of atmospheric pressures between 40°S and 65°S, called the Southern Annular Mode (SAM). SAM acts to contract and expand the circulation of weather systems around Antarctica. This, in turn, influences Victorian climate, with impacts dependent on the season, and varying across the State. SAM has trended positively since the late 1950s and this may have contributed to the observed ongoing deficit in cool season rainfall. While large-scale modes of variability are important in understanding the observed variability of the climate of Victoria, they do not fully explain the randomness of the weather. Therefore the local climate is never perfectly predictable at any timescale. The randomness of weather noise also is embedded in historical climate model runs and future climate projections, which explain why they are not deterministic in nature. Besides the various modes of interannual variability relevant to Victorian rainfall, recent research points to the importance of decadal variability. Particularly relevant are the change of phase of the Inter-decadal Pacific Oscillation (IPO) in influencing the interaction between the interannual modes, affecting the climate of Victoria, and also the long-term trends in the expansion of the tropics and the Hadley Cell (which is a key component of the mean meridional circulation).

Projections of future changes to the climate for Victoria presented in this report are based on international efforts to gather all existing global climate model (GCM) simulations, as well as a national program that delivered nation-wide climate change projections. The climate will change in response to future human activities, the specifics of which are unknown as this stage. Therefore the climate models are forced with plausible estimates of future greenhouses gas concentrations according to likely socio-economic scenarios. These scenarios are known as Representative Concentration Pathways or RCPs. In this report results are presented for several of these scenarios, focusing on a higher scenario (RCP8.5 which is similar to a 'business as usual' approach) and a lower scenario (RCP4.5 which is achievable only if substantial emission reduction measures are put in place).

Projections of the evolution of the climate system in response to the human induced forcings are produced using complex mathematical models representing both the atmospheric and oceanic components of the global climate system. In order to capture the uncertainties of the future projections of the climate, and because climate models contain limitations (especially for small-scale features), it is best practice to make use of results from a large number of simulations from existing climate models within the international community. The climate models underpinning the future projections have been evaluated based on their ability to reproduce the observed past and present climate, as well as the key mechanisms influencing the climate. These evaluations are helpful in determining which processes the models simulate well and, therefore, in guiding the selection of individual models for impact studies. These evaluations are made for important surface climate variables across Victoria as well as for large-scale mechanisms known to drive the variability of the climate of Victoria. We find that GCMs can capture large-scale aspects of the climate well but are not designed to provide local information at scales finer than their spatial resolution. To obtain local-scale projections, additional techniques are required to downscale this information to a scale relevant for impact studies. Amongst the numerous

existing approaches, this report makes extensive use of results from a statistical downscaling model based on meteorological analogues.

The future climate projections for Victoria presented in this report are based on the recently released Australian Climate Change projections (*Climate Change in Australia Information for Australia's Natural Resource Management Regions: Technical Report)*. This national program delivered data as well as a series of reports which are useful background information in support of this report and are available through the *Climate Change in Australia* website: http://www.climatechangeinaustralia.gov.au/. In particular, the website provides methods and tools to enable the selection of climate dataset(s) required to perform more advanced analysis of the impact of climate change. While the national project went far beyond the scope of this study, we provide additional and more local details of projected changes to Victoria's climate.

Climate change projections for Victoria based on data released by CSIRO and the Bureau of Meteorology have also been included in the Victorian Government's Climate-Ready publications, released in 2015. Climatic trends have been used to highlight the impacts climate change will have on Victoria's regions and provides examples of how people are already becoming climate-ready, with links to more detailed information. The Climate-Ready publications are available at http://www.climatechange.vic.gov.au/understand

Continued substantial warming for Victoria for mean, maximum and minimum temperature is projected with very high confidence, taking into consideration the robust understanding of the driving mechanisms of warming and the strong agreement on direction and magnitude of change amongst GCMs and downscaling results. For the near future (2030), the mean projected warming shows only minor differences between RCPs and reaches a median of around 1 °C in maximum temperatures in both the cool and warm seasons with slightly smaller increases in minimum temperatures. For late in the 21st century (2090), warming is markedly larger for RCP8.5 reaching a median of about 4 °C above the 1986–2005 level during the warm season for both maximum and minimum temperature and 3.5 °C during the cool season. In line with the mean warming, hot temperature extremes are also projected to increase while frost risk is projected to decrease.

In the near term (2030), there is high confidence that natural climate variability will remain the major driver of rainfall changes from the climate of 1986–2005. Late in the century (2090) under both RCP4.5 and RCP8.5, there is *high confidence* that cool season rainfall will continue to decline and there is no clear leaning in the models towards either wetter or drier conditions in the warm season. Apart from the simulated direction of future changes from GCM and downscaling results, this assessment also takes into account the physical understanding of the relationship between the atmospheric circulation and rainfall across Victoria—specifically, how well the models represent this relationship, and what the projected changes in the circulation are. The understanding of physical processes coupled with high model agreement results in *high confidence* that the intensity of heavy rainfall events will increase. Snowfalls are projected to continue to decline for all RCPs with *high confidence*, particularly under RCP8.5. Rainfall changes will be driven by changes in general atmospheric circulation, in particular a broadening of the mean meridional circulation, and accompanying changes in mean sea level pressure (MSLP). MSLP over southern Australia is projected to increase with *high confidence*, mostly during the cool season; this is driven by an increase in the strength of the well-known belt of high pressures, the subtropical ridge, and a shift of this ridge southward consistent with the

observed trend over the last 30 years. As climate models tend to underestimate the rainfall response to changes in the position and intensity of the subtropical ridge, these models may underestimate the projected rainfall decline in the cool season. Other large-scale drivers (e.g. ENSO and SAM) are also projected to change and impact future rainfall projections.

Changes in mean and extreme wind are uncertain. Mean wind is likely to decrease during the cool season while increased occurrence of more intense frontal systems and wind changes during the warm season is possible.

Important changes are projected in the hydrological cycle. Linked to the rainfall projections, there is medium confidence that the time spent in meteorological drought, and the frequency of extreme droughts, will increase over the course of the century under RCP8.5. Beside the changes in rainfall and temperature, changes in other variables will also contribute to changes in the hydrological cycle. Small changes are projected for solar radiation and relative humidity by 2030 with clear increases seen by 2090. In particular, an increase in solar radiation is linked to reduced cloud cover and rainfall decline in conjunction with a decrease in relative humidity. Potential evapotranspiration is projected to increase in all seasons. As a result, soil moisture and runoff are projected to decrease with medium confidence.

There is *high confidence* that climate change will result in a harsher fire-weather climate regime in the future. However, there is only low confidence in the magnitude of the projected change to fire weather, as this depends on rainfall projections and their seasonal variation. The summer rainfall increase projected by some climate models, if it eventuates, would moderate the number of severe fire-weather days, although there is very little confidence about this projection.

Sea level, which has risen around Australia at an average rate of 1.4 mm/year between 1966 and 2009, is projected to continue to rise during the 21st century (*very high confidence*). By 2090, the projected range of sea level rise for the Victorian coastline is between 0.39 m and 0.84 m under the high emissions scenario (RCP8.5). Sea surface temperature (SST) has increased significantly across the globe over recent decades and is projected to further rise with very *high confidence*. Across the coastal waters of Victoria in 2090, further warming is projected in the range of 1.6 to 3.4 °C for RCP8.5. There is also very *high confidence* that the ocean pH is expected to decrease around Australia.

1. THE CLIMATE OF THE STATE OF VICTORIA

1.1 Defining climate regions

The State of Victoria was divided into three regions which are meaningful from a climatic, vegetative and hydrological perspective: the Murray Basin, the South-West and South-East regions. These regions are formed as groupings of the ten existing Catchment Management Authority (CMA) areas.

In this report, the State of Victoria is divided into three regions (Fig. 1). The regions were derived by grouping the ten existing Victorian Catchment Management Authorities (CMAs) or Natural Resources Management (NRM) boundaries (which are defined by catchments and bioregions), into three regions that are meaningful from a climatic perspective (discussed in Section 1.2):

- The Murray Basin section of Victoria (blue shading in Fig. 1) comprises an area to the north of the Great Dividing Range (GDR), encompassing the Victorian section of the larger Murray Basin NRM Cluster. This includes the Mallee, Wimmera, North Central, Goulburn Broken and North East CMA regions;

- South-West Victoria (red shading in Fig. 1), southwest of the GDR which includes the Glenelg-Hopkins, Corangamite and Port Philip and Westernport CMA regions; and

- South-East Victoria (green shading in Fig. 1), southeast of the GDR, which includes the West and East Gippsland CMA regions.

Each region is characterised by distinct topographical and climatological features as described in Section 1.2.

These three regions follow the clustering used in the NRM reports (shown by the thick coloured boundaries in Fig. 1) but are restricted to the Victorian sections of the relevant clusters (shaded on Fig. 1). The individual Victorian CMAs are shown by the thin black boundaries. Results are presented using these three Victorian regions where possible (primarily for temperature and rainfall). However for variables for which results are unavailable at this scale (most other variables), the broader NRM clusters are used - in particular the Murray Basin cluster, encompassing the Murray Basin region, and the Southern Slopes cluster, encompassing both the South-West and South-East regions of Victoria.

A range of climate change impacts and adaptation challenges have been identified across Victoria, including temperature and rainfall impacts on agriculture, water resources and other natural assets, as well as shifting habitats for terrestrial and marine flora and fauna (Department of the Environment 2013). Across the State, broad acre cropping and intensive agriculture, invasive species and biodiversity management, water security, bushfire risk, alpine tourism and coastal inundation are priorities for the natural resource management and planning community.
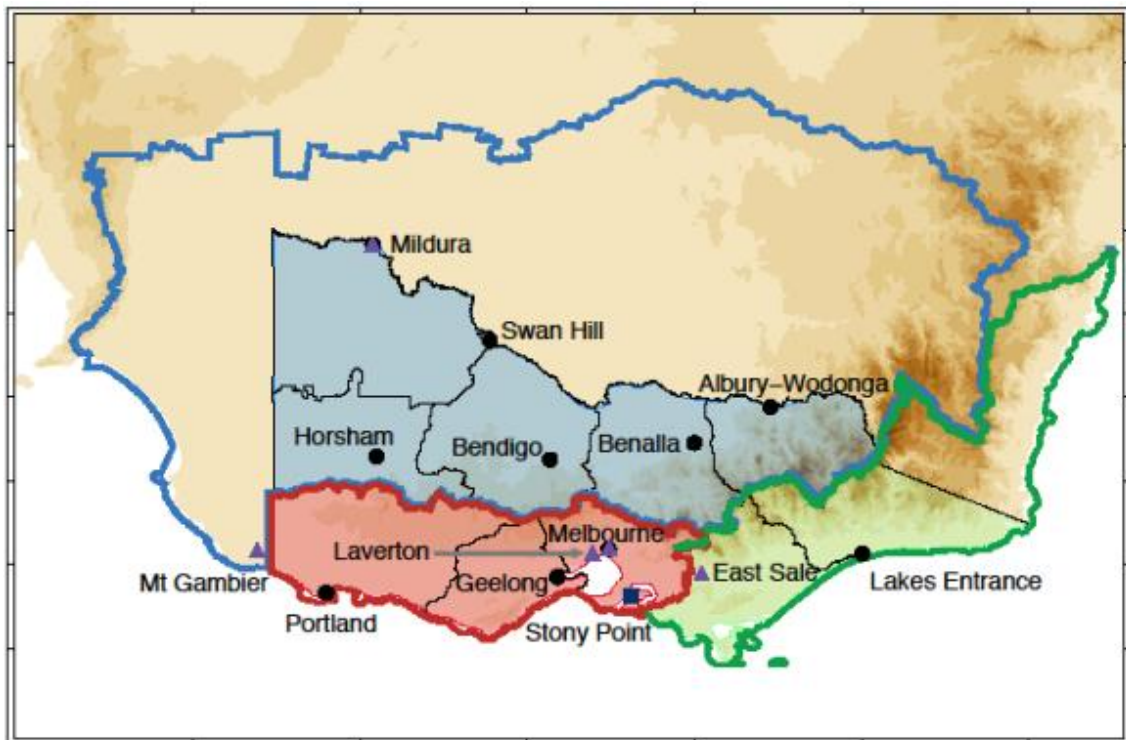
Fig. 1: The three climatic regions identified across the State of Victoria: Murray Basin (blue shading), the South-West of Victoria (red shading) and the South-East of Victoria (green shading) based on boundaries of individual CMA subregions (thin black lines). Cluster regions used for the latest national projections for Australia (CSIRO and BoM 2015) of relevance to Victoria are indicated by coloured boundaries: the Murray Basin cluster (thick blue line), and the Southern Slopes cluster encompassing the South-West of Victoria (thick red line) and South-East of Victoria (thick green line). The regional topography is shown in the background shading. Black circles indicate major towns for each CMA subregion, fire data stations are shown by purple triangles (see Sections 1.3 and 4.6) and Stony Point, used as an example for sea level rise, is shown by a blue square (see Section 4.7).

1.2 Regional mean climate

Victoria experiences a temperate climate: mean temperature ranges from 10 °C in winter to 20 °C in summer (with geographical differences); and rainfall, which is more abundant in the southern regions, occurs predominantly in the cool season (April-October). The climate is highly variable from year to year, particularly in summer.

The State of Victoria, located at latitudes 34–38°S, is within the 'extra-tropics' or 'mid-latitudes' of the global climate system, generally falling between the subtropical ridge (STR) of high pressure at approximately 30–40°S (the descending arm of the Hadley Cell—see Section 2.1 for further details) and the northern edge of the so called 'Roaring Forties' of westerly circulation in 40–50°S. As such, the State is influenced by a number of synoptic-scale and large-scale phenomena, further discussed in Section 2.
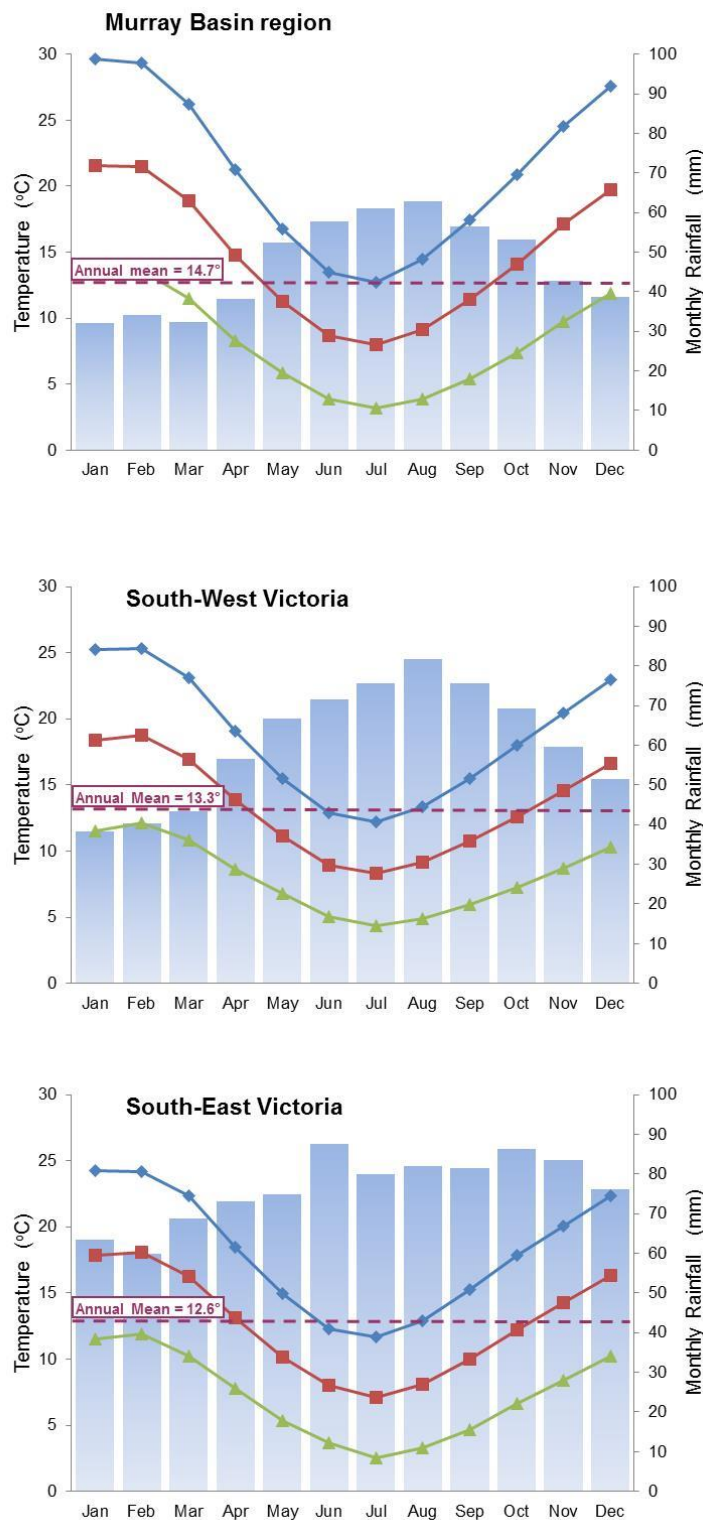
Fig. 2: Average characteristics of monthly rainfall (bars, right axis) and temperature (lines, left axis; mean in red, maximum in blue and minimum in green, as well as the annual mean temperature in the dashed line) over 1900–2014 for rainfall and 1911–2014 for temperature for the three regions of Victoria: Murray Basin (top), South-West region (middle) and South-East region (bottom). Temperature and rainfall data are from the Bureau of Meteorology operational 5 km gridded monthly data.

According to the Bureau of Meteorology records, annual mean temperatures across the State range from around 12.6 °C in the South-East region to 14.7 °C in the inland Murray Basin region (Fig. 2) with much larger spatial variability around individual locations. The South-West and South-East regions, extending to the coast, experience relatively temperate, maritime climates while the more inland Murray Basin region has a slightly warmer climate with larger diurnal (the difference between minimum and maximum) and seasonal (the difference between mid-summer and mid-winter maximum, mean and minimum) temperature ranges.

Total rainfall is larger in the South-East (917 mm/year) and South-West (730 mm/year) regions compared to the drier Murray Basin region (562 mm/year); larger and smaller values are recorded around the State at individual locations. The annual cycle of rainfall averaged across the northern part of the State shows the dominance of the cool season rainfall (top panel in Fig. 2). In this report, the 'cool season' is defined as the period for which the monthly long-term temperature average is below the annual average. Across the State, the cool season is April to October. The 'warm season' correspondingly is November to March. In general, a winter-dominated seasonal cycle of rainfall occurs in the northern and western part of the State (May–October peak), with a more uniform seasonal cycle in the eastern part of the State (Fig. 2).

Climate anomalies such as droughts and floods are a common feature of the Australian climate, and Victoria is no exception. Their occurrences are partly explained by influences of well-known large-scale natural modes of climate system variability (CSIRO 2012). These modes and their relevance to Victorian climate are described in more detail in Section 2. It is important to understand that these known modes, combined or individually, cannot explain the majority of year-to-year variability—a large part of the variability is due to the randomness of weather systems or as-yet unknown climate modes. Year-to-year standard deviations of monthly total rainfall averaged across the State are consistently between 22 and 29 mm per month (Fig. 3). When divided by the mean rainfall and expressed in percentage terms (three coloured lines in Fig. 3), they tend to be lower for spring months, when modes such as the El Niño–Southern Oscillation (ENSO) and the Indian Ocean Dipole (IOD) have the largest impact on Australian climate (see Section 2.2). This indicates that cool season rainfall is more reliable than warm season rainfall. Furthermore, rainfall in the Murray Basin region is more variable almost all year around than for the two southern regions (Fig. 3).
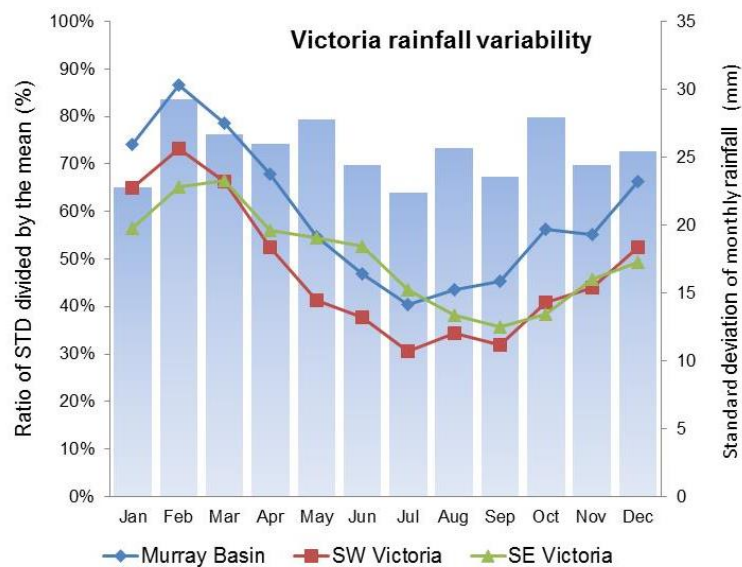
Fig. 3: Annual cycle of the standard deviation (STD) of monthly rainfall in mm (blue bars, right axis shown for the entire State) and divided by the mean monthly rainfall expressed in percentage terms (coloured lines, left axis, computed for the three regions). All values are based on rainfall from the Bureau of Meteorology operational 5 km gridded monthly data from 1900 to 2014.

1.3 Trends and variability of the regional climate

Victoria's warming trend over the last century has averaged 0.06 °C per decade (1911–2014), in line with global warming. This warming trend is accompanied by natural climate variability on year-to-year and decadal timescales. There has been no long-term trend in annual total rainfall over the historical instrumental record, and this record exhibits marked decadal variability. When split into two seasons, warm season rainfall has increased and cool season rainfall has decreased. The cool season rainfall deficit, in relation to the long-term mean, has accelerated in the second half of the 20th century and became statistically significant. This was a significant factor in the Millennium Drought from 1997 to 2009. The Millennium Drought was the most severe protracted drought of the instrumental record and was predominantly due to a cool season rainfall deficit. Along with the declining trend in cool season rainfall, the State has also experienced declining streamflows and increasing bushfire risk.

Surface air temperatures in Victoria have been increasing by about 0.06 °C per decade (Table 1) since national records began in 1911 (Fig. 4). Daytime maximum temperatures have risen slightly more (0.07 °C per decade) than overnight minimum temperatures (0.05 °C per decade). All trends are highly statistically significant for all durations considered (100, 50 and 30 years) and across all parts of the State. The warming is fairly uniform across the three regions of the State (Table 1) with lower warming in the South-West region and higher warming in the Murray Basin region. The warming across the State is broadly in keeping with global temperature changes, with the rate of warming increasing in the most recent part of the historical period; this can be seen in a comparison of the 1911–2014 period, the last 50 years and the last 30 years' trends (Table 1). As a result, trends computed over the last 30 years are substantially larger, in particular for daily maximum temperature and for the warm season (up to 0.63 °C per decade, Table 1).

Tmax	Victoria	MB	SW	SE	Tmin	Victoria	MB	SW	SE
Annual Mean	0.07** 0.20** 0.45**	0.06** 0.22** 0.50**	0.09** 0.17** 0.37*	0.06** 0.16** 0.41**	**Annual Mean**	0.05** 0.11** 0.16*	0.03* 0.08 0.13	0.08** 0.12** 0.17*	0.09** 0.20** 0.28*
Cool Season	0.06** 0.18** 0.32**	0.06** 0.20** 0.37**	0.08** 0.15** 0.22*	0.06** 0.14** 0.28**	**Cool Season**	0.03* 0.08 0.00	0.01 0.04 -0.08	0.06** 0.11** 0.05	0.07** 0.19** 0.18*
Warm Season	0.07** 0.22** 0.63**	0.06* 0.25** 0.67**	0.10** 0.19* 0.58**	0.07** 0.18* 0.58**	**Warm Season**	0.08** 0.15* 0.40**	0.05** 0.13* 0.42**	0.10** 0.13* 0.33*	0.13** 0.21** 0.42**

Table 1: Linear trends computed for daily maximum (Tmax; left) and minimum (Tmin; right) surface temperature (°C/decade) for the State average and the three regions (MB; Murray Basin, SW; South-West and SE; South-East), annually and for the cool and warm seasons. In every case trends are provided for the full record (1911– 2014, top row), the last 50 years (1965–2014, middle row) and the last 30 years (1985–2014, bottom row). Statistical significance of trends at the 95% level is indicated with * and at the 99% level with **. Cooling trends are shown in blue.
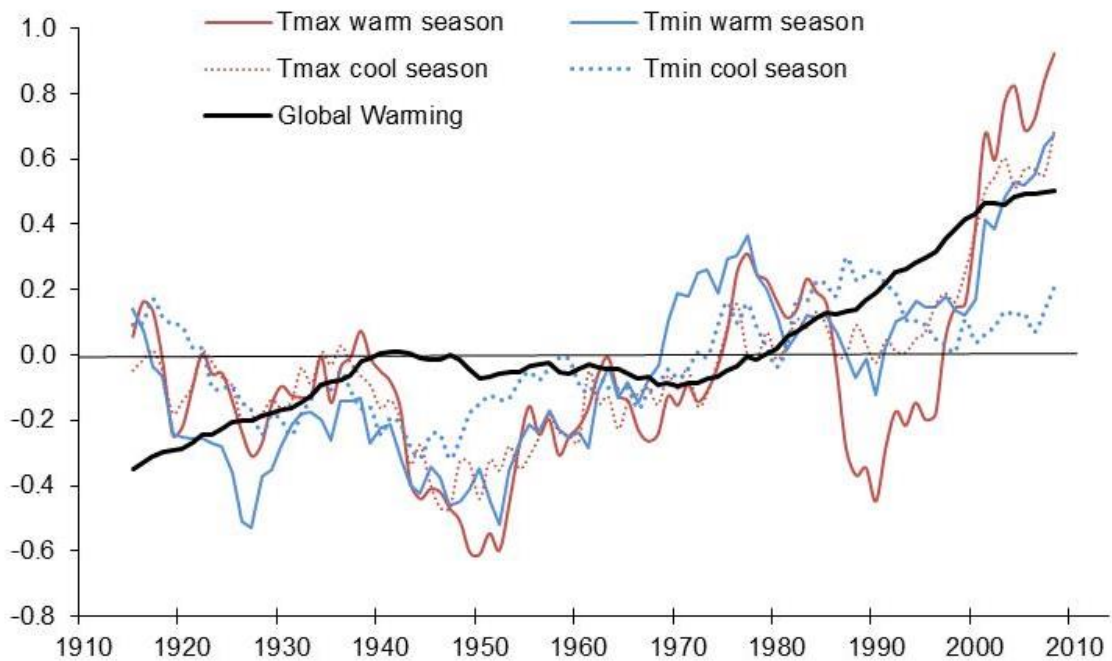
Fig. 4: 11-year running means of Victoria average daily minimum (blue lines) and maximum (red lines) air temperature as anomalies (°C) relative to the 1911–2014 average; solid lines show the April to October (cool) seasonal average and dashed lines show the November to February (warm) seasonal average. These values are based on the Bureau of Meteorology operational 5 km gridded monthly temperature data from 1911 to 2014. The black line shows the global average temperature anomalies (relative to the 1961– 1990 reference period) from the Climatic Research Unit website (HadCRUT4, Morice et al. 2012).

It is worth noting that the lower rate of warming across Victoria in the early part of the record (compared to global warming), as noted in Fig. 4, is very likely in part due to a warm bias in the gridded temperature data used in this report. Trends computed using the Bureau of Meteorology's newly developed Australian Climate Observation Reference Network – Surface Air temperature (ACORN-SAT) data (Trewin 2013; Fawcett et al. 2012) are higher than the trends obtained here using the gridded temperature dataset. However, the increased rate of warming since the 1970s appears concomitant with the acceleration of the global warming (black curve on Fig. 4) with marked differences due to naturally occurring decadal variability, as expected for a small region. This is an important reminder that while the warming observed across Victoria is primarily driven by the increase of anthropogenic greenhouse gas emissions that are causing global warming, year-to-year and even decadal anomalies are also driven by regional factors. For example, daily minimum temperatures increased at a slower rate than daily maximum temperatures during the last 30 years. This is particularly true for the cool part of the year, when the trend in minimum temperature is nil in some areas and even negative for the Murray Basin region, being consistent with observations of increased frost in some part of the State over the last few decades (Dittus et al. 2014). The different warming rates for maximum and minimum temperature observed in the last 30 years are consistent with the observed rainfall trend discussed in Section 2.2, as there is a strong relationship between rainfall reduction and an increase in diurnal temperature range (Power et al. 1998).

Annual rainfall across the State is highly variable and exhibits a small and statistically non-significant drying trend over the full instrumental record (1900–2014; Table 2). However, trends strengthen when the last 50 years are considered and, with the exception of the South-East region, strengthen even further when the last 30 years are considered (although on an annual basis these 50 and 30 year trends are still not statistically significant). The State has experienced some remarkable rainfall variability in the last 15 years (Fig. 5), including the record breaking Millennium Drought which affected most of southeastern Australia, including the Murray Basin (Leblanc et al. 2012). The rainfall anomalies during this event were particularly large compared to previous historical droughts—for example, as discussed in Timbal et al. (2015b) for the high rainfall hydrological catchments on both sides of the Great Dividing Range. The Millennium Drought ended with two of the wetter years on record for Australia in 2010–11 (Beard et al. 2011, Bureau of Meteorology 2012). However, across Victoria, while these two years were very wet and contributed to a recovery of surface water resources, they were not the highest on record. This arose because exceptionally high rainfalls were limited to the northern part of the State (Bureau of Meteorology, 2012)—for 2010–11, the 2-year Victorian average was 845 mm per year, which was the third wettest 2-year period after 1973–74 (927 mm) and 1955–56 (860 mm) (Bureau of Meteorology, 2012). In addition to seasonal totals, evidence has emerged that extreme rainfalls are also increasing across Australia, including locations in Victoria (Gallant et al. 2014).

Rainfall	Victoria	MB	SW	SE
Annual Mean	-1.6%	-0.8%	-2.4%	-2.3%
	-9.9%	-11.2%	-9.0%	-8.0%
	-12.9%	-15.6%	-13.7%	-6.2%
Cool Season	-7.3%	-9.5%	-3.9%	-5.9%
	-15.8%	-21.7%	-10.2%	-8.5%
	-26.1% *	-37.5% **	-17.0%	-9.7%
Warm Season	9.7%	17.6%	1.0%	3.3%
	1.9%	11.0%	-6.4%	-7.1%
	13.3%	30.9%	-6.7%	-0.6%

Table 2: Linear trends computed for rainfall for the State average and the three regions (MB; Murray Basin, SW; South-West and SE; South-East); in every case trends are provided for the full record (1900–2014, top row), the last 50 years (1965–2014, middle row) and the last 30 years (1985–2014, bottom row) and are expressed as a percentage of the mean over the period considered. Statistical significance at the 95% level is indicated with * and at the 99% level with **. Drying trends are shown in red.
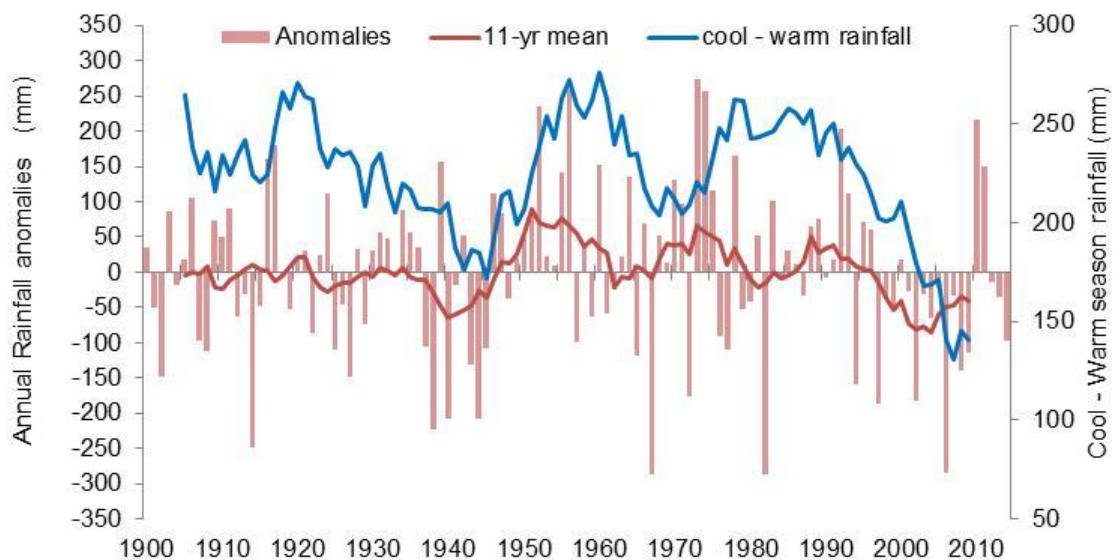
Fig. 5: Average Victorian observed annual rainfall anomalies in mm (red bars, from 1900 to 2014, left axis) and the 11-year running mean (bold red line, left axis). Additionally, the 11-year running mean of the difference between the April–October (cool season) and November–March (warm season) rainfall is shown (bold blue line, right axis). All values are based on rainfall from the Bureau of Meteorology operational 5 km gridded monthly data from 1900 to 2014.

The Millennium Drought was dominated by autumn and early winter rainfall declines (primarily within the cool season); in contrast, the very wet La Niña-driven 2010–11 period was dominated by warm season rainfall. These dry and wet events have contributed to a marked ongoing difference between cool and warm season rainfall due to both a decline in cool season rainfall and an increase in warm season rainfall. As was the case for the warming trend discussed earlier, these two opposite trends in seasonal rainfall accelerated in the latter part of

the historical period, illustrated by comparing the trends of the last 50 and 30 years with those of 1900–2014 (Table 2). However, in contrast to temperature trends, the rainfall trends are not statistically significant, with the exception of the last 30-year cool season rainfall trend, despite being large in percentage terms. This is due to the high natural variability of rainfall discussed earlier (Fig. 3). The spatial extent of the decreasing cool season rainfall (and the trend's acceleration in the latter part of the instrumental record) is consistent across the State and is most pronounced north of the Great Dividing Range (the Murray Basin region), and least pronounced south of the Range, in particular in South-East Victoria (Table 2). The increasing warm season rainfall trend is not consistent across the State and in the more recent period is only a feature of the Murray Basin region. In this case, it is nearly as large as the cool season rainfall decline in percentage terms, albeit from a much lower mean rainfall (381 mm for the cool season versus 180 mm for the warm season on average across the Murray Basin region, Fig. 1).

Streamflow data have been compiled by the Bureau in the Hydrological Reference Stations (HRS) dataset (Turner et al. 2012). The HRS dataset catchments were chosen to track the influence of climate change on streamflow and, hence, are relatively unimpaired by human activities and located generally at the headwaters of major drainage basins (Sinclair Knight Merz 2010). Twenty-seven catchments across Victoria, selected from the HRS dataset by Fiddes and Timbal (2016a), have experienced declines in the total streamflow received per year since the 1970s (Fig. 6), with most of the decline experienced since the 1990s. This decline in annual streamflow is primarily driven by cool (April–October) season rainfall decline, and is coincident with the traditional filling season for water storages in Victoria. The catchments in close proximity to the Great Dividing Range show weaker trends than the lower elevation catchments further away from the range. During the warm season there is a large increasing trend in percentage terms. However, this is small in absolute terms, and warm season streamflow does not compensate for the cool season decline. On both annual and seasonal time scales, linear trends in streamflow decline are highly related to the runoff via a log-linear relationship: the catchments that generate higher runoff north of the Great Dividing Range, in the Murray Basin region, experienced the least effect (in percentage terms) of the negative rainfall trend since the 1970s (Fig. 6). Hence, the difference in streamflow response during the Millennium Drought or the reduction since the 1970s (e.g. stronger decline in the northwest of the State compared to the northeast) has more to do with the catchment's physical properties and mean runoff than the magnitude of the changes in cool season rainfall (Fiddes and Timbal 2016a).

Trends in climatic variables are also reflected in trends in the risk of bushfires. Bushfire occurrence depends on four 'switches': 1) ignition, either human-caused or from natural sources such as lightning; 2) fuel abundance or load; 3) fuel dryness, where lower moisture contents are helpful for fire propagation and; 4) suitable weather conditions for fire spread, generally hot, dry and windy (Bradstock 2010). The settings of most of these switches depend on meteorological conditions across a variety of timescales and, given this strong dependence on the weather, climate change will have a significant impact on future fire weather. Fire weather is estimated here using the McArthur Forest Fire Danger Index (FFDI, McArthur 1967). This index includes a drought factor that depends on both long-term and short-term rainfall. Therefore, temperature, relative humidity and wind speed are direct inputs into the calculation of FFDI. Fire weather is considered 'severe' when the FFDI index exceeds 50. Climatological

time series of FFDI are limited to locations where long records exist for the meteorological variables used in computing the FFDI. At five stations across Victoria (either within the State or close to State boundaries), historical records are sufficient to evaluate the evolution of FFDI from 1973 to 2015 (Table 3 and Fig. 7). These locations provide a broad indication of fire danger in the surrounding area, covering different climate zones, but not capturing the alpine regions of Victoria. At all locations but one, the FFDI has been increasing during this period, which gives a State-wide significant increase. This increase is most significant in the spring season leading to an overall lengthening of the fire season. At the tail of the distribution of fire danger, the number of days when FFDI reaches the severe threshold (above 50) has seen a significant increase, larger than the increase in annual cumulative FFDI (Table 3).
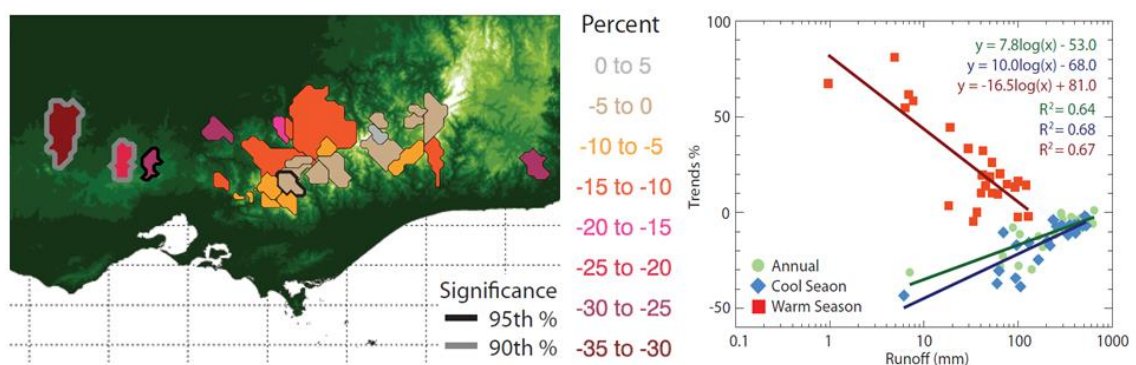
Fig, 6: Decadal linear trends (expressed as a percentage of the 1977–2012 mean) for annual streamflow for the period of 1977–2012 across a selection of Victorian catchments (left panel). Trends significant at the 90% (thick grey borders) and 95% (thick black borders) confidence levels are highlighted. The relationship of the trends' magnitude across the 27 catchments to the log-transformed runoff in these catchments is shown for the annual mean and the cool and warm seasons (right panel). Compared to rainfall, the seasons for streamflow are shifted by a month: cool is May to November and warm is December to April. All streamflow data are extracted from the Hydrological Reference Stations data assembled by the Bureau of Meteorology. (Source: Fiddes and Timbal 2016a).

Station	Mean annual cumulative FFDI (1981-2010)	Linear trend in percentage of the mean (1973-2015)	Averaged number of days per year with FFDI > 50 (severe)	Linear trend in number of days for FFDI > 50 (1973-2015)
Melbourne Airport	2553	37%	2.7	4.6
Laverton	2208	20%	1.7	1.0
Mt Gambier	2026	17%	1.6	3.6
Mildura	5488	42%	7.2	8.6
East Sale	1849	21%	0.5	0.0
Station average	2824	28%	2.7	3.6

Table 3: Individual station and average composite of key statistics of the Forest Fire Danger index (FFDI): mean annual cumulative FFDI and the linear trends of that quantity expressed as a percentage of the mean value for the full available record (1973–2015); number of days per years of severe FFDI (above 50); and the linear trend of that quantity. N.B: FFDI year are reported from 1st of July to end of June (i.e. 2015 FFDI is from 1 July 2014 to 30 June 2015).
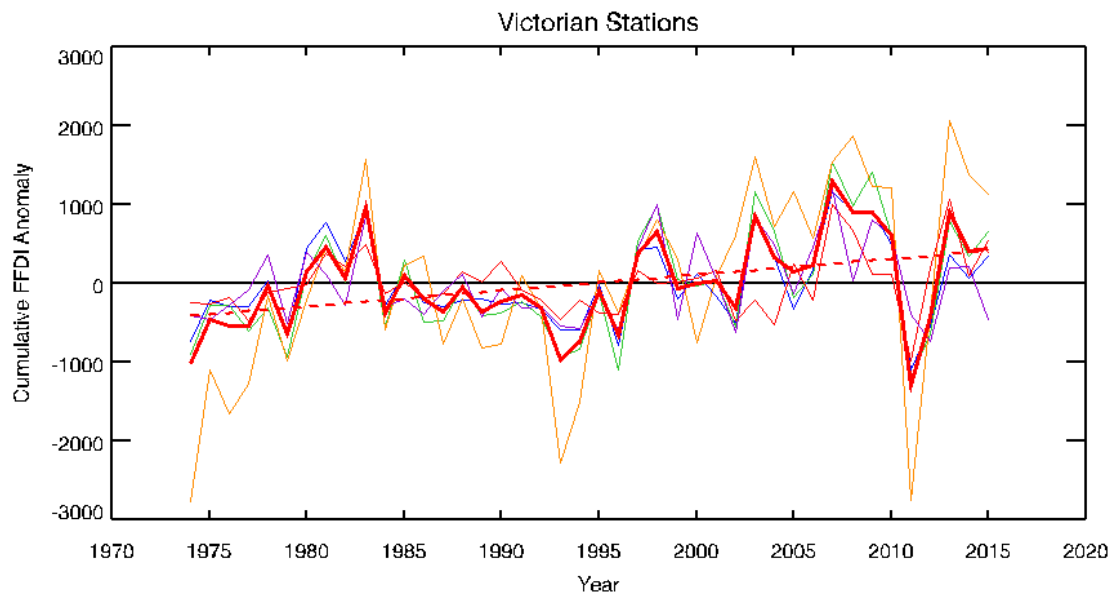
Fig. 7: Annual cumulative Forest Fire Danger Index (FFDI) for five locations relevant to Victoria (Laverton, blue line; Melbourne Airport, green line; Mildura, orange line; Mt Gambier (South Australia), red line; East Sale, purple line) expressed as anomalies from the long-term mean (1973–2015) with the five stations average overlay (thick red line) as well as the trend line for the historical period (dashed red line).

1.4 The implications of Climate Change for the definition of a climate baseline

Ongoing climate change means that climate is non-stationary. Together with the high natural variability that characterises Victoria's climate, this makes it difficult to define a baseline that adequately characterises current climate. The last 30 years are a significant departure from the long-term historical record, being warmer than any previous 30-year period and with lower cool season rainfall. It is important that users of climate change projections understand which period has been used as the reference (or baseline). In the case of the latest CMIP5 climate change projections, the reference period is 1986–2005. Some climate change signal is present in this period. However the warming anomalies are less for 1986–2005 than for the last 30 years and the rainfall anomalies also differ due to decadal variability.

Up until the Millennium Drought the planning and management of water resources across the State was generally based on the assumption of a stationary climate. However, it is now recognised that climate change has affected the climate during the recent decades, and that this needs to be taken into account in planning and management processes. Because there is uncertainty in the degree to which climate change has affected the most recent decades of climate and weather observations, and because of the large natural variability observed in the historical record, it is difficult to select a baseline that is representative of the current climate

while also encompassing an appropriate range of natural climate variations. The recommendation of the World Meteorological Organization (WMO) is to use a period of at least 30 years to define a reference period. It is therefore of interest to evaluate how unusual the last 30 years (1985–2014) of rainfall and temperature have been across the three Victorian regions (Fig. 8). It emerges that for all regions, for both warm and cool seasons and the annual mean, the last 30 years have been the warmest of any 30-year period in the historical record (e.g. coloured bars with stars in left column of Fig. 8 are furthest to the right). For rainfall, in the last 30 years the cool season has been the driest 30-year period observed in the historical record for the Murray Basin and South-West regions (e.g. blue bars with stars in the right column of Fig. 8 are further to the left); however this is not the case for annual or warm season rainfall. From this analysis, it appears that any approach which samples the full historical record to estimate the likelihood of a particular outcome may be biased with respect to the current state of the climate in Victoria.

It is also important that users of future climate change projections understand from which reference period differences are computed. In this document, in line with the latest IPCC report (IPCC 2013) and the Technical Report for the National Climate Change Projections (CSIRO and BoM 2015), climate change projections for the 21st century are calculated as changes relative to the 1986–2005 baseline period. For the three Victorian regions, annual, cool and warm season rainfall anomalies are indicated for this baseline period in Fig. 8 with coloured arrows. For the two southern regions of Victoria, rainfall anomalies for the IPCC baseline period are relatively similar to those of the last 30 years (1985–2014); for the Murray region, however, there is a difference of 6–7% for the cool and warm season anomalies with the 1985–2014 period being wetter than the last 30 years. These differences reflect the high decadal variability in rainfall. However, because of the more consistent longer term trends in temperature, average annual temperatures for the 1986–2005 baseline period are usually only 0.1 to 0.4 °C cooler then the last 30 years anomalies. Therefore, while consistent with international best practice, choosing 1986–2005 as the reference period for the future projections introduces some differences compared to the climate as defined for the last 30 years. These differences are common when switching between baseline periods, and it is recommended that this be clearly understood when making use of the projections information.
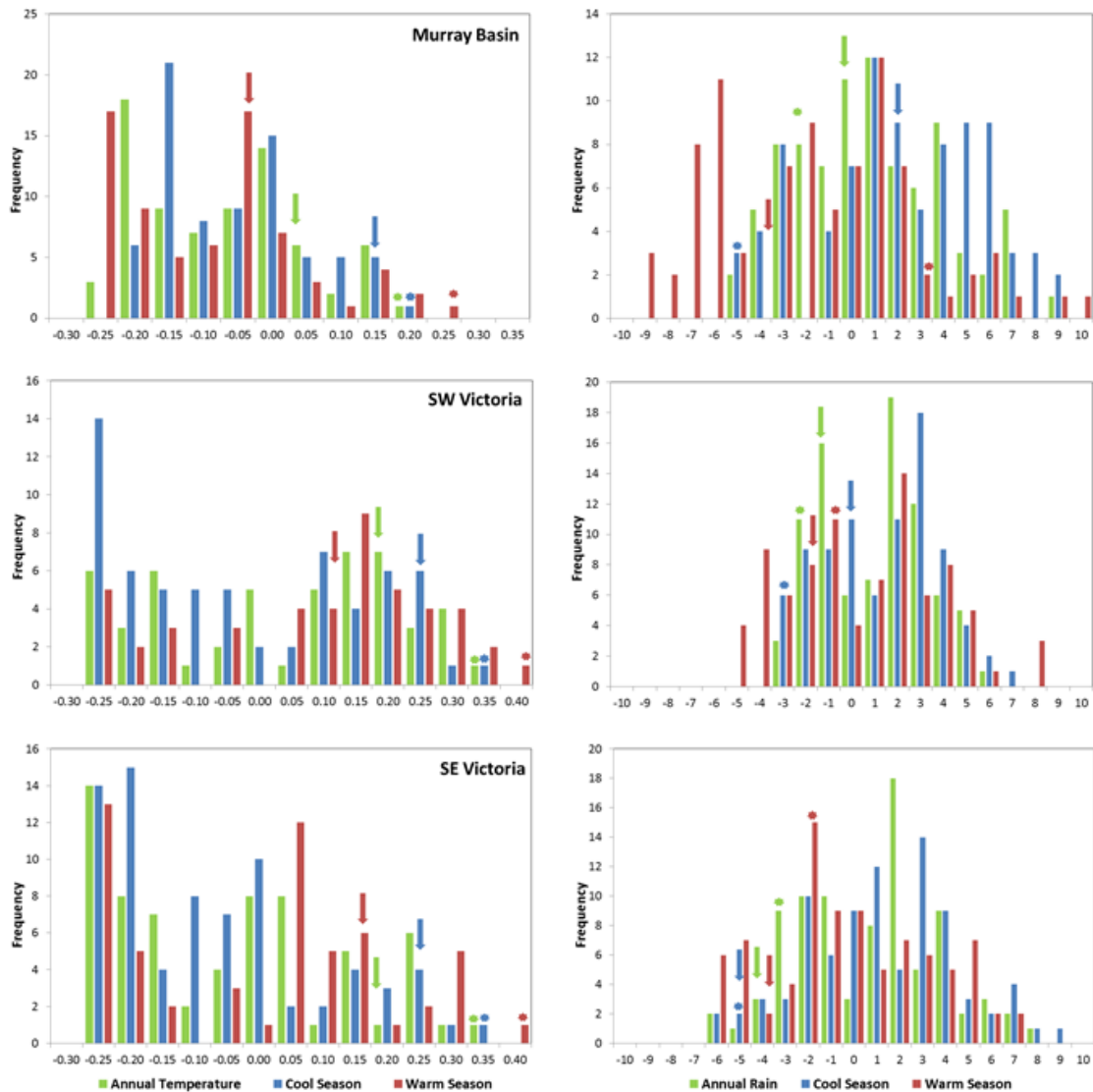
Fig. 8: Frequency distribution of 30-year anomalies of mean temperature (left, anomalies in °C relative to the 1911–2014 mean) and rainfall (right, in percentage terms relative to the 1900–2014 mean), averaged across the three Victorian regions (Murray Basin top, South-West region middle and South-East region bottom). Shown are annual results (green bars) and results for the cool (blue bars) and warm (red bars) seasons. Anomalies for the most recent 30-year period (1985–2014) are indicated by coloured stars while anomalies for the reference period for the projections (1986–2005) are indicated by coloured arrows. Note: the warm season rainfall anomaly for the 1986–2005 period (red arrow in top left panel) was never observed amongst all possible 30 years periods.

2. LARGE-SCALE INFLUENCES ON VICTORIAN CLIMATE

Victorian climate experiences natural variability on interannual and longer timescales in response to a complex interplay of large-scale climatic phenomena. An understanding of these phenomena, and how they influence the climate of Victoria now and into the future, is required to both appreciate local climate and also to predict its future evolution over a range of timescales (e.g. seasonal and long-term changes).

2.1 Mean meridional circulation and the subtropical ridge

The transfer of excess energy from the tropics to the pole(s) takes place via the mean meridional circulation, which controls the mean climate of Victoria, the position of the band of high pressure systems (the subtropical ridge) and the passage of rain-bearing weather systems. There are multiple lines of evidence showing that the characteristics of this particular global circulation has been changing over the last 50 years, in part due to anthropogenic forcings as well as natural fluctuations. These changes can be related to some of the observed changes in rainfall across Victoria.

Victoria is located under the descending arm of the Hadley Cell, which is a part of the global mean meridional circulation (MMC) depicted in Fig. 9. This shows a north-south cross-section through the Southern Hemisphere atmosphere above eastern Australian longitudes. The MMC is the main mechanism by which the planet transfers excess heat received at the Equator to the Poles. The descending arm of the Hadley Cell is tightly linked to surface high pressure systems (H in Fig. 9), resulting in relatively warm and dry air and little rainfall. This band of high pressure is called the subtropical ridge (STR). Rainfall over Victoria is associated with low pressure systems observed in between high pressure systems that are associated with either mid-latitude storm tracks (predominantly south of the STR) or cut-off lows (predominantly north of the STR).

Further south, the 'roaring 40s' and '50s' constitute a band of strong westerly winds and storms that encircle Antarctica (Sturman and Tapper 1996) and are very important for Victorian climate during the cool season. The centres of these storms in the surface westerlies are generally located south of Australia (Simmonds and Keay 2000); however, fronts associated with these storms are far reaching and have a large impact on Victoria. Along with cut-off lows, they are a major source of rainfall across Victoria (Risbey et al. 2009a and 2009b, Pook et al. 2012) all year around and especially during the cool season. During the warm season, cold fronts in south eastern Australia bring the classic 'cool change'—a significant change in air temperature (from warm to cool), accompanied by a change in wind direction at the boundary of a front. Fronts are associated with strong winds and increased fire danger (Mills 2005). Recent climatologies indicate the prevalence of fronts as rain bearing systems, particularly cold fronts, across southern Australia (Berry et al. 2011, Simmonds et al. 2012). Any trends in observed winds are difficult to establish due to sparse coverage of wind observations, difficulties with instruments and the changing circumstances of anemometer sites (Jakob 2010). McVicar et al. (2012) and Troccoli et al. (2012) have reported weak and conflicting trends in observed winds across Australia (although they considered winds at different levels). Circumventing the surface wind observation issues, Alexander et al. (2011) reported, using the gradient in MSLP, that storminess affecting southeastern Australia has experienced a significant reduction during the 20th century.

Changes have been observed in key components of the MMC affecting the climate of Victoria. It is now well accepted that the tropics have expanded in recent decades: the edge of the tropical tropopause (symbol A in Fig. 9) has trended poleward during the last 30 years (Lucas et al. 2012); the subtropical jet (B in Fig. 9) has decreased in intensity, while the polar front jet (C in Fig. 9) has increased in intensity (Frederiksen et al. 2011). The position of the descending arm of the Hadley Cell (D in Fig. 9) has also moved poleward during the last 30 years (Nguyen et al. 2013). All these large-scale changes indicate a poleward extension of the southern hemisphere Hadley circulation (Lucas et al. 2014).
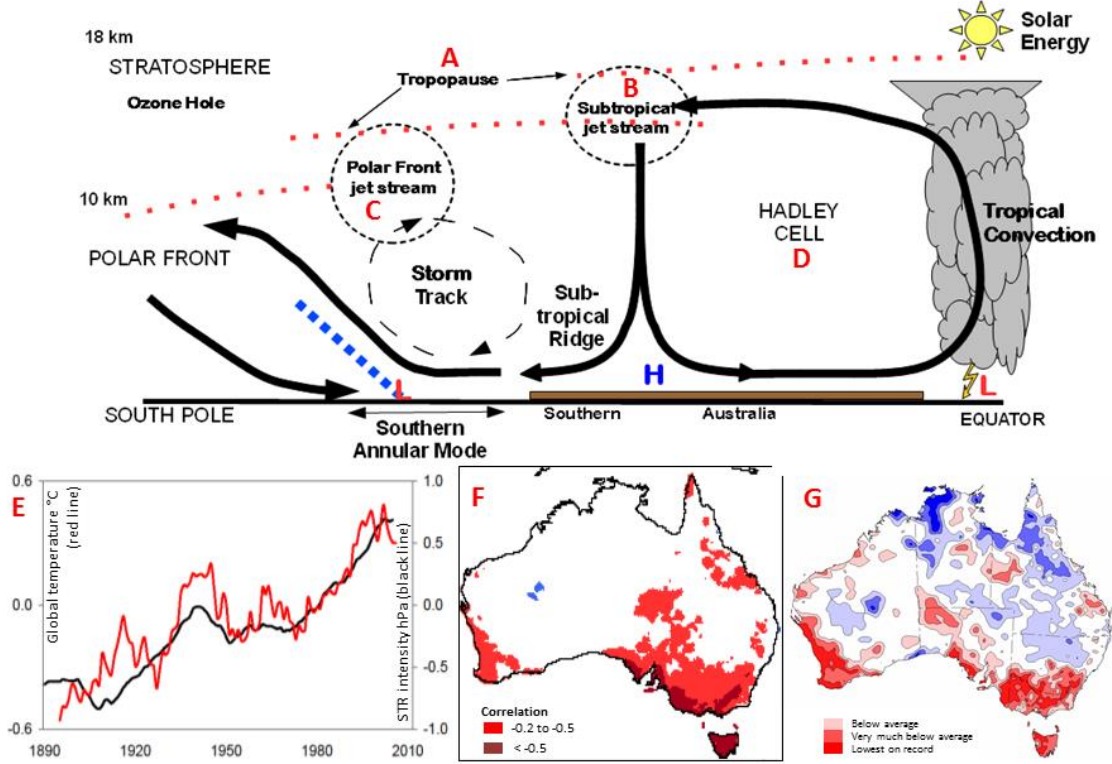
Fig. 9: Sketch of the mean meridional circulation (MMC) across the Southern Hemisphere; H and L denote regions of high and low pressure at the surface; A, B, C and D denote features discussed in Section 2.1; E shows time series of 11-year running mean of global surface temperature (black) and STR intensity (red); F shows map of the correlation between annual rainfall and STR intensity; G shows April–July rainfall decile map for the period 1986–2015. (Adapted from CSIRO and BoM 2012).

MMC expansion affects the climate across Australia and, in particular, Victoria. Intensification of the STR (i.e. increased surface pressure) observed during the last 120 years has occurred in conjunction with global warming of the planet (see E in Fig. 9) (Timbal and Drosdowsky 2013). MSLP changes over southern Australia are likely to have been in part driven by human influences (Grose et al. 2015c). Annual rainfall in much of southern Australia has a significant negative relationship with the intensity of the STR (see F in Fig. 9), in particular across Victoria and for cool season rainfall (Timbal and Drosdowsky 2013). The spatial extent of drying in the

early part of the cool season (April to July) during the last 30 years (see G in Fig. 9) coincides with the areas where the STR influences rainfall, and is particularly significant across Victoria.
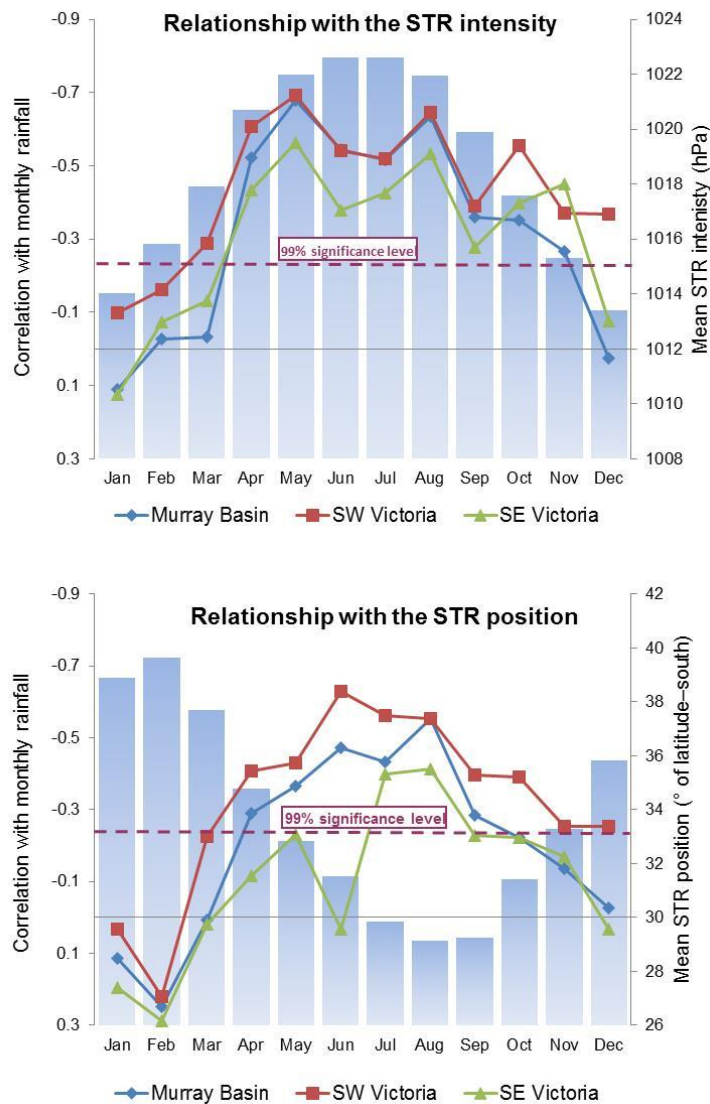
Fig. 10: Annual cycle of the correlation coefficients between the subtropical ridge (STR) intensity (left) and position (right) and rainfall for the three regions of Victoria (left Y-axis, Murray Basin in green, South-West region in red and South-East region in blue). Mean values of the subtropical ridge are shown as blue bars (right Y-axis), for intensity (in hPa, left panel) and position (latitude in degrees south, right panel). Higher negative values above the dashed lines are significant at a 99% significance level. Rainfall values are based on the Bureau of Meteorology operational 5 km gridded monthly data from 1900 to 2014 and subtropical ridge values are computed from de-trended data using the Drosdowsky (2005) methodology.

During summer the STR is weaker (close to the global average mean sea level pressure of 1013 hPa) and located further south (about 40°S), while during winter it is stronger (up to 1022 hPa) and further north (about 30°S) (Fig. 10). This behaviour influences seasonal rainfall

in Victoria with a more intense STR associated with declines in cool season rainfall, amplified—albeit to a lesser degree—by a poleward shift of the STR, also associated with reduced cool season rainfall. The relationship between the STR variability and Victorian rainfall is highly consistent across the three regions and is stronger and usually highly statistically significant during the cool season (Fig. 10). Small differences do exist across Victoria: the relationship with the intensity of the STR is stronger in the South-West and Murray Basin regions and weaker in the South-East region (Fig. 10) where major rainfall events are associated with easterly systems which are not influenced by the STR.

2.2 Tropical modes of variability

Victorian climate is highly variable. On interannual timescales the variability is often driven by remote large-scale mechanisms in the tropical oceans, in particular the Pacific Ocean where ENSO variability (El Niños and La Niñas) has a strong influence. In addition to ENSO, the behaviour of the Indian Ocean, either in response to ENSO or independently, plays an important role.

The weather and climate features described in the Section 1 are modulated from year-to-year by the main modes of natural tropical climate variability: the El Niño–Southern Oscillation (ENSO) and the Indian Ocean Dipole (IOD). ENSO originates in the Pacific Ocean and is the major driver of global interannual climate variability. Its link to Australian climate variability is well established (e.g. McBride and Nicholls 1983). Under normal conditions (the ENSO 'neutral' phase) the Walker Circulation and Pacific sea surface temperatures (SSTs) are in balance, with the easterly equatorial trade winds feeding moisture into the strong convection over the West Pacific Warm Pool. This produces high rainfall over the Maritime Continent and to the north of Australia. In other years the trade winds weaken or reverse, the Warm Pool expands eastward and convection moves away from the Australian region. During these 'El Niño' conditions, SSTs are warmer in the eastern Pacific and cooler than average around northern Australia. As a result rainfall is often below average over much of eastern Australia. In some other years, the trade winds strengthen, the eastern Pacific cools and SSTs around northern Australia are warmer than average. During these 'La Niña' conditions convection over northern Australia is enhanced and rainfall is often above average over eastern Australia. While El Niño and La Niña events are natural variations in the climate system, occurring on average every 4–7 years, ENSO also displays significant decadal variability (Power and Colman 2006). Australia's wettest 2-year period on record (2010–11), which ended the Millennium Drought across southeastern Australia (including Victoria), was associated with a strong, prolonged La Niña. The influence of ENSO on Australian rainfall is strongest in the later part of the calendar year.

The IOD is active in the tropical Indian Ocean, influencing interannual climate variability across tropical and extratropical Australia. The IOD is characterised by changes in SSTs off the Sumatran coast in the eastern Indian Ocean basin and changes of the opposite sign in the western Indian Ocean (Saji et al. 1999). Low SSTs in the east (and high in the west) form the 'positive' phase of the IOD and these conditions come about when southeasterly winds off northwest Australia induce upwelling in the eastern Indian Ocean (England et al. 2006). The IOD is usually active from May to November and is often terminated by the wind reversal accompanying the arrival of the northern Australia monsoon (e.g. Hendon et al. 2014). A

positive IOD has been found to contribute to below-average rainfall in southeastern Australia; the opposite rainfall pattern occurs during the negative phase, when eastern Indian Ocean SSTs are above average (Meyers et al. 2007).

IOD events are rarely independent of ENSO variability, as most positive (negative) IOD events are recorded when El Niño (La Niña) events are underway (Meyers et al. 2007; Hendon et al. 2014). The correlation between the two phenomena is very high in spring and less so in the other seasons. The impact of ENSO variability on rainfall across southeastern Australia, including most of Victoria, is modulated by the IOD response during ENSO events. This arises because the ability of tropical Pacific Ocean conditions (indicated by ENSO) to affect rainfall in southeastern Australia occurs primarily via the Indian Ocean (indicated by the IOD) (Cai et al. 2011). A convenient way to summarise the tropical influences of both ENSO and IOD on southeastern Australia rainfall is to use the tripolar index developed by Timbal and Hendon (2011). This index takes into account average SSTs over the central Pacific, northern Australia and north western Indian Ocean, providing a stronger relationship with rainfall for the three Victorian regions compared to ENSO or the IOD index alone.

The influence of the tropics on Victorian rainfall peaks during spring, most strongly over the Murray Basin region, whilst the Great Dividing Range acts as a barrier that weakens the relationship in other areas, particularly for the South-East region (Fig. 11). During August to November, the relationship is moderate and explains at most 20% of the year-to-year variability of any particular month. This August–November period was noted earlier as being a less variable time of year for rainfall. Despite this relationship between the tropical modes of variability and Victorian rainfall, it is not possible to relate the observed rainfall decline during the cool season to change in tropical SSTs (Timbal and Hendon 2011). The tropical modes of variability have little influence in the early part of the cool season when the rainfall deficit is the largest (CSIRO 2012). During the latter part of the cool season, when the relationship is moderate, negative trends in the tropical SST tripole index suggest, if anything, a small positive contribution to Victorian rainfall. This mitigates the overall reduction driven by STR intensification (Timbal and Hendon 2011). As expected from their impacts on rainfall, the tropical modes of variability are important in understanding the year-to-year variability of streamflow across Victorian catchments (Timbal et al. 2015b, Fiddes and Timbal 2016a) but do not explain the trends in streamflow discussed in the Section 1.3.
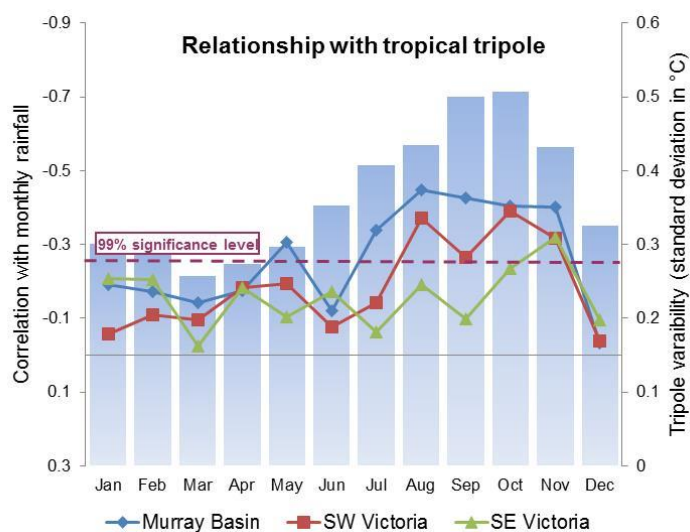
Fig. 11: Annual cycle of the correlation coefficients between the tropical tripole index and rainfall for the three regions in Victoria (left Y-axis, Murray Basin in green, South-West region in red and South-East region in blue). Monthly standard deviations of the tripole index are shown as blue bars (right Y-axis, in °C). Negative correlations values above the dashed line are significant at the 99% significance level. Rainfall values are based on the Bureau of Meteorology operational 5 km gridded monthly data from 1900 to 2014 and tripole values are computed from de-trended HadISST data (reference) using Timbal and Hendon (2011) methodology.

2.3 High latitude modes of variability

Besides tropical modes of variability, the trajectories of weather systems delivering rainfall across Victoria are affected by a hemispheric see-saw of atmospheric pressures between 40°S and 65°S, called the Southern Annular Mode (SAM). It acts to contract and expand the circulation of weather systems around Antarctica. This, in turn, influences Victorian climate, with impacts dependent on the season, and varying across the State. SAM has trended positively since the late 1950s and this may have contributed to the observed ongoing deficit in cool season rainfall.

The northern extent of the westerly winds (often referred to as the 'westerlies') shifts north and south on a range of timescales, influencing rainfall variability across southern Australia. This north–south shift in the westerlies, and the embedded low pressure systems, are also part of the hemispheric mode of variability known as the Southern Annular Mode (SAM, Thompson and Wallace 2000). SAM reflects the variability in the hemispheric pattern of lower pressures around Antarctica and higher pressures over southern Australia, and is monitored using the SAM index (Marshall 2003). Higher values of the SAM index mean higher pressures over southern Australia and a poleward contracted band of westerlies. The impact of SAM varies with location and season (Hendon et al. 2007). In winter, a positive SAM phase shifts low pressure systems to the south, thus shifting rainfall away from southeastern Australia. In spring and summer a positive SAM phase shifts the westerlies southward, allowing more tropical incursions from the north and anomalous easterly winds over the eastern seaboard, bringing above-average rainfall. These spatial patterns across southeastern Australia are reflected in the correlation coefficients between the SAM index (Marshall 2003) and rainfall averaged across

the three Victorian regions (Fig. 12). The largest negative relationship (positive SAM phase correlating with less rainfall) is seen in the middle of the cool season (July) and is largest in the South-West region. The positive relationship (positive SAM phase correlating to more rainfall) is seen in late spring to early summer and is most prominent in the Murray Basin region. For the South-East region, the relationship is weak and insignificant all year round.

The annual cycle of the variability of SAM is fairly even all year around (not shown); instead the annual cycle of the linear trend of the SAM index is shown in Fig. 12. The SAM index has been trending upward since the late 1950s with the largest trend in summer and autumn extending into the early part of the cool season (July). For this reason, SAM is likely to have contributed to the cool season rainfall decline, at least early in the season. This contribution is not necessarily independent of the contribution from the STR intensification, as a trend towards a more positive SAM implies an increase in intensity of the zonal belt of high pressure.
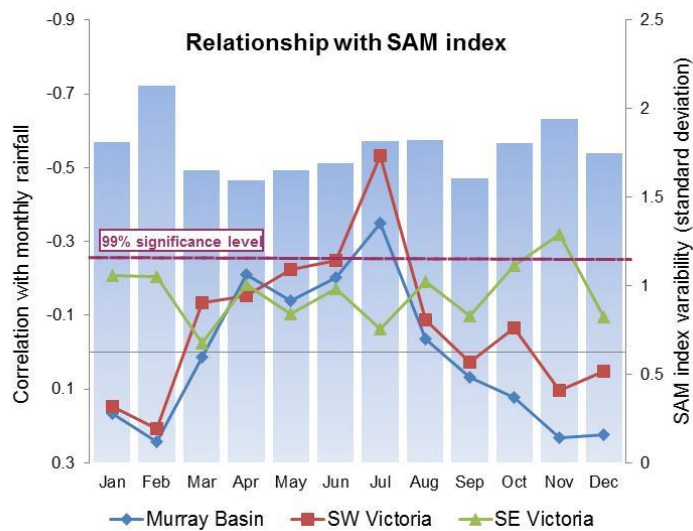
Fig. 12: Annual cycle of the correlation coefficients between the Southern Annular Mode (SAM) and rainfall for the three regions in Victoria (left Y-axis, Murray Basin in green, South-West region in red and South-East region in blue). Monthly linear trends of the SAM index are shown as blue bars (right Y-axis, normalised values). Negative (positive) values above (below) the dashed line are significant at the 99% significance level. Rainfall values are based on the Bureau of Meteorology operational 5 km gridded monthly data from 1900 to 2014 and the SAM index is from Marshall (2003).

2.4 Synoptic variability or 'weather noise'

While large-scale modes of variability are important in understanding the observed variability of the climate of Victoria, they do not fully explain the randomness of the weather. Therefore the local climate is never perfectly predictable at any timescale. The randomness of weather noise is also embedded in historical climate model runs and future climate projections from global climate models, which explains why they are not deterministic in nature.

The term 'synoptic variability' refers to the high frequency (day-to-day) variability of weather due to the passage of fronts or lows (often rain-bearing) and high pressure systems (which can last for extended periods in the case of blocking events). The modes of variability internally

generated by the climate system described above (either tropical, ENSO and IOD; or extratropical, SAM) are felt on the regional climate of Victoria through their impact on the synoptic variability. These impacts are well understood and contribute greatly to the ability to deliver seasonal climate predictions. It is important however to remember that while these large scale modes influence Victorian climate, for any given month they account for less than 20% of the year-to-year variability in any part of the State (see Section 1.2). Therefore, a large part of the naturally occurring synoptic variability is random and unpredictable: from a climatological perspective this is referred to as 'the weather noise'.

In addition to the frontal systems affecting southern Australian rainfall and temperatures, some low pressure systems separated from the westerly storm track (known as 'cut-off lows') are particularly important, bringing large rainfall totals to southern Australia (Pook et al. 2012). On the Australian east coast, cut-off lows can sometimes form over the Tasman Sea, and are commonly referred to as East Coast Lows (ECLs). These systems are responsible for some of the more damaging natural disasters and for major flows within water catchments (Dowdy et al. 2013a). ECLs predominantly impact the eastern seaboard, east of the Great Dividing Range, extending to the southeastern regions of Victoria. Interestingly, the large-scale modes of variability (described above) do not appear to have a significant influence on ECL occurrence (Dowdy et al. 2013a). As ECLs are a major contributor to southeastern Victorian rainfall, this explains the weaker relationship between rainfall in the South-East region and the tropical (Fig. 11) and extratropical (Fig. 12) modes of variability over large parts of the year (Pepler et al. 2014).

2.5 Interactions between modes of variability

Besides the various modes of interannual variability relevant to Victorian rainfall, recent research points to the importance of decadal variability. Particularly relevant are the change of phase of the Inter-decadal Pacific Oscillation (IPO) in influencing the interaction between the interannual modes, affecting the climate of Victoria, and also the long-term trends in the expansion of the tropics and the Hadley Cell (which is a key component of the mean meridional circulation).

The various modes of variability described in Sections 2.2, 2.3 and 2.4 are not independent of one another. The ways they interact vary on decadal time scales, with a flow-on effect on rainfall in Victoria. These variations are related to the phase of the Inter-decadal Pacific Oscillation (IPO) (Lim et al. 2016). The IPO is a fluctuation of SSTs in the Pacific Ocean, spatially broader than the ENSO variability, and operating on a non-regular multi-decadal timescale; typically taking 15 to 30 years to shift from a warm to a cold phase. Unlike ENSO, the IPO may not be a single physical 'mode' of variability but rather the result of several processes with different origins. Currently, there appears to be no predictability in the phase swings of the IPO. The most recent phase change of the IPO was in 1999, transitioning to its cold phase (that is, cooler sea-surface temperatures in the east Pacific and warmer in the west, in terms of a decadal mean). This is associated with reduced variability and predictability of ENSO and, as such, impacts on seasonal prediction capabilities. A cold IPO phase means a warming of the waters north of Australia. Thus the IPO cold phase has a similar signature to global warming in the sea-surface temperatures north of Australia. These combined factors enhanced recent La Niña events, which in turn fostered a strong positive SAM, further

triggering greater spring and summer rainfall during 2010 (Lim and Hendon 2015a). This relationship between ENSO and SAM is relevant in dry years as well as in wet years; the strong drought over Victoria in the spring of 2002 has been shown to be due to both the moderate El Niño event and the strong negative phase of SAM at that time (Lim and Hendon 2015b). Furthermore, the phase of the IPO also influences the strength of the ENSO–IOD relationship and modulates the spatial patterns of their teleconnections to Australian climate. For instance, the recent cold phase of the IPO appeared to create stronger links with Victorian rainfall, despite reducing the strengths of ENSO and IOD (Lim et al. 2016). Victorian rainfall tends to vary more directly with ENSO indicators during wet years (La Niña) and with IOD indicators during dry years (El Niño and subsequent positive IOD). Fig. 13 provides an overview of these large-scale influences on Victorian climate.

On decadal timescales, the expansion of the Southern Hemisphere Hadley cell is associated with a La Niña-like state (Hope et al. 2015b) in the tropical Pacific. During the last 30 years, tropical expansion has been additionally promoted by the shift to the cold phase of the IPO after 1999. It is therefore possible that decadal modes of variability such as the IPO have contributed to the observed (and accelerating) trends in Victoria's climate (i.e. temperature and rainfall) in the last 30 years. As yet, global climate model simulations are unable to capture the full extent of the observed Hadley Cell expansion, nor the timing of the decadal variability of the IPO in the last 30 years, making it difficult to confidently attribute these to recent trends in climate.
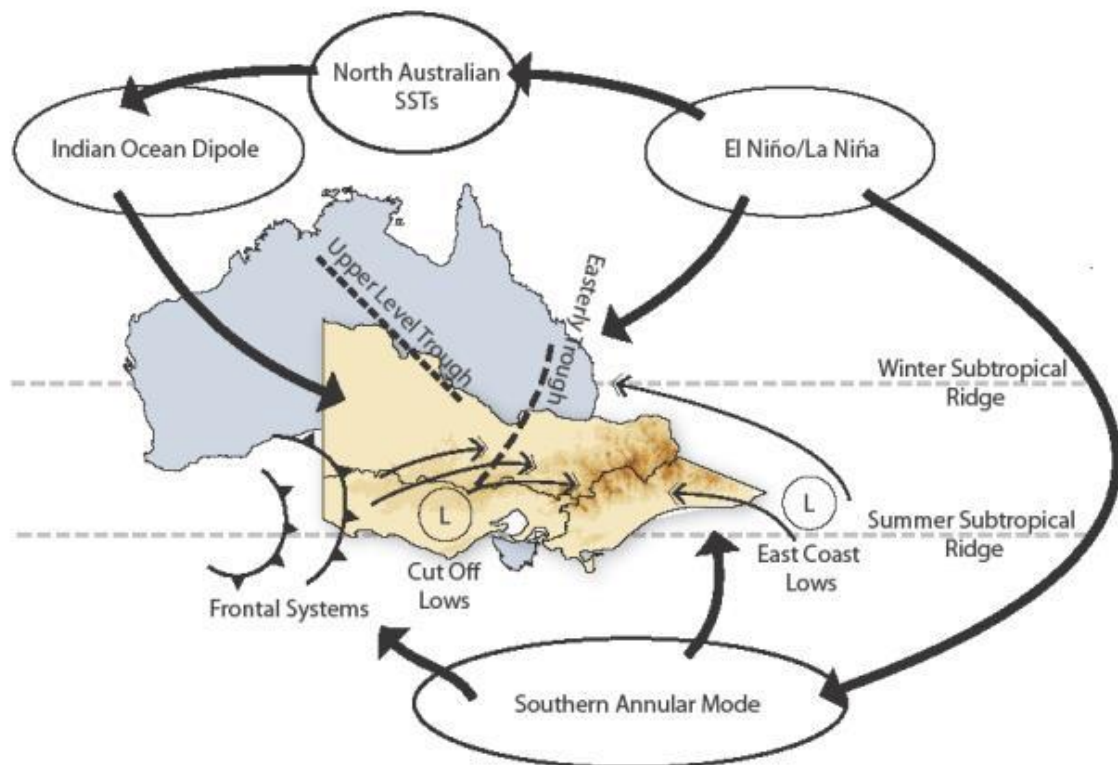
Fig. 13: Large-scale climate features of relevance to local climate in Victoria. Thick arrows show the influences each climate mode has upon either synoptic weather types affecting Victoria or another climate mode. Thin arrows indicated wind directions associated with certain synoptic weather types.

3. DEVELOPING FUTURE PROJECTIONS

Projections of future changes to the climate for Victoria presented in this report are based on international efforts to gather existing global climate model simulations, as well as a national program that delivered nation-wide climate change projections.

The projections of future climate for the State of Victoria are based on our current understanding of the climate system, observed historical trends and model simulations of the climate response to increasing greenhouse gas and aerosol emissions. The simulated climate response is that of models in the Coupled Model Intercomparison Project, phase 5 (CMIP5) climate model archive. The CMIP5 model archive also underpins the science of the Fifth Assessment Report of the Intergovernmental Panel on Climate Change (IPCC 2013) and the Technical Report for the National Climate Change Projections (CSIRO and BoM 2015).

3.1 Emission pathways

The climate will change in response to future human activities, the specifics of which are unknown as this stage. Therefore the climate models are forced with plausible estimates of future greenhouses gas concentrations according to likely socio-economic scenarios. These scenarios are known as Representative Concentration Pathways or RCPs. In this report results are presented for several of these scenarios, focusing on a higher scenario (RCP8.5 which is similar to a 'business as usual' approach) and a lower scenario (RCP4.5 which is achievable only if substantial emission reduction measures are put in place).

The climate projections presented in this report are based on climate model simulations following a set of greenhouse gas and aerosol scenarios that are consistent with a range of socio-economic assumptions of how the future may evolve. There are four Representative Concentration Pathways (RCPs) and these are labelled according to the radiative forcing (in W/m^2) associated with that particular pathway by the end of the 21st century (Van Vuuren et al. 2011). The highest scenario, RCP8.5, represents a future with little curbing of emissions, resulting in carbon dioxide concentrations reaching 940 ppm (part per millions in volume) by 2100. The higher of the two intermediate concentration scenarios (RCP6.0) assumes implementation of some mitigation strategies, with carbon dioxide concentrations reaching 670 ppm by 2100. The lower intermediate scenario, RCP4.5, describes somewhat higher emissions than RCP6.0 until the mid-century, but peaks earlier with stabilisation of the carbon dioxide concentration at about 540 ppm by 2100. The very low scenario (RCP2.6) describes emissions that peak around 2020 and then rapidly decline, with carbon dioxide concentration at about 420 ppm by 2100. It is likely that active removal of carbon dioxide from the atmosphere would be required later in the century for this scenario to be achieved.

In this report, the focus is on two of these scenarios: RCP4.5, representing a pathway only achievable if substantial emission reduction measures are put in place to avoid 'dangerous climate change' and RCP8.5, the pathway if little or no action is taken to limit emissions. The previous generation of climate model experiments that underpinned the science of the IPCC's Fourth Assessment Report in 2007 used a different set of emission scenarios. These are described in the IPCC's Special Report on Emissions Scenarios (SRES) (Nakićenović and

Swart 2000). The RCPs and SRES scenarios do not correspond directly to each other, though we note that RCP8.5 has a resultant radiative forcing close to that of SRES scenario A1FI, and carbon dioxide concentrations under RCP4.5 closely mimic those of SRES scenario B1. More details on the emission pathways can be found in the recent IPCC report (IPCC 2013) and Van Vuuren et al. (2011). A comparison between RCPs and SRES are provided in the Technical Report for the National Climate Change Projections (p. 26, CSIRO and BoM 2015).

3.2 Global climate models

Projections of the evolution of the climate system in response to the human induced forcings are produced using complex mathematical models representing both the atmospheric and oceanic components of the global climate system. In order to capture the uncertainties of the future projections of the climate, and because climate models contain limitations (especially for small-scale features), it is best practice to make use of results from a large number of simulations from existing climate models within the international community.

Future climate changes cannot be simply extrapolated linearly from past climate due to the non-stationary nature of the climate system and our influence upon it, resulting in different possible future emissions pathways. The best tools for climate change projections are general circulation models; also called global climate models (GCMs). These are mathematical representations of the climate system, run on powerful supercomputers. Their fundamentals are based on the laws of physics, including conservation of mass, energy and momentum, and parameterisation of small-scale weather phenomena. GCMs are closely related to models used by the Bureau of Meteorology to produce Australia's weather forecasts. Climate models have undergone continuous development for the last three decades, and now incorporate interactions between the atmosphere, oceans, sea ice and land surface. Some latest generation models can additionally represent the interactions between oceanic, atmospheric and land surface carbon cycles, including interactive atmospheric chemistry and vegetation, evolving towards full 'earth system models'.

GCMs represent the atmosphere and ocean as three dimensional grids, with a typical resolution of around 200 km, and 20 to 50 vertical levels, in both the ocean and the atmosphere. Models explicitly simulate large-scale synoptic features of the atmosphere, such as the progression of high and low pressure systems, and large-scale oceanic currents and overturning. However many important physical processes occur at finer spatial scales. Examples include radiation and precipitation processes, cloud formation and atmospheric and oceanic turbulence. The impacts of such processes are included in 'parameterisations', whereby their effects are expressed in approximate form on the coarser model grid. Parameterisations are typically the result of intensive theoretical and observational study, and essentially represent an additional detailed physical modelling within the climate model itself. The actual warming projected by a model depends on the forcing and the global climate sensitivity to the forcing.

Direct comparison of the CMIP3 and CMIP5 results is hampered by the different emission scenarios used (as discussed earlier). However, based on a range of studies and methods, the Fifth Assessment Report found that there is 'no fundamental difference' in the overall sensitivities of the two ensembles (IPCC 2013). More details on the set of GCM simulations

assembled for the projections used in this work (listed in Appendix 3) can be found in the Technical Report for the National Climate Change Projections (CSIRO and BoM 2015).

3.3 Climate model evaluation

The climate models underpinning the future projections have been evaluated based on their ability to reproduce the observed past and present climate, along with the key mechanisms influencing the climate. These evaluations are helpful in determining which processes models simulate well and, therefore, in guiding the selection of individual models for impact studies. These evaluations are made for important surface climate variables across Victoria as well as for large-scale mechanisms known to drive the variability of the climate of Victoria.

The skill of a climate model is assessed by comparing model simulations of the current climate with observational datasets (primarily Bureau of Meteorology operational gridded datasets) and reanalysis datasets (see Appendix 1). Some differences in model output relative to the observations are to be expected, as GCMs reproduce their own version of the current climate. Comparison of the observed and simulated climate mean and variability, and the trends attributable to external forcings, are part of the confidence assessment of climate projections (Bhend and Whetton 2015).

GCMs from the CMIP5 database considered for this report simulate Victoria's regional annual cycle of temperature over the baseline period 1986–2005 (left panels in Fig. 14) with little scatter amongst models and usually within 2 °C of observations for any month. The strong similarities between simulated and observed seasonal patterns give confidence in the simulation of realistic future projections. The ability of the models is similar for all three regions in Victoria.

For rainfall, climate models show a very large scatter around the observations with different seasonal patterns for the three regions in Victoria (right panels in Fig. 14). For the Murray Basin region, the largest errors are found for the warm season rainfall, while errors for the cool season, particularly for the early part of the season, are lower. About ten CMIP5 models have a poor representation of the annual cycle, showing a summer maximum in rainfall. These models contribute to a bias in the ensemble mean toward a wetter than observed warm season rainfall, although the ensemble mean remains close to the observations for most of the cool season rainfall. For the southern parts of the State, there is also a fairly wide spread amongst models. The largest errors for some models are found in the simulation of the winter maximum rainfall and, generally, an underestimation of the rainfall in spring. This is especially so for the South-East region, due to that part of the State not being captured due to the global models' spatial resolution.

The ability of CMIP5 models to capture one of the important measures of the general circulation relevant to Victoria is evaluated by looking at the reproduction of the annual cycle of mean sea level pressure (MSLP) for all three regions. The annual cycle of MSLP is reasonably simulated (middle panels in Fig. 14), although the scatter amongst models is large. Individual models have errors up to 6 hPa, which is substantial in comparison to an annual cycle range of 10 hPa, but in general it is a systematic bias (a systematic shift all year around) and the critical movement of the annual cycle is well captured.
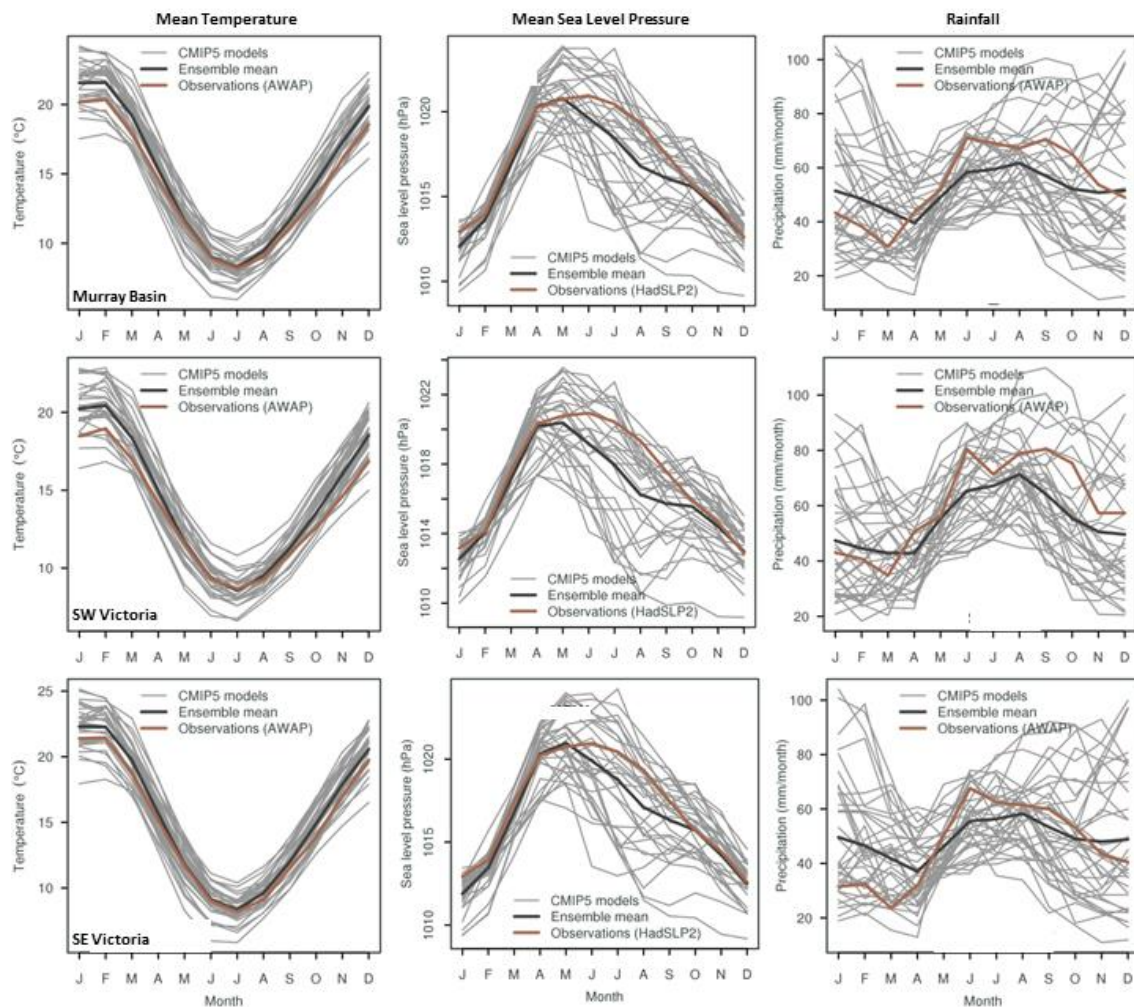
Fig. 14: The annual cycle of temperature (left panels), MSLP (middle panels) and rainfall (right panels) for the three regions in Victoria, (Murray Basin top row, South-West region middle row and South-East region bottom row) as simulated by the CMIP5 models (grey lines) computed for the baseline period of 1986–2005. Model ensemble mean is shown in black and the observed climatology over the same period in brown. Rainfall and temperature observations are from the Bureau of Meteorology operational gridded observations and MSLP observations are from HadSLP2 (Allan and Ansell 2006).

Local MSLP is linked to the STR, an important modulator of the rainfall across Victoria (see Section 2.1). It is therefore useful to evaluate the models' ability to reproduce the intensity (STR-I) and positon (STR-P) of the STR (left panel in Fig.15), as well as how well models relate the behaviour of the STR to rainfall across Victoria (right panel in Fig. 15). The CMIP5 model mean annual cycle of STR-I and STR-P for the 1948–2002 period is within the observed uncertainty in most months of the year, although with a slight northerly bias in August and September. Overall the bias in current climate models (CMIP5) is less than in the previous generation (CMIP3) in some respects, but not for all months of the year. The correlation coefficients between CMIP5 model rainfall computed over a box encompassing Victoria and each model's STR-I highlights that this relationship is generally too weak in the GCMs throughout the entire cool season, and especially so for the April to August period (right panel in Fig. 15).
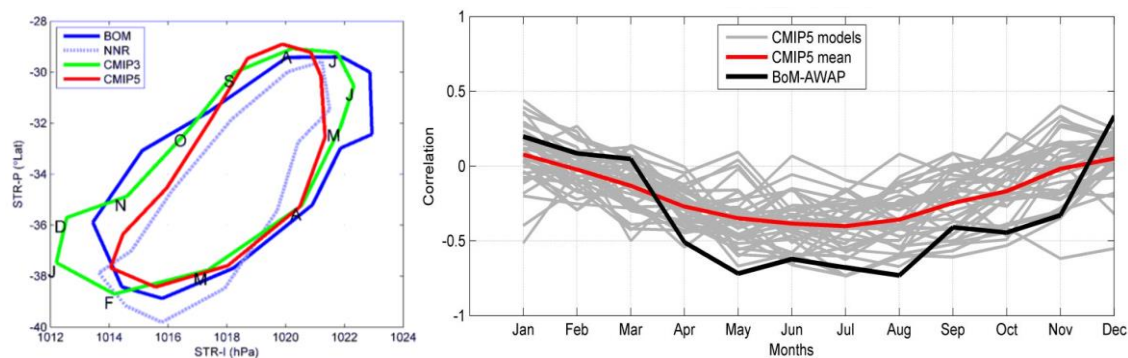
Fig. 15: Combined mean annual cycles (letters denote the initial of each calendar month) of the intensity (STR-I) and position (STR-P) index of the STR for the period 1948–2002 (left panel) as indicated using observations from the Bureau of Meteorology (BOM, blue curve; Drosdowsky 2005), the National Center for Environmental Prediction (NCEP) and the National Center for Atmospheric Research (NCAR) reanalyses (NNR, light blue curve), the multi-model mean of CMIP3 models (green curve; Kent et al. 2013; the reference period here is 1948–1974) and the multi-model mean of CMIP5 models (red curve; Grose et al. 2015b). Correlation coefficients (right panel) between STR-I and rainfall for southeastern Australia (a larger region encompassing Victoria) for 1948–2002, from 35 CMIP5 models (grey), the ensemble mean (red), and the observed relationship using the Bureau of Meteorology operational gridded rainfall (black). (Source: Grose et al. 2015b)

The ability of the CMIP5 models to capture significant observed trends for key climatic variables in Victorian climate is also an important consideration in the overall confidence assessment. The magnitude of the observed temperature trend between 1911 and 2005, as well as the acceleration of the warming since the 1960s, are fairly well matched by the multi-model mean, but with large model spread around this mean (not shown). However the distinct seasonal variation in observed temperature trends (largest in the warm season and weaker in the cool season) is not captured. Similarly, models simulate the increase in annual mean sea level pressure seen in observations, but do not capture the seasonal differences in this trend (not shown). In particular, models generally do not match the observed increase in MSLP during autumn. The CMIP5 models do capture an expansion of the MMC, in particular for the Hadley Cell and the strengthening of the STR (Nguyen et al. 2014), albeit with a reduced intensity compared to the reanalyses and observations (Grose et al. 2015b). However the same models are not able to reproduce the observed rainfall trends across Victoria over the last 30 years (Bhend and Whetton 2015). There is a large range of responses across models, but the ensemble mean shows no tendency towards drying during the cool season and a weak tendency towards wetter conditions for the warm season (not shown). As a consequence, when these climate models are used, via statistical downscaling, to generate streamflow simulations, insubstantial trends are found in simulated streamflow for many Victorian catchments. Only 6 out of 22 downscaled GCMs have a downward trend in excess of a 5% decline for the 27 hydrologic reference catchments considered across the State, while two models produce an average decline (for the 27 catchments) of 9%, similar to that of the observations (Fiddes and Timbal 2016b). It is worth noting that the catchments considered covered about 10% of the State; however, they are expected to be representative of surrounding areas.

It is informative to assess how well the CMIP5 climate models are able to capture the important relationship between rainfall across Victoria and the modes of variability identified in Section 2,

again contributing to the overall model assessment. The ability of 36 CMIP5 models to reproduce tropical SST variability (top panel in Fig. 16) and its relationship to Victorian rainfall (lower panel in Fig. 16) was analysed. The climate models have a realistic annual cycle but tend to overestimate the magnitude of the tropical variability, as diagnosed from the standard deviation of SST anomalies in the tripole boxes. This is a systematic bias present all year around, although some models are closer to the observed variability. This is consistent with the known problems within climate models regarding their ability to reproduce ENSO variability despite an improvement in GCMs from CMIP3 to CMIP5 (see for example Guilyardi et al. 2009; chapter 14 in IPCC 2013). Despite the overestimation of the tropical variability, models tend to underestimate the strength of the relationship with Victorian climate, albeit showing a realistic annual cycle of the variation of the strength of this teleconnection.
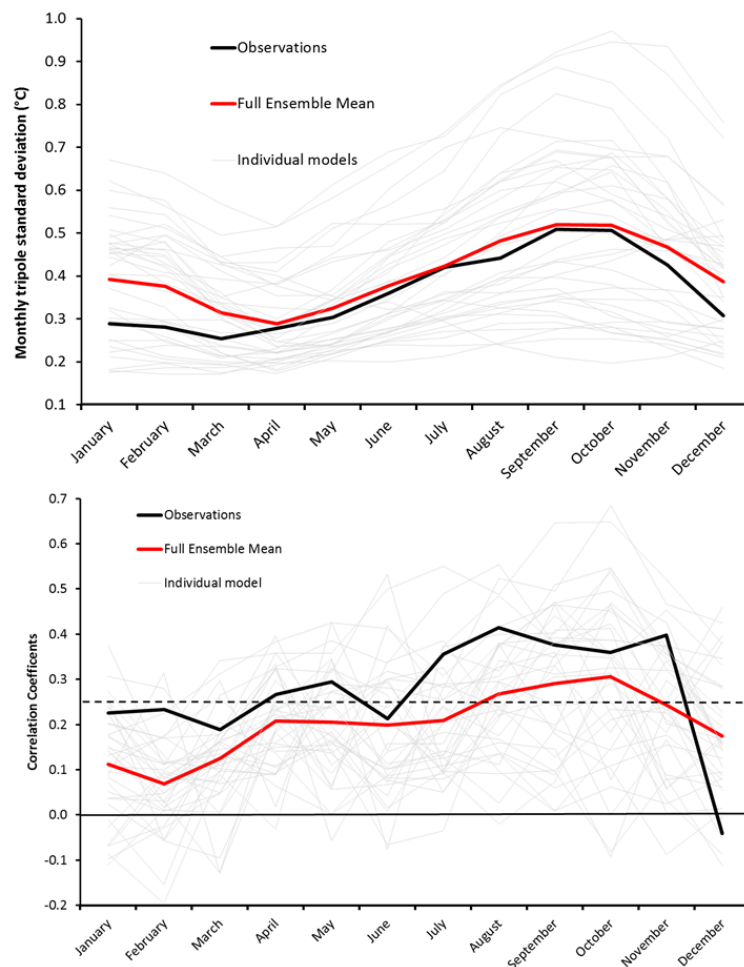
Fig. 16: Annual cycle of tripole index variability (standard deviation in °C, top panel) and relationship with rainfall across Victoria (correlation coefficient, bottom panel) for the observations (black line), 36 CMIP5 models (grey lines) and the ensemble mean (red line). The dashed line indicates the 99% confidence level. Rainfall observations are from the Bureau of Meteorology operational gridded rainfall; all quantities are computed for the baseline period of 1900–2005.

Across all these assessments, individual models were evaluated and ranked for a range of metrics. Detail of the skill scores of individual GCMs can be found in the Technical Report for the National Climate Change Projections (CSIRO and BoM 2015) and a summary of the evaluation of relevance to Victoria is provided in Appendix 3. The approach adopted for determining climate change projections for Victoria has been to equally weight all participating CMIP5 models, as all models are plausible. As part of the release of the national projections using CMIP5 models, the range of projected change factoring in model performance (by weighting or model elimination) was investigated. It was found that this did not have a significant impact on the resultant projections (see CSIRO and BoM 2015 for details); however some models were listed as having deficiencies which need to be considered if their results are to be used for impacts work (p. 75, CSIRO and BoM 2015).

Overall, model evaluation is an important tool and its result is applied in two other key areas. First, it is considered when formulating the confidence rating that is attached to all CMIP5 projections (see Section 4). Secondly, poor performing models are flagged in the Climate Futures tool (Whetton et al. 2012) to guard against these models being included in a smaller set of selected models used in impact assessment modelling (see Section 3.5 on accessing and using climate change information). Appendix 3 summarises key findings from various evaluations of the CMIP5 models used in this report which are relevant to Victoria.

3.4 High resolution climate projections

Global climate models can capture large-scale aspects of the climate well but are not designed to provide local information at scales finer than their spatial resolution. To obtain local-scale projections, additional techniques are required to downscale this information to a scale relevant for impact studies. Amongst the numerous existing approaches, this report makes extensive use of results from a statistical downscaling model based on meteorological analogues.

Section 3.3 highlights that while climate models are generally able to reproduce large-scale features of the climate system, larger biases emerge for smaller regions (e.g. the biases shown for rainfall averaged across the Victorian regions, Fig. 14). Climate models, which solve the equations of mass transport in the atmosphere globally on a finite grid, are not designed to provide meaningful information at spatial scales below their grid resolution or even across only few grid cells. Therefore, when climate information is required locally or for small regions (including for the Victorian regions presented here, which are only covered by a small number of GCM grid boxes), techniques to provide higher resolution information are used. Downscaling is the process by which GCM climate change outputs, with a typical spatial resolution of 100–300 km, are translated into finer resolution climate change projections. Downscaling can produce more physically plausible changes compared to that of the host GCMs, and in a few compelling situations there is a case for using downscaled data in preference to GCM outputs for impact analysis at the regional scale. These situations are typically regions where topography or coastlines greatly influence local climate, and where there are distinct climatic zones within a relatively small area. The three Victorian regions considered in this report are prime candidates to benefit from using downscaled climate change projections.

There are many different ways in which GCM outputs can be translated to finer resolutions or even point locations (Ekström et al. 2015). Some methods are nearly as complex as the GCMs themselves, whilst others merely involve adding the mean change between two time slices, as derived directly from the GCMs, to observed data. As a general guide, downscaling methods can typically be categorised into three groups: dynamical downscaling, statistical downscaling and change factor methods. Dynamical downscaling involves running a dynamical climate model, also known as a regional climate model (RCM), using output from a GCM as its input. Statistical downscaling does the same but applies a statistical model to GCM output. Change factor methods are techniques of combining the change signal from comparatively coarse GCM outputs with high resolution observed datasets and thus are not a complete downscaling approach. In this case only the observed climate has a high spatial and temporal resolution, whilst the climate change signal remains as that of the coarse resolution climate model. All methods of downscaling typically require some form of bias correction in order to match observations, and this correction is generally assumed to remain valid when applied to future projections.

Statistical downscaling refers to a method that uses a statistical relationship between the local-scale variable of interest (e.g. local rainfall) and larger-scale atmospheric fields (e.g. large-scale pressure fields). This is achieved through regression methods, weather typing or through the use of weather generators calibrated to the large-scale atmospheric fields. In this report, results from the Bureau of Meteorology analogue-based statistical downscaling model (SDM) for Australia (Timbal et al. 2009) are used to complement the projections obtained directly from the GCMs. Statistical downscaling will almost certainly produce greater climate realism than the host model, but may still have some level of bias compared to an observed dataset, both in spatial and temporal distributions. In terms of physically plausible change, statistical downscaling is likely to produce more spatial and temporal detail in the climate change signal compared to the GCM, especially around areas of significant topography and coastlines. This is limited however to the variables for which this method has been used: precipitation and temperature. A further limitation is that the method requires a substantial number of predictors and, hence, could only be applied to the 22 CMIP5 models (out of full CMIP5 database for which all the necessary data were available. In this regard the projections obtained from the SDM do not span the full range of model uncertainties as seen for the other projections using the complete CMIP5 database.

Other high resolution projections have been generated for Australia using the dynamical Conformal Cubic Atmospheric Model (CCAM, McGregor and Dix 2008). These were done as part of the completion of the national climate change projections (CSIRO and BoM 2015). In addition, simulations covering Victoria were performed using the Weather Research Forecast (WRF) model as part of the NSW and ACT regional Climate Modelling program (NARCLIM: www.ccrc.unsw.edu.au/NARCliM/). These simulations are valuable resources for detailed impact studies.

3.5 Understanding climate projections and further information

The future climate projections for Victoria presented in this report are based on the recently released Australian climate change projections. This national program delivered data as well as a series of reports which are useful background information in support of this report and are available through the *Climate Change in Australia* website. In particular, the website provides methods and tools to enable the selection of climate dataset(s) required to perform more advanced analysis of the impact of climate change. While the national project went far beyond the scope of this study, we provide additional and more local details of projected changes to Victoria's climate.

The Climate Change in Australia website (www.climatechangeinaustralia.gov.au) provides information on the science of climate change in a global and Australian context with material supporting regional planning activities. It gives access to the published material in support of the national projections: in particular the associated Technical Report (CSIRO and BoM 2015). It also provides access to eight cluster reports including the two clusters of direct relevance to the State of Victoria: the Murray Basin cluster (Timbal et al. 2015a), encompassing the Victorian, New South Wales and South Australian Murray–Darling Basin, and the Southern Slopes cluster (Grose et al. 2015a) which encompasses both the South-West and South-East regions of Victoria, as well as Tasmania. The website provides information in addition to these reports, such as a different time periods or emission scenarios.

The Climate Change in Australia website is a useful resource in adaptation planning. The fundamental role of adaptation is to reduce the adverse impacts of climate change on vulnerable systems, using a wide range of actions directed by the needs of the vulnerable system. While this report presents information about possible future climate responses to increasing greenhouse gas concentrations, the website allows stakeholders to direct the information into guidance for adaptation, using tools such as the Climate Futures web tool.

Since projected changes for Victoria are either obtained from the publications mentioned above or are re-computed specifically for regions within Victoria using the same methodology, the various Climate Change in Australia resources (e.g. reports and website) are useful background material for this report.

In the following section, projected changes are expressed as a range of plausible changes in individual variables as simulated by CMIP5 models or derived from their outputs. However, many users are interested how the climate as a whole may change, rather than changes in single variables. To do this, we must consider concurrent variable changes into the future. For these studies, data from *individual* models should be considered because each model simulates changes that are internally consistent across many variables. The challenge for impact and adaptation researchers lies in selecting which models to look at, since models vary in their simulated response to increasing greenhouse gas emissions. In order to alleviate this situation, climate models can be organised according to their simulated climate response. For example, sorting according to rainfall and temperature responses would show how models fall into a set of discrete future climate scenarios, framed in terms such as: *much drier and slightly warmer, much wetter and slightly warmer, much drier and much hotter,* and *much wetter and much hotter.* This approach has been generalised and the Climate Futures web tool (Whetton et al.

2012) facilitates visualisation and categorisation of model results, and selection of datasets, that are of interest to the user. It is described in full detail in box 9.1 of CSIRO and BoM (2015).

The example presented in Fig.17 represents the changes in temperature and rainfall in the South-West region of Victoria for 2060 (years 2050–2069) under the RCP8.5 scenario. The table organises the models into groupings according to their simulated changes in rainfall (rows) and temperature (columns). The largest number of models falls into the *hotter* and *drier* category (17 of 42 global climate models and 2 out of 6 regional climate models), which could be considered the maximum consensus case. In a risk assessment context, a user may want to consider not only the maximum consensus climate, but also the best case and worst case scenarios. A water-supply manager, for example, is likely to determine from the matrix shown in Fig. 17 that the best case scenario would be a *wetter and warmer* climate (3 GCMs out of 42) and the worst case the *warmer* and *much drier* scenario (2 out of 42 GCMs). Assuming that the user has identified what futures are likely to be of interest, Climate Futures allows exploration of the numerical values for each of the models that populates such scenarios. Through this approach users can select a small subset of models from the CMIP5 ensemble to provide representative scenarios for their application, taking into consideration model spread, as well as additional information regarding model skill and the sensitivity of their application to climate change. Alternatively, the user may wish to consider a small set of scenarios defined irrespective of emission scenario or date (but with their likelihood of occurrence being time and emission scenario sensitive). This may be in circumstances where the focus is on critical climate change thresholds. This strategy is best investigated using the Climate Future Composite Matrix approach, also provided as part of the Climate Change in Australia website. As the complexity of this type of analysis increases, it is recommended that the authors of these analysis tools be consulted to ensure maximum accuracy and relevance.
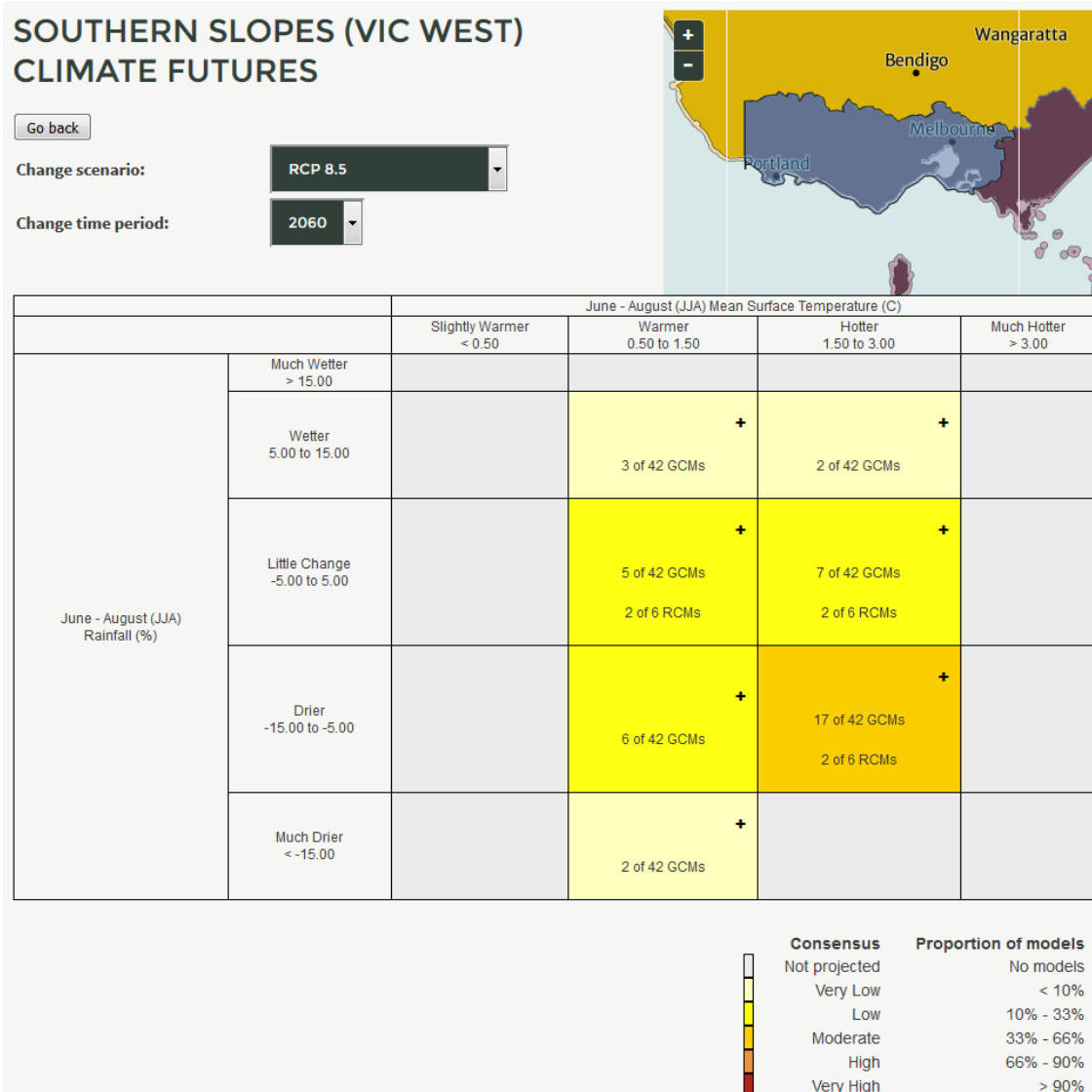
Fig. 17: An example table based on the outputs from the Climate Futures web tool showing results relevant for the South-West of Victoria when assessing plausible climate futures for 2060 under the RCP8.5 emission pathway, as defined by simulated changes in winter rainfall (% change) and temperature (°C of warming). (Source: www.climatechangeinaustralia.gov.au)

4. THE FUTURE CLIMATE OF VICTORIA

This section presents projections of climate change to the end of the 21st century for a range of climate variables of relevance to Victoria.

4.1 Temperature projections

Continued substantial warming for Victoria for mean, maximum and minimum temperature is projected with very high confidence, taking into consideration the robust understanding of the driving mechanisms of warming and the strong agreement on direction and magnitude of change amongst GCMs and downscaling results. For the near future (2030), the mean projected warming shows only minor differences between RCPs and reaches a median of around 1 °C in maximum temperatures in both the cool and warm seasons with slightly smaller increases in minimum temperatures. For late in the 21st century (2090), warming is markedly larger for RCP8.5 reaching a median of about 4 °C above the 1986–2005 level during the warm season for both maximum and minimum temperature and 3.5 °C during the cool season. In line with the mean warming, hot temperature extremes are also projected to increase while frost risk is projected to decrease.

The modelled increase in the mean temperature (averaged for Victoria) over the 20th century shows similar rates to observed trends in temperatures (Fig. 18). Daily maximum and minimum temperatures are roughly consistent with the mean warming. For the 21st century, stronger warming rates are found for the higher emission scenarios (see right-hand bars plotted in Fig. 18 and results in Table 4), as enhanced radiative forcing is directly linked to atmospheric warming. Model spread increases with time due to variation in model sensitivity to forcing.

By 2030, projections for all RCPs indicate a similar magnitude of warming, reaching a median of around 1 °C in maximum temperatures in both the cool and warm seasons with slightly smaller increases in minimum temperatures. The uncertainty in the projected warming, due to different models' sensitivity, is larger than the uncertainty due to different emission pathways. Therefore results from both RCP4.5 and 8.5 are presented together (Table 4). In contrast, by the end of the century there is clear separation between the two emissions pathways as shown in Table 4 and for all three Victorian regions. Results for the two RCP scenarios are presented separately for this time period.

The graphs in Fig. 18 show sustained warming under the high-emission scenario which by 2090 reaches a median of around 4.0 °C for both maximum and minimum temperature during the warm season and 3.5 °C during the cool season. There are some variations between minimum and maximum median values across the three regions of Victoria (see bar plots in Fig. 18). When comparing the projected warming to the spread of interannual variability estimated by the climate models (grey bars in Fig. 18), projected warming is well outside the spread of natural variability with the exception of projections for RCP2.6, and therefore it is highly significant. Daily minimum temperatures increase at a slightly slower rate than daily maximum temperatures during the cool part of the year. This is consistent with their different warming rates observed in the last 30 years (see Fig. 4).
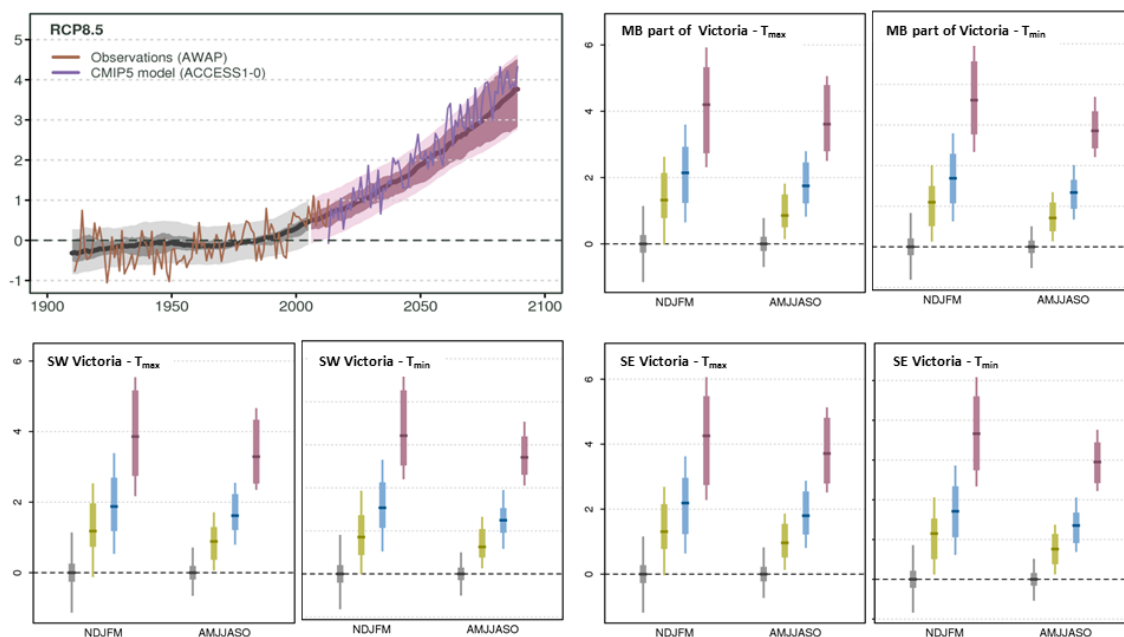
Fig. 18: Time series (top left panel) of annual average surface air temperature (°C) for Victoria from 1911 to 2090, as simulated by CMIP5 models relative to the 1950–2005 mean for the RCP8.5 scenario. The central line is the median value, and the shading is the 10th and 90th percentile range of 20-year means (inner dark) and single year values (outer light). The grey shading indicates the period of the historical simulation, while the future scenario (RCP8.5) is shown with shading in purple. Observations from the Bureau of Meteorology gridded temperature dataset (brown line) and projected values from a typical model are shown (purple line). Bar plots show the projected range for seasonal change in daily maximum and minimum temperature for 2080–99 with respect to 1986-2005 for RCP2.6 (green), RCP4.5 (blue) and RCP8.5 (purple) across the three Victorian regions (top right: Murray Basin; bottom left: South-West Victoria; bottom right: South-East Victoria). Natural climate variability is represented by the grey bars.

Included in the top left-hand graph of Fig. 18 is an example of an individual model simulation. This is included to illustrate that individual model runs produce temporal variability similar to that of observed temperature. The projected model data show individual years that are warmer or cooler than preceding years. When comparing the trajectory of warming to the spread of natural variability, the warming signal due to increased emissions appears to emerge from the natural variability around the 2050s. Here, 'emergence' means when the range of temperatures in the future moves beyond the range of current climate observations.

Table 4 shows that direct model outputs and those from the statistical downscaling of climate models are overall very consistent, with generally small differences in magnitude of the warming. The SDM results show less warming annually for the South-West region in general and less warming State-wide in the warm season. A stronger warming for maximum daily temperature and a smaller warming for daily minimum temperature exists, which is consistent with the enhanced rainfall decline projected using the SDM (see Section 4.2). The geographical distribution of mean annual temperature projected by 2090 for median warming under the high emissions scenario across the southeast of Australia including Victoria is illustrated in Fig. 19. This has both direct global climate model output and the result from the statistical downscaling of 22 of the GCMs. Under this high emissions scenario, the area with a mean temperature below

14 °C (large blue region in Fig. 19a) is reduced drastically to the high elevation alpine regions, straddling the Murray Basin and South East regions (see also topography shown in Fig. 1). Overall, the two maps of projected temperature change are fairly consistent. However, compared to the results obtained directly from GCMs, those obtained by downscaling show some small differences: a stronger temperature increase at the foothills of the Great Dividing Range (i.e. the 19 °C contour is aligned more closely to the high elevation terrain on the northern flank of the Range), and also a stronger contraction of the cool areas in the Victorian Alps. There are also small differences along the coast, most notably in the South-East region.

Taking into consideration the strong agreement on both the direction and magnitude of temperature change amongst GCMs and downscaling results, and the robust understanding of the driving mechanisms of warming and its seasonal variation, there is very *high confidence* in substantial increases for daily mean, maximum and minimum temperature for across Victoria.

T_{max}		2030		2090			
		RCP4.5 & 8.5		RCP4.5		RCP8.5	
		GCM	SDM	GCM	SDM	GCM	SDM
Cool season	MB Vic	0.5 to 1.4	0.6 to 1.5	1.2 to 2.5	1.5 to 2.1	2.8 to 4.8	3.1 to 4.7
	SW Vic	0.4 to 1.3	0.6 to 1.4	1.2 to 2.2	1.3 to 1.9	2.5 to 4.3	2.8 to 4.3
	SE Vic	0.5 to 1.4	0.6 to 1.3	1.2 to 2.5	1.6 to 2.2	2.8 to 4.8	3.3 to 4.9
Warm season	MB Vic	0.6 to 1.7	0.8 to 1.5	1.2 to 2.9	1.7 to 2.7	2.7 to 5.3	3.2 to 5.5
	SW Vic	0.5 to 1.7	0.5 to 1.1	1.2 to 2.7	1.5 to 2.4	2.7 to 5.2	2.9 to 5.1
	SE Vic	0.5 to 1.7	0.8 to 1.6	1.2 to 3.0	1.7 to 2.8	2.7 to 5.5	3.5 to 5.6

T_{min}		2030		2090			
		RCP4.5 & 8.5		RCP4.5		RCP8.5	
		GCM	SDM	GCM	SDM	GCM	SDM
Cool season	MB Vic	0.4 to 1.0	0.5 to 0.9	0.9 to 1.7	1.2 to 1.6	2.4 to 3.3	2.4 to 3.2
	SW Vic	0.3 to 1.1	0.4 to 0.8	1.0 to 1.5	1.0 to 1.5	2.3 to 3.2	2.1 to 2.7
	SE Vic	0.4 to 1.1	0.5 to 1.0	0.9 to 1.7	1.2 to 1.7	2.4 to 3.4	2.5 to 3.3
Warm season	MB Vic	0.5 to 1.3	0.5 to 1.1	1.1 to 2.3	1.1 to 1.9	2.8 to 4.6	2.4 to 3.9
	SW Vic	0.4 to 1.4	0.4 to 1.0	1.1 to 2.1	1.0 to 1.7	2.5 to 4.3	2.2 to 3.7
	SE Vic	0.5 to 1.4	0.5 to 1.2	1.1 to 2.3	1.2 to 2.0	2.7 to 4.6	2.5 to 4.2

Table 4: Projected changes in seasonal (cool season: April–October, warm season: November–March) maximum (top) and minimum (bottom) daily temperature for the 2020–2039 period (2030; RCP4.5 and RCP8.5 combined) and 2080–2099 period (2090; RCP4.8 and RCP8.5 separately) expressed in degree Celsius relative to the 1986–2005 period for the three regions of Victoria. The table compares the 10th to 90th percentile range extracted directly from 35 global climate models (GCM) to those from the statistical downscaling models (SDM) sourced from 22 of the global climate models.
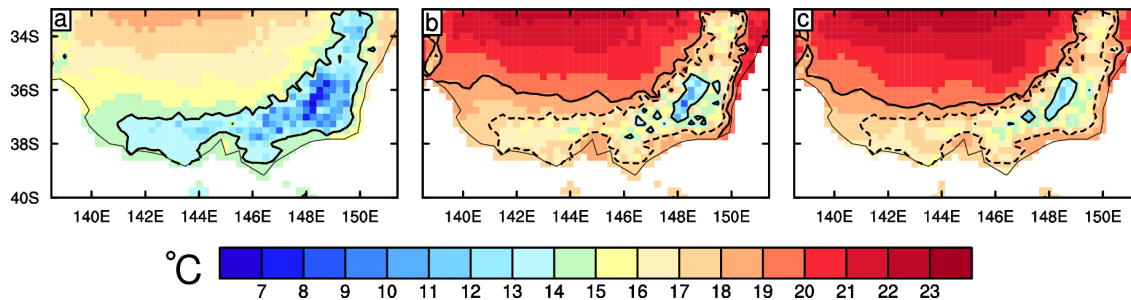
Fig. 19: Annual mean surface temperature (°C), for the present (a) and for 2090 using GCM projected warming (b) and the statistical downscaling of GCMs (c). The 15 and 20 °C contours are shown with solid black lines; in (b) and (c) the same contours from the original climate are plotted as dotted lines. Observed temperature values are based on the Bureau of Meteorology operational 5 km gridded monthly data from 1986 to 2005. The future case is using the median change at 2090 under the RCP8.5 scenario from all CMIP5 models (b) and for the 22 models for which the SDM was applied (c). Results were produced on a 5 km grid and averaged over a 0.25° grid.

Changes to temperature extremes often lead to greater impacts than changes to the mean climate. To assess these, researchers examined CMIP5 projected changes to measures such as the hottest day in the year, the return period of hottest day in a year, warm spell duration and frost risk days. In general it was found that measures of extremes, such as the hottest day in a year, are projected to increase in line with the mean warming, dependent on the period considered and the emissions scenario. To better define changes in extreme hot temperatures, several metrics can be used to quantify the magnitude, frequency and duration of maximum/minimum values of rare events. To better approximate future behaviour of heatwaves, relevant extremes can be thought of as 'extended lengths of warm spells'. This is defined as the annual count of events with at least six consecutive days with daily temperature maxima above the 90th percentile, as measured against a baseline climate. The GCM projections indicate a marked increase in the warm spell duration index through the century. The baseline is near zero, as this is a rare event in summer across Victoria. There are very large increases projected for RCP8.5 by 2090; median warming gives an increase in warm spells of 75 days compared to 1986–2005 mean for the Murray Basin cluster, and in excess of 100 days for the Southern Slopes cluster (Fig. 20).

Changes in the frequency of surface frost are of importance to agriculture, energy and other sectors, and to the environment. Assessing frost occurrence directly from GCM output is not reliable, in part because of varying biases in land surface temperatures and in part due to competing influences of temperature, mean sea level pressure and rainfall. For this report, we examined results from the 22 statistically downscaled CMIP5 models. The statistical technique has the ability to describe local temperature with minimal bias and hence it is possible to analyse the number of days with minimum temperatures below 2 °C as a proxy for the risk of frost occurrences. Average numbers of frost occurrences across the greater Murray Basin cluster are projected to decrease for all months of the annual cycle (Fig. 21) with a greater reduction by century end (2080–2099) than by 2030. It is interesting to note that spring frosts decline less rapidly than those in autumn and winter, which indicates that, when combined with advanced plant phenology due to generally warmer conditions, risks associated with late frost occurrences may not necessarily decline. This is a complex area which requires careful modelling based on individual plant phenology.
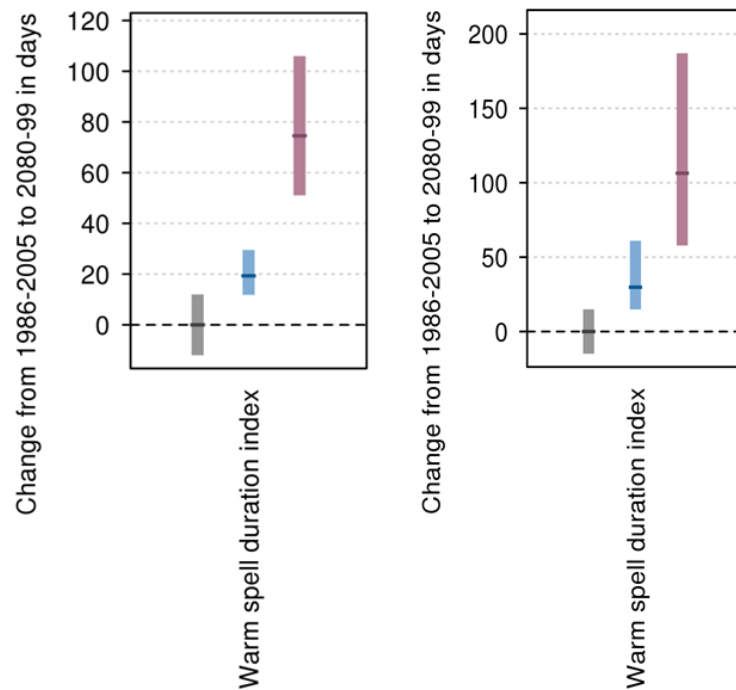
Fig. 20: Projected changes in the number of days of warm spells (see text for definition of variables) by 2090 (2080–2099) for the Murray Basin cluster (left panel) and the Southern Slopes cluster (right panel). Results are shown for RCP4.5 (blue) and RCP8.5 (purple) relative to the 1986–2005 mean. The central line is the median value, and the shading is the 10th and 90th percentile range. Natural climate variability is represented by the grey bars. (Source: Timbal et al. 2015a, Grose et al. 2015a).
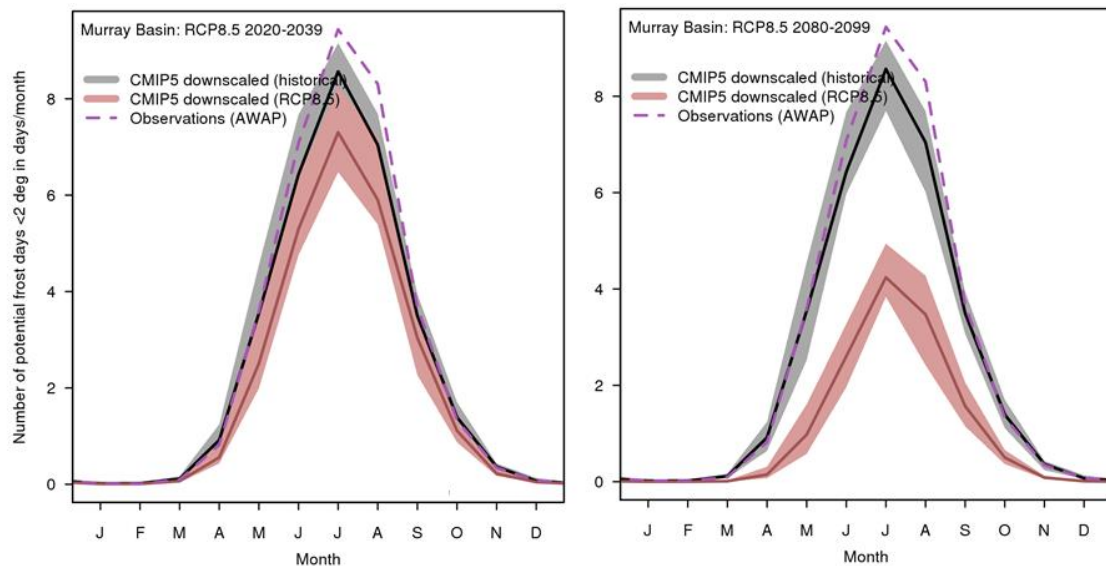
Fig. 21: Annual cycle of the number of potential frost days per month averaged over the Murray Basin cluster for two 20-year future periods shown in red, 2030 (left panel) and 2090 (right panel), as simulated by 22 statistically downscaled CMIP5 models for the RCP8.5 scenario. The central line is the median value, and the shading shows the 10th and 90th percentile range. The historical record (1950–2005) is shown by the black line and shading respectively. The observed values from the Bureau of Meteorology operational gridded dataset is shown by the dashed purple line.

4.2 Rainfall and snowfall projections

In the near term (2030), there is high confidence that natural climate variability will remain the major driver of rainfall changes from the climate of 1986–2005. Late in the century (2090) under both RCP4.5 and RCP8.5, there is high confidence that cool season rainfall will continue to decline and there is no clear leaning in the models towards either wetter or drier conditions in the warm season. Apart from the simulated direction of future changes from GCM and downscaling results, this assessment also takes into account the physical understanding of the relationship between the atmospheric circulation and rainfall across Victoria: specifically, how well the models represent this relationship, and what the projected changes in the circulation are. The understanding of physical processes coupled with high model agreement results in high confidence that the intensity of heavy rainfall events will increase. Snowfalls are projected to continue to decline for all RCPs with high confidence, particularly under RCP8.5.

Annual mean rainfall projections are shown until 2090 under RCP8.5 (time series in Fig. 22) as well as the projected percentage change averaged over 2080–2099 relative to 1986–2005 for the warm and cool seasons for three emissions scenarios (bar plots in Fig. 22). Tabulated results for two emission scenarios for 2030 and 2090 are given in Table 5 for both the direct GCM output from 35 CMIP5 models and for the statistical downscaling of 22 of those models. Under any RCP, model spread is large and the signal is not clearly separated from natural variability and systematic biases. Model spread increases with time due to compounding uncertainty, depending on different forcings and emission scenarios, and the models simulating more drying events. Hence the relatively weak long-term trend in rainfall is very difficult to separate from the effects of very large natural variability and model uncertainty, which continue during the 21st century. For the cool season, the projected drying trend is more severe and also more robust as the magnitude of the median decline increases with the severity of the emission scenarios (from RCP 2.6 to 8.5). In contrast, while the mean signal also indicates a rainfall decline during the warm season, no relationship with the severity of the emission scenarios is found, as the decline is less in the RCP8.5 pathway compared to other two mid-range scenarios, at least for the Murray Basin and South-East regions. This non-linearity between the magnitude of the climate forcing and the warm season rainfall response suggests that opposing mechanisms, acting to both increase and decrease rainfall, are at play. Therefore increased summer rainfall cannot be ruled out and several models do project an increase of warm season rainfall.

The severity of the observed rainfall decline over the last 30 years stands out as exceptional (Table 2). In comparison to the envelope of the climate model simulations of the 20th century (grey shading in top left panel in Fig. 22), it represents a very extreme case, albeit one that falls largely within the modelled range of natural variability. In comparison with the future projections, it is on par with the most extreme modelled projections by 2090 using RCP8.5. It is also interesting to note the similarity in the spatial pattern of the cool season rainfall decline. Of the three Victorian regions, the Murray Basin region experienced the largest historical decline in cool season rainfall. Declining trends are projected to be slightly larger in this region compared to the southern regions by the end of the 21st century under all three emissions scenarios (top right panel in Fig. 22). It is worth remembering that while climate models do reproduce the

changes (MMC and STR changes, see Section 3.3 on climate model evaluation) driving the observed cool season decline, they do so with a much reduced magnitude. Hence, it is possible that climate models are not as sensitive as the real climate system to the overall change in circulation impacting the region. For this reason, projected reductions in cool season rainfall may be underestimates, and the large reductions in cool season rainfall at the extreme end of the modelling results should not be discarded for planning purposes.
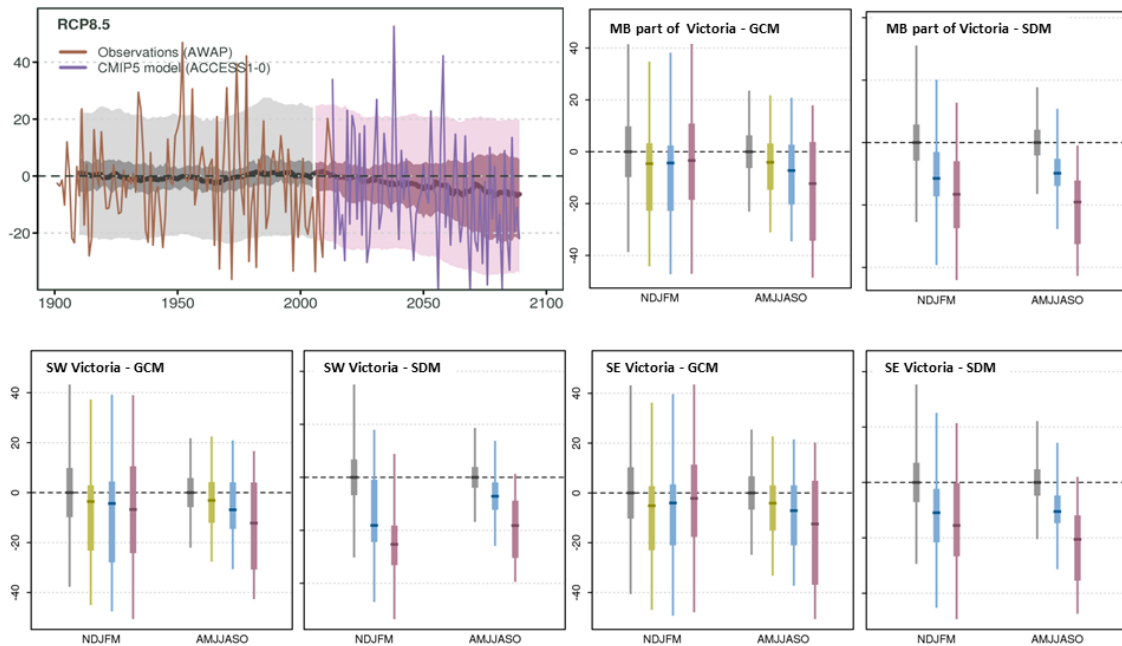
Fig. 22: Time series (top left panel) of annual average rainfall (%) for Victoria from 1900 to 2090, as simulated by CMIP5 models relative to the 1950–2005 mean for the RCP8.5 scenario. The central line is the median value, and the shading shows the 10th and 90th percentile range of 20-year means (inner dark) and single year values (outer light). The grey shading indicates the period of the historical simulation, while the future scenario (RCP8.5) is shown with purple shading. Observations from the Bureau of Meteorology operational gridded rainfall dataset (brown) and projected values from a typical model (purple) are shown. Bar plots show the projected range for mean rainfall (change in percentage term) for 2080–99 with respect to 1986–2005 for RCP 2.6 (green), RCP4.5 (blue) and RCP8.5 (purple) across the three Victorian regions (top right: Murray Basin; bottom left: South-West Victoria; bottom right: South-East Victoria) for the CMIP5 models (GCM) and for the statistical downscaling (SDM) of 22 of the CMIP5 models (only for RCP4.5 and 8.5). Natural climate variability is represented by the grey bars.

For geographical reasons, downscaling has the potential to be of benefit in further revealing spatial details in the projected climate change signal across Victoria. Using the SDM method, overall agreement is found with the thrust of the CMIP5 model projections (Fig. 22 and Table 5) for the 2080–2099 periods averaged across the three regions of Victoria. Some differences emerge due to the smaller sample of GCMs considered (22 instead of 35 GCMs for RCP8.5). For both warm and cool seasons, the rainfall decrease is enhanced using statistical downscaling of the GCMs. Furthermore, the consistency amongst the projections, in particular for the cool season, is increased, although this is partly driven by the subsampling from the CMIP5 suite of models. For example, in the case of the RCP8.5 scenario, all statistically

downscaled models project a cool season rainfall decline in the Murray Basin region (Table 5). This convergence amongst projections and increase of the severity of the projected drying when the statistical downscaling method is used, is worth remembering when considering related projections in regards to snow (later in this section) and streamflow (Section 4.5).

| | | 2030 | | 2090 | | | |
| | | RCP4.5 & 8.5 | | RCP4.5 | | RCP8.5 | |
		GCM	SDM	GCM	SDM	GCM	SDM
Annual mean	**MB Vic**	-14 to +4	-11 to 0	-18 to +2	-14 to -7	-31 to +8	-28 to -11
	SW Vic	-14 to +3	-13 to 0	-17 to +3	-15 to -5	-27 to +5	-28 to -12
	SE Vic	-15 to +4	-12 to +3	-18 to +3	-15 to -7	-34 to +8	-29 to -10
Cool season	**MB Vic**	-14 to +4	-11 to +2	-20 to +3	-14 to -5	-34 to +4	-33 to -12
	SW Vic	-13 to +3	-11 to +4	-15 to +4	-12 to -2	-31 to +4	-30 to -9
	SE Vic	-15 to +4	-12 to +4	-21 to +3	-15 to -5	-37 to +5	-35 to -12
Warm season	**MB Vic**	-16 to +10	-16 to +2	-23 to +2	-17 to -3	-19 to +11	-27 to -6
	SW Vic	-21 to +12	-20 to +1	-28 to +5	-24 to -1	-24 to +11	-33 to -18
	SE Vic	-17 to +11	-18 to +3	-21 to +4	-22 to -3	-18 to +11	-27 to 0

Table 5: GCM projected changes in rainfall for the 2020–2039 period (2030) and 2080–2099 period (2090) expressed as a percentage change relative to the 1986–2005 period for the three regions of Victoria. The table compares the 10th to 90th percentile range extracted directly from 35 global climate models (GCM) and from the statistical downscaling of 22 of these climate models (SDM). Results are given for RCP4.5 and RCP8.5 for the annual mean, the cool season (April to October) and the warm season (November to March).

Taking into account the physical understanding of the relationship between the mean meridional circulation, the subtropical ridge and rainfall across Victoria (see Section 2.1) and these projections, including the results from statistical downscaling, there is *high confidence* that cool season rainfall will decline in the future. The magnitude of this decline is, however, uncertain. In contrast, there is *little confidence* that future warm season rainfall will remain unchanged across Victoria indicating that positive or negative changes are also possible. There is also *high confidence* that natural variability will remain large relative to any anthropogenic changes, at least for the near future.

The frequency of heavy rainfall events and associated flooding is projected to increase across Victoria, despite the overall projected rainfall decline in both cool and warm seasons. In a warming climate, heavy rainfall events are expected to increase in magnitude mainly due to a warmer atmosphere holding more moisture (Sherwood et al. 2010). The CMIP5 models simulate an increase in the magnitude of the annual maximum 1-day rainfall value (i.e. the amount of rainfall that falls on the wettest day of the year) and an even greater increase in the magnitude of the 20-year return value for maximum 1-day rainfall (where a 20-year return value is equivalent to a 5% chance of occurrence within any one year) for the period 2080–2099 relative to the baseline period 1986–2005 (Fig. 23). The magnitudes of the changes in extreme rainfall are strongly dependent on the emission scenario and time into the future. Comparing the trends in the two extreme indices with that of annual mean rainfall (Fig. 23), it is evident that

while the projections for mean rainfall are decreasing, the rainfall extremes are projected to increase. The magnitude of this increase in heavy rainfall events is more clearly differentiated from natural variability than is the case for average rainfall. This pattern (change in extremes relative to the mean) is consistent across Australia (CSIRO and BoM 2015).

During part of the cool season the higher altitude mountains of Victoria are snow-covered. The long-term prospects for snow cover have implications for the tourism industry, natural resources management, and the seasonality and magnitude of streamflow from high elevation catchments. The spatial resolution of GCMs is too coarse to represent snow-covered areas in the Australian Alps directly. The highest elevation in most CMIP5 models for grid boxes in southeastern Australia representative of the Australian Alps is between 450 m and 650 m; hence no CMIP5 model can represent the snow-covered Alpine area. Projected changes in snowfall have therefore been assessed using statistically downscaled CMIP5 climate model results. Accumulated precipitation falling on days where maximum temperature stays below 2 °C has been used to create an annual total of equivalent snowfall. This has been done for two locations: a 5 km grid box (148.40°E, 35.95°S, elevation 1419 m), and the highest 5 km grid box (148.40°E, 36.15°S, elevation 1923 m). These two locations provide an insight into future changes in snowfall across a range of elevations spanning the area where snow is currently observed. At these two locations (Fig. 24), simulated snowfall showed a decline in the last 50 years, in agreement with the decline in snow accumulation observed at several locations across the Victorian (Fiddes et al. 2015) and NSW (Davis 2013) Alps. A decline in the frequency of the smaller daily snowfall events (under 10cm) across the Victorian Alps in the last 25 years has been observed (Fiddes et al. 2015).
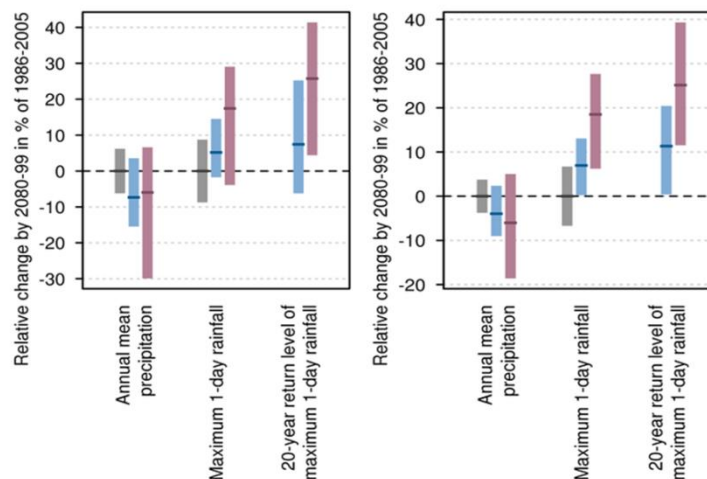
Fig. 23: Projected changes in mean rainfall, the magnitude of the annual maximum 1-day rainfall and the magnitude of the 20-year maximum return value for the 1-day rainfall, for 2090 (see text for definition of variables) for the Murray Basin cluster (left panel) and the Southern Slopes cluster (right panel). Relative rainfall anomalies are given as a percentage relative to the 1986–2005 mean for the RCP4.5 (blue) and RCP8.5 (purple) scenarios. The central line is the median value, and the shading is the 10th and 90th percentile range. Natural climate variability is represented by the grey bars. (Source: Timbal et al. 2015a, Grose et al. 2015a).
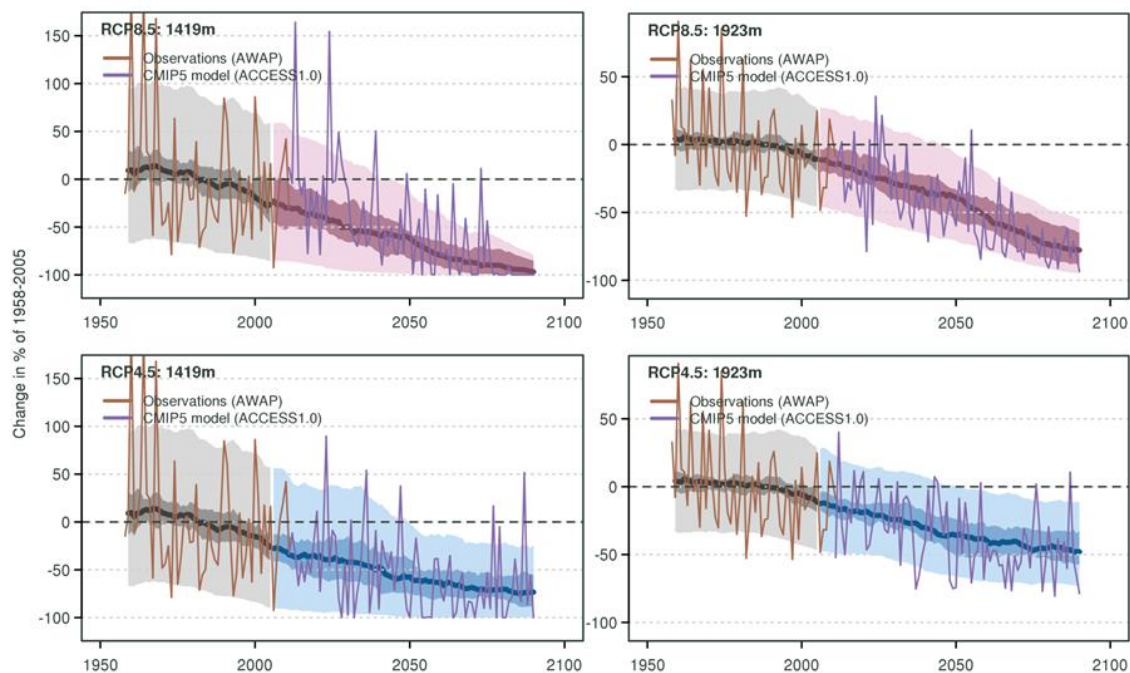
Fig. 24: Change in snowfall for two grid boxes in the Bureau of Meteorology operational 5 km gridded observations, corresponding to a lower alpine elevation consistent with the current snowline (left panels) and for the highest elevation in the gridded observations (right panels). Future projections are provided from 2006 onward for the RCP8.5 (top row) and RCP4.5 (bottom row) scenarios. Each panel shows the model ensemble median (thick line), the 10th and 90th percentile of annual snowfall (light shading) and the 10th and 90th percentile of the 20-year mean snowfall (dark shading), operational 5 km gridded observations (brown line) and an example of a possible future time series (light purple) from a single model (ACCESS-1.0). (Source: CSIRO and BoM 2015)

Projections clearly show a continuing reduction in snowfall during the 21st century. The magnitude of decrease depends on the altitude of the region and on the emission scenario. At the lower alpine elevation grid box (1419 m), years without snowfall start to be observed from 2030 in some models. By 2090, these years become common with RCP8.5. Fig. 24 displays the result from a single downscaled model (ACCESS 1.0) illustrating how this model depicts interannual variability of snowfall. It highlights the fact that with RCP4.5, while years without snowfall will become possible, years with normal snowfalls (by today's standard) still occur at the end of the 21st century but less frequently. At the high alpine elevation grid box (1923 m), the reduction of snowfall is less in percentage terms, averaging about 50% by 2090 with RCP4.5 and 80% with RCP8.5. The reduction in simulated snowfall is primarily due to warming rather than a decline in precipitation, i.e. an increase in the ratio of rain to snow, and is in agreement with previous snow simulations (Bhend et al. 2012). Fiddes et al. (2015) suggest that extreme snowfall events, when accompanied by cold air out-breaks, will continue under warming scenarios. These projections are for snowfall only, and exclude the additional impacts of climate change on snow-melt and ablation. Hence the full picture in terms of snow depth, area and duration of cover is not available.

4.3 Mean sea level pressure and circulation changes

Rainfall changes will be driven by changes in general atmospheric circulation, in particular a broadening of the mean meridional circulation, and accompanying changes in mean sea level pressure (MSLP). MSLP over southern Australia is projected to increase with high confidence, mostly during the cool season; this is driven by an increase in the strength of the well-known belt of high pressures, the subtropical ridge, and a shift of this ridge southward consistent with the observed trend over the last 30 years. As climate models tend to underestimate the rainfall response to changes in the position and intensity of the subtropical ridge, these models may underestimate the projected rainfall decline in the cool season. Other large-scale drivers (e.g. ENSO and SAM) are also projected to change and impact future rainfall projections.

As discussed earlier, changes in mean sea level pressure (MSLP) are important as they relate to rainfall change across Victoria, in particular during the cool season when the intensity of the subtropical ridge (STR) has a strong influence on regional rainfall. Across southern Australia (which includes the area where the STR is measured) annual mean MSLP is projected to increase, reaching 1 hPa by 2090 for the RCP8.5 scenario (time series in Fig. 25). Based upon results for the Murray Basin cluster, the projected annual mean change is made up of a small increase during the warm season and a large increase during the cool season (bar plot in Fig. 25). The cool season is the time of the year where the relationship between the STR intensity and rainfall in Victoria is important. For 2090, there is *high confidence* in the direction of the change, but the increase is gradual during the 21st century and its magnitude depends on the emission scenario.

A separate analysis of the CMIP5 projections of the STR confirms that most climate models project an increase in the intensity of the STR, depending on the magnitude of the projected warming (Grose et al. 2015b). The STR is projected to strengthen and move poleward under RCP8.5, a result that is highly consistent among all the climate models examined (Fig. 26). There is a greater emphasis on an increase in intensity of the ridge rather than a shift in position in CMIP5 (Grose et al. 2015b) compared to CMIP3 (Kent et al. 2013). An intensification of the STR is expected to be associated with a reduction in rainfall, and is therefore consistent with the CMIP5 model projections of a reduction of rainfall for the cool season from April to October across Victoria (see Section 3.3). However, there is a large range in the magnitude of projected reductions, and the poor simulation of the connection between the STR and rainfall in the current climate suggests that the projected rainfall decline may be underestimated under RCP8.5. A simple linear analysis using the observed relationship between STR changes and rainfall to interpret the STR changes simulated by the climate models, suggests that the underestimation could be around 4% in the multi-model mean but more for some single models. The underestimation of recent trends in the intensity of the STR-I (see Section 3.3) by models also suggests that the projected decrease in rainfall by the CMIP5 GCMs may be underestimated. The intensification and poleward shift of the STR is consistent with the observed trend in the last 30 years and the observed broadening of the MMC (see Section 2.1).
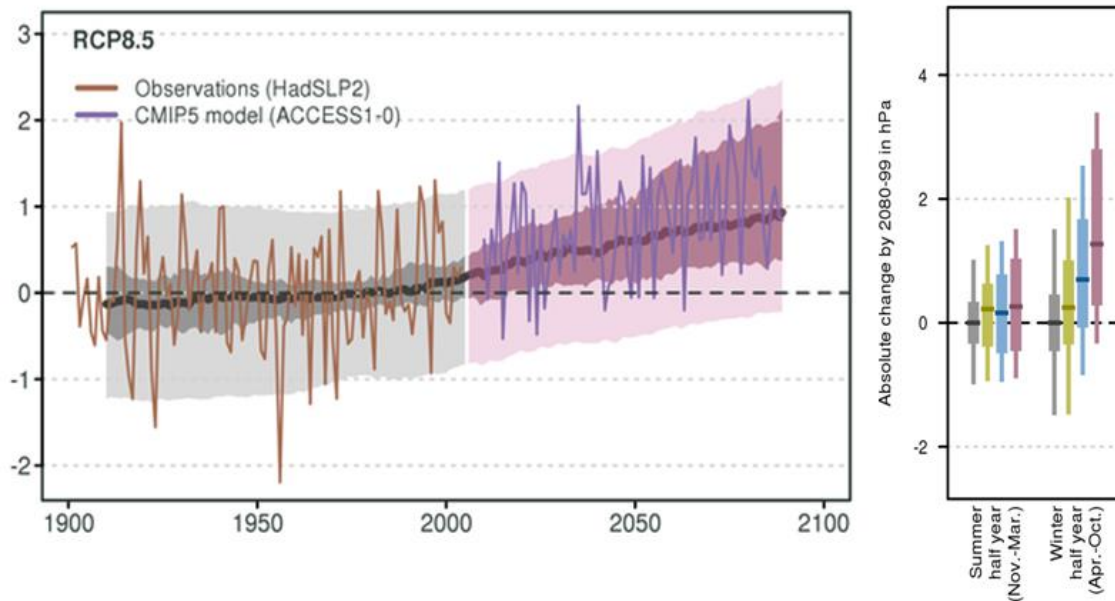
Fig. 25: Time series for the Murray Basin cluster annual average MSLP (hPa), as simulated by CMIP5 models relative to the 1950–2005 mean for RCP8.5 (left). The central line is the median value, and the shading shows the 10th and 90th percentile range of 20-year means (inner dark) and single year values (outer light). The grey shading indicates the period of the historical simulation, while the future scenario is shown with purple shading. HadSLP2 observations are shown in brown and projected values from a typical model are shown into the future in purple. Bar plots (right) show seasonal changes (hPa) for southern Australia (from Western Australia to South-Eastern Australia) for 2080–2099 with respect to 1986–2005 for RCP2.6 (green), RCP4.5 (blue) and RCP8.5 (purple). The central line is the median value, and the shading is the 10th and 90th percentile range. Natural climate variability is represented by the grey bars. (Source: Timbal et al. 2015a)
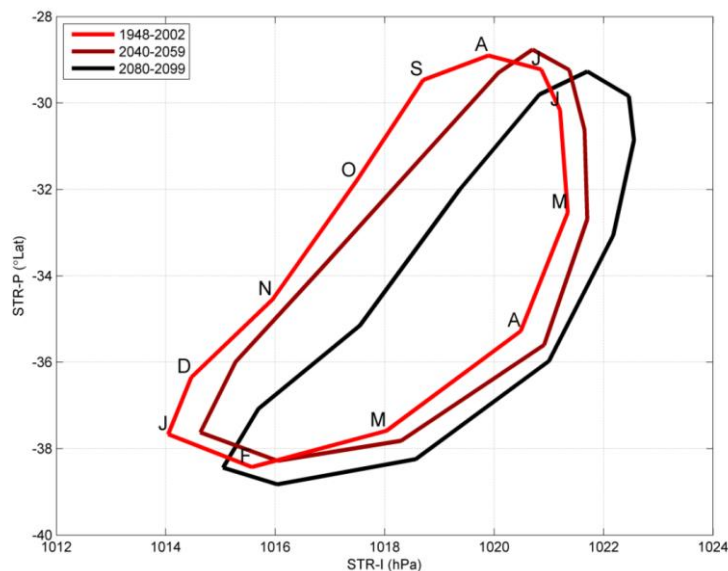
Fig. 26: GCM simulations of the annual cycle of STR intensity (STR-I) and position (STR-P) for the historical period (1948–2002; light red) and for the middle (2040–2059; dark red) and end (2080–2099; black) of the 21st century under the RCP8.5 scenario. Months are denoted by their initial letter. (Source: Grose et al. 2015b).

Grose et al. (2015b) also noted that there is a relationship between the ability of models to reproduce the STR and rainfall projections for some areas along the Australian eastern seaboard; this finding is relevant for the South-East region of Victoria. Models in which the main longitudinal band of the STR is shifted west appear to generate much drier future projections for the eastern seaboard (Grose et al. 2015b). This is worth considering when selecting particular climate models for impact studies.

Other large-scale climate features of relevance to Victorian climate (as discussed in Section 2) have been extensively studied. Future climate projections indicate a consensus amongst models toward a further broadening of the MMC (IPCC 2013). The IPCC report (Chapter 12 in IPCC, 2013) also concluded that 'there is *high confidence* that the El Niño-Southern Oscillation will remain the dominant mode of year-to-year variability in the tropical Pacific, with global effects in the 21st century. Due to the increase in moisture availability, ENSO-related precipitation variability on regional scales will likely intensify. Natural variations of the amplitude and spatial pattern of ENSO are large and thus confidence in any specific projected change in ENSO and related regional phenomena for the 21st century remains low'.

Additionally, more recent work concluded that global warming will intensify El Niño-driven drying in the western equatorial Pacific and further increase El Niño driven rainfall increases in the central and eastern Pacific during El Niño events (Power et al. 2013, Cai et al. 2014). In the Indian Ocean, the overall frequency of IOD events (positive and negative) is not projected to change (Ihara et al. 2008, IPCC 2013). Changes in the Southern Annular Mode (SAM) have exhibited a positive trend in southern summer and autumn (Marshall 2007, Jones et al. 2009a), a change attributed to the effects of ozone depletion and the increase in greenhouse gases (Thompson et al. 2011, IPCC 2013). While stratospheric Ozone is projected to recover, greenhouse gas increases will be the principal driver of SAM changes into the future (assessed as likely in chapter 14 in IPCC 2013).

4.4 Wind and weather systems

Changes in mean and extreme wind are uncertain. Mean wind is likely to decrease during the cool season while increased occurrence of intense frontal systems with abrupt wind 'changes' during the warm season are possible.

For 2030, changes in wind speed are projected with *high confidence* to be small under all RCPs (± 5%) (not shown). By 2090 under RCP4.5 and RCP8.5, there is an indication in the model results of decreased wind speed in winter (see Timbal et al. 2015a and Grose et al. 2015a for details). This aligns with changes in atmospheric circulation already discussed and is of *medium confidence*. Small or inconsistent changes are present in the other seasons. Overall, no large changes in surface wind are expected across the State, except in winter.

Changes in extreme winds are likely to be more important for impact studies than mean wind. Summer extreme winds occur primarily due to intense cold fronts and thunderstorms. In that season, the interactions between frontal systems and the continent are markedly different than during the cool season due to a stronger thermal contrast between the land and the ocean. For

example, using a selection of CMIP3 models, Hasson et al. (2009) found that intense frontal systems affecting southeastern Australia, associated with extreme winds and dangerous fire, will increase strongly by end of the 21st century, although this increase is strongly affected by the emission scenario. As these fronts tend to have the greatest impact on the western part of the State these findings are most relevant for the South-West and Murray Basin regions. For the South-East region changes in extreme winds are more likely to be related to any change in ECLs. Studies in the literature suggest a continuation of the observed decreasing trend in ECLs since the 1970s (Speer 2008), with a reduction of about 30% of ECL formation in the late 21st century compared to the late 20th century (Dowdy et al. 2013b) based on an analysis of CMIP5 models. While the number of cut-off lows may reduce, there is some indication that their average intensity may increase (Grose et al. 2012).

4.5 Changes in the hydrological cycle

Important changes are projected in the hydrological cycle. Linked to the rainfall projections, there is medium confidence that the time spent in meteorological drought, and the frequency of extreme droughts, will increase over the course of the century under RCP8.5. Beside the changes in rainfall and temperature, changes in other variables will also contribute to changes in the hydrological cycle. Small changes are projected for solar radiation and relative humidity by 2030 with clear increases seen by 2090. In particular, an increase in solar radiation is linked to reduced cloud cover and rainfall decline in conjunction with a decrease in relative humidity. Potential evapotranspiration is projected to increase in all seasons. As a result, soil moisture and runoff are projected to decrease with medium confidence.

One important consequence of the projected change in key climate variables (temperature, rainfall and wind) is a follow-on effect on the frequency, duration and severity of droughts. Drought in general means acute water shortage. The primary cause of any drought is a lack of rainfall over an extended period of time, resulting in a water shortage for some activities, groups, or sectors. The response of different entities (e.g. agricultural and hydrological systems) to water shortage conditions varies substantially as a function of time scale and socio-environmental conditions.

To assess the implications of projected climate change for drought occurrence, the Standardised Precipitation Index (SPI) was selected as a measure of meteorological drought (McKee et al. 1993, Lloyd-Hughes and Saunders 2002). This index is based solely on rainfall. More details on the calculation of the SPI can be found in the Technical Report for the National Climate Change Projections (CSIRO and BoM 2015). The projected change in the percentage time spent in drought, as well as the projections for the duration and frequency for extreme drought, are shown in Fig. 27 for the two NRM clusters overlapping with the Victorian regions. The proportion of time spent in any category of drought (from mild to extreme) is projected to increase through the century, especially by 2090 under RCP8.5. This result is associated with the projected decline in annual and cool season rainfall, although changes in rainfall variability may contribute. The duration and frequency of droughts in the extreme category are also projected to increase, with smaller changes in lower categories. Median projections are similar for the two clusters north and south of the Great Dividing Range; the range of projections is larger for the Murray Basin cluster, potentially leading to very large increases in extreme

drought duration as well as possible decreases. Because the projections of meteorological drought depend on projections of mean rainfall, the direction of any change in drought is typically the same as that of the mean annual rainfall, although they also reflect changes in variability. There is some indication that ENSO events, which have a strong influence on Victorian rainfall (Section 2.2), will have an increased influence over western equatorial Pacific Ocean under global warming (Power et al. 2013) leading to a possible intensification of El Niño related droughts over Victoria.

Surface water availability across Victoria is affected by more than rainfall, temperature and wind changes, discussed in Sections 4.1, 4.2 and 4.4. Changes in incoming solar radiation will affect the energy budget and partitioning across the landscape, leading in turn to changes in humidity at the surface, evapotranspiration and subsequently soil moisture, runoff across the landscape and streamflow. Projecting these changes requires methodologies able to resolve these finer scale processes.
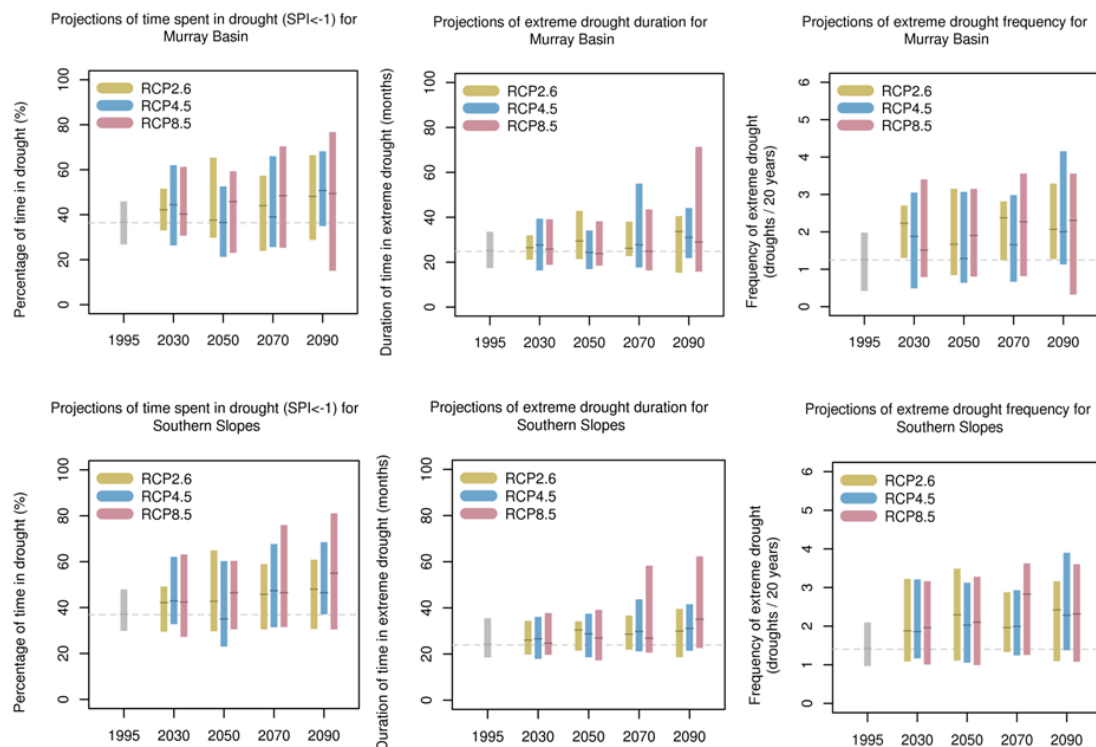
Fig. 27: CMIP5 simulated changes in drought based on the Standardised Precipitation Index (SPI) for the Murray Basin cluster (top panels) and the Southern Slopes cluster (bottom panels). The multi-model ensemble results show the percentage of time in drought (i.e. for SPI less than –1) (left panels), duration of extreme drought (middle panels) and frequency of extreme drought (right panels) for each 20-year period centred on 1995, 2030, 2050, 2070 and 2090 under RCP2.6 (green), RCP4.5 (blue) and RCP8.5 (purple). Natural climate variability is represented by the grey bars. See CSIRO and BoM (2015), chapter 7.2.3 for definition of drought indices. (Source: Timbal et al. 2015a, Grose et al. 2015a).

The CMIP5 models project small changes in radiation (in general less than 5%) for all RCPs considered (RCP2.6, RCP4.5 and RCP8.5) to 2090 across southeast Australia (Fig. 28). The largest projected mean change is up to 7% for the Murray Basin cluster for RCP8.5 in winter and about half that in spring; while for the Southern Slopes cluster, the projected increase is similar for winter and spring, at close to 5%. Winter and spring are the two seasons where most (but not all) models tend to agree on an increase. Projected changes in summer and autumn are smaller with models showing both increases and decreases (Fig. 28, left panels). As expected, the strongest trend is found in the seasons where the largest rainfall decline is projected. It is worth noting that an Australia-wide model evaluation suggested that some models are not able to adequately reproduce the climatology of solar radiation (Moise et al. 2015). Globally, CMIP5 models appear to underestimate the observed trends in some regions due to underestimation of aerosol direct radiative forcing and deficient aerosol emission inventories (Allen et al. 2013). Taking this into account, we have *high confidence* in increased winter and spring radiation projections by 2090.

Relative humidity depends on the absolute amount of moisture in the atmosphere and the ambient temperature and pressure. For example, for the same absolute amount of moisture, an atmosphere with higher temperature will have a lower relative humidity compared to a cooler atmosphere. For this reason, without circulation changes, absolute atmospheric moisture is expected to increase with global warming but relative humidity will decrease. Across Victoria, the magnitudes of the projected decreases in relative humidity depend on the emission scenario and are modulated by the direction of the rainfall projections (Fig. 28, middle panels). By 2090, mean decreases are up to 5% in spring for the Murray Basin cluster, and close to 3% for the Southern Slopes cluster; the mean projected decrease is larger for spring than for winter, and for these two seasons most models agree on the direction of the change consistent with the rainfall and radiation projections. In contrast, projected changes in summer and autumn are smaller, with models showing both increases and decreases. In all seasons, there are, however, models that simulate increases in relative humidity, as evident by large positive 90th percentile values. Climate models have a reasonable ability to simulate the climatology of global humidity, and we conclude that for winter and spring there is *high confidence* for substantial decrease while for summer and autumn there is *medium confidence* in a small decrease.

Amongst the various possible measures of evaporation, this report uses Morton's wet-environmental potential evapotranspiration, which is a derived measure of potential evaporation and transpiration demand assuming a wet environment (McMahon et al. 2013). This measure combines inputs of air temperature, relative humidity and downward solar radiation at the surface. Overall, the Morton method compares favourably with other methods used to calculate potential evaporation in rainfall-runoff modelling (Chiew and McMahon 1991) and is strongly correlated to pan evaporation observations (Kirono et al. 2009). With increasing temperatures due to global warming and an intensified hydrological cycle, potential evapotranspiration is generally expected to increase. For Victoria, projected seasonal changes for potential evapotranspiration relative to the 1986–2005 baseline period are shown for the end of the 21st century (Fig. 28, right panel). Climate models strongly agree on an increase of wet-environment potential evapotranspiration across all seasons. The increases are similar in both clusters (Murray Basin and Southern Slopes) with the largest increases in percentage terms for winter (20–25%) and 10–15% in the other seasons. As potential evaporation is much larger during the warm part of the year, in absolute terms, the largest increases in potential evaporation are found

in summer and autumn, with smaller increases in winter and spring. Although there is *high confidence* in an increase, there is only medium confidence in the magnitude of this change.
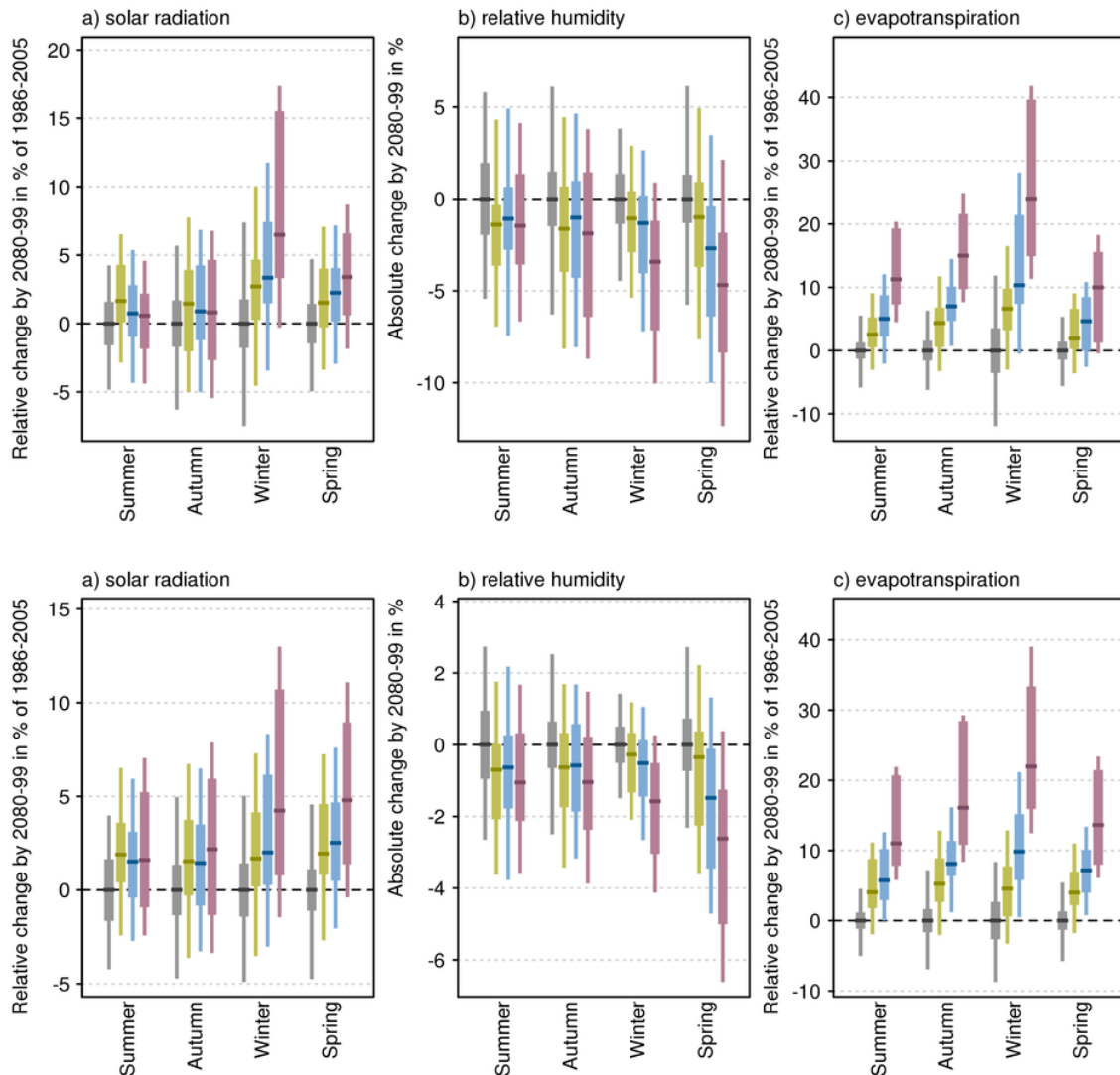
Fig. 28: Projected changes by 2090 in (a) solar radiation (%), (b) relative humidity (%, absolute change) and (c) wet-environmental potential evapotranspiration (%) for the Murray Basin cluster (top panels) and the Southern Slopes cluster (bottom panels). The bar plots show seasonal projections with respect to the 1986–2005 mean for RCP2.6 (green), RCP4.5 (blue) and RCP8.5 (purple). Natural climate variability is represented by the grey bars. (Source: Timbal et al. 2015a, Grose et al. 2015a).

As a consequence of the changes in surface temperature and rainfall projected across Victoria, the land surface partitioning of energy and moisture is projected to change as was described for solar radiation, humidity and evapotranspiration across Victoria. In turn a reduction in soil moisture, runoff and streamflow is expected. However, soil moisture, runoff and streamflow are difficult to simulate. This is particularly true in climate models where, due to their relatively coarse resolution, the models cannot simulate much of the rainfall detail that is important to many hydrological processes. For these reasons, additional tools were used to provide these projections.

As a first estimate, hydrological models were forced by CMIP5 simulated rainfall and potential evapotranspiration to derive a soil moisture estimate based on an extension of the Budyko framework (Zhang et al. 2008) as a part of the NRM reports. The projected seasonal soil moisture changes across Victoria for 2090 are summarised in Fig. 29 (left panels) for the Murray Basin (top panels) and the Southern Slopes (lower panels) NRM clusters. Decreases dominate, particularly in winter and spring and are largest for RCP8.5. The annual mean changes for the high emission scenario range from around −1 to –10%. The largest declines are projected for the Murray Basin cluster in winter and spring. In summer and autumn where the mean decline is smaller, larger values are projected for the Southern Slopes cluster compared to the Murray Basin cluster. Consistent with the directly simulated surface moisture, the percentage changes in soil moisture are strongly influenced by those in rainfall, but tend to be more negative due to the increase in potential evapotranspiration.
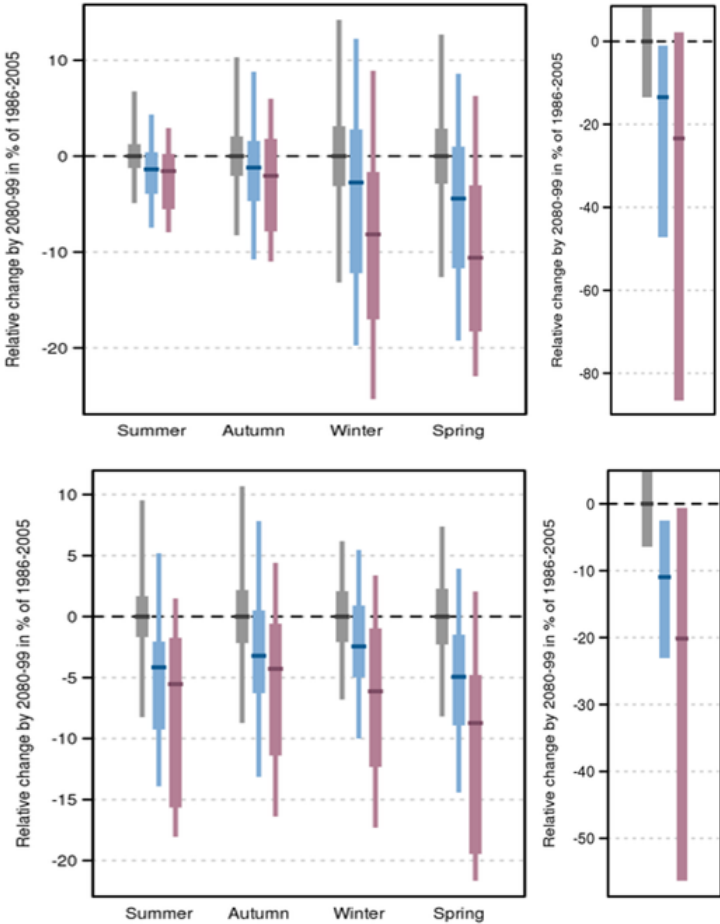
Fig. 29: Projected change in seasonal soil moisture (left) and annual runoff (right) (Budyko method—see text) for the Murray Basin cluster (top panels) and the Southern Slopes cluster (bottom panels). Anomalies are given for 2080–2099 in percentage term with respect to the 1986–2005 mean for RCP4.5 (blue) and RCP8.5 (purple). Natural climate variability is represented by the grey bars. (Source: Timbal et al. 2015a, Grose et al. 2015a).

Runoff was also derived from the long-term annual water and energy balance using the Budyko framework (Teng et al. 2012) and is presented as change in 20-year averages. Projected runoff is inferred from 30-year means of rainfall and potential evapotranspiration for each CMIP5 model for which data are available. The median and ranges for the Murray Basin cluster in the final 20-year period are shown in the right panels of Fig. 29. The median change for 2090 under RCP8.5 is a decrease of about 20% for the southern part of the State and slightly more for the Murray Basin, with the majority of models giving a decrease in both regions; it is noteworthy that these estimates have a very large uncertainty range. Despite the *high confidence* about the mean rainfall decline during the cool season, there is only low confidence in these projections. This arises because the method used is not able to consider changes to rainfall intensity, seasonality and changes in vegetation characteristics, which are all factors that could impact future runoff. More detailed runoff and streamflow projections for Victoria are being prepared as part of the Victorian Climate Initiative and will be reported separately.

4.6 Change in bushfire risk

There is high confidence that climate change will result in a harsher fire-weather climate regime in the future. However, there is only low confidence in the magnitude of the projected change to fire weather, as this depends on rainfall projections and their seasonal variation. The summer rainfall increase projected by some climate models, if it eventuates, would moderate the number of severe fire-weather days, although there is very little confidence about this projection.

Change in bushfire risk is assessed using three CMIP5 models, chosen to provide a wide spread of results across Victoria. Using a method similar to that of Hennessy et al. (2005), monthly-mean changes to maximum temperature, rainfall, relative humidity and wind speed from these models are applied to observation-based high-quality historical fire-weather records (Lucas 2010). A period centred on 1995 (i.e. 1981–2010, the last 30 years of existing observations when that study was completed) serves as the baseline. These records are modified using the changes from the three models for two 30-year time slices (centred on 2030 and 2090) and the RCP4.5 and RCP8.5 emission scenarios; more details on the methodology used are provided in CSIRO and BoM (2015). In Victoria, significant fire activity occurs primarily in areas characterised by forests and woodlands; fuel is abundant and the 'weather switch', well-characterized by FFDI, is key to fire occurrence (see Section 1.3 for details).

Five stations are used to describe the spatial changes of fire risk across Victoria: Mt Gambier (in South Australia but close to the western border of the State), Mildura, Laverton, Melbourne Airport and East Sale (all are shown in Fig. 1); and an average of these five stations is provided. It should be noted that, as large parts of the State—including all the Alpine regions—are not covered, it should not be regarded as a State average. Focusing on the 2030 and 2090 time slices, the results indicate increased fire-weather risk in the future (Table 6). Across the State, the sum of all daily FFDI values over a year is broadly indicative of general fire-weather risk. This index increases by about 10% by 2030, about 15% under RCP4.5 by 2090, and 35% under RCP8.5 by 2090. The number of days with a 'severe' fire danger rating increases by about 30% by 2030, and by 30–60% with RCP4.5 to 85–185% with RCP8.5 by 2090.

| Station | 2030 | | 2090 | | | |
| | RCP4.5 and 8.5 | | RCP4.5 | | RCP8.5 | |
	Change in mean annual cumulative FFDI	Change in number of days per year with FFDI > 50	Change in mean annual cumulative FFDI	Change in number of days per year with FFDI > 50	Change in mean annual cumulative FFDI	Change in number of days per year with FFDI > 50
Melbourne Airport	10.7%	24%	13.7%	36%	35.7%	84%
Laverton	9.7%	22%	12.6%	33%	35.9%	114%
Mt Gambier	11.0%	30%	17.4%	56%	40.4%	94%
Mildura	7.9%	30%	12.3%	42%	25.0%	186%
East Sale	7.3%	33%	14.6%	56%	35.0%	123%
Station average	9.3%	28%	14.1%	45%	34.4%	120%

Table 6: Changes in FFDI characteristics expressed in percentage terms relative to the reference (1980–2010) period for future time-slices (2020–2040 and 2080–2100) under the RCP4.5 and RCP8.5 scenarios for mean annual cumulative FFDI and the number of days per years of severe FFDI (above 50). These results are an average across three climate models. For 2030, results for RCP4.5 and RCP8.5 were combined.

Table 6 depicts the spatial variability of fire risk across the State. Fire risk is largest by 2090 with the higher emission scenario; but the changes in percentage terms are rather different across the five locations due to diverse baseline fire climate risk (see Section 1.3). Considerable variability in the projections is driven by the choice of models for this analysis (not shown). While projected temperatures show some variation, rainfall variability is particularly large. On the whole, the wetter models show smaller increases in fire weather—in particular for those models that indicate an increase of warm season rainfall. This reflects the interplay between the variables influencing fire danger. The higher summer rainfall acts to moisten the fuel (captured by the lower drought factor—one of the variables used in the FFDI) during the peak fire season, hence reducing the overall fire-weather risk in that season while potentially providing higher fine fuel growth and, thus, higher risk later in the season. In the mean, changes to relative humidity and wind speed have little influence on future fire-weather climate. In summary, there is *high confidence* that climate change will result in a harsher fire-weather climate for Victoria in the future.

4.7 Marine projections

Sea level, which has risen around Australia at an average rate of 1.4 mm/year between 1966 and 2009, is projected to continue to rise during the 21st century (very high confidence). By 2090, the projected range of sea level rise for the Victorian coastline is between 0.39 m and 0.84 m under the high emissions scenario (RCP8.5). Sea surface temperature (SST) has increased significantly across the globe over recent decades and is projected to further rise with very high confidence. Across the coastal waters of Victoria in 2090, further warming is projected in the range of 1.6 to 3.4 °C for RCP8.5. There is also very high confidence that the ocean pH is expected to decrease around Australia.

Changes in sea levels and their extremes, as well as sea surface temperatures and ocean pH (acidity) have the potential to impact both the coastal terrestrial and marine environments. This is discussed at length in chapter 8 of the Technical Report for the National Climate Change Projections (CSIRO and BoM 2015). Of particular significance for the terrestrial environment of coastal Victoria is the impact of sea level rise and changes to the frequency of extreme sea levels. Impacts will be felt through coastal flooding and erosion. For the adjacent marine environment, increases in ocean temperatures and acidity may alter the distribution and composition of marine ecosystems and impact vegetation and coastal fisheries.

Changes in sea level are caused primarily by changes in ocean density (e.g. 'thermal expansion') and changes in ocean mass due to the exchange of water with the terrestrial environment, including from glaciers and ice sheets. Sea levels have risen around the Australian coastline at an average rate of 2.1 mm/year over 1966–2009; including an accelerated rise of 3.1 mm/year over 1993–2009. Projections of future sea level changes are shown for Stony Point in Victoria (Fig. 30). The rate of sea level rise during the 21st century will be larger than the average rate during the 20th century as radiative forcing from greenhouse gas emissions continues to grow (Fig. 30). For the first decades of the 21st century the projections are almost independent of the emission scenario. The rate of rise continues to increase through the 21st century and for the RCP8.5 scenario the sea level ends up being about 30% higher than with the RCP4.5 level by 2100. Significant interannual variability will continue through the 21st century as indicated by the dotted lines in Fig. 30. These ranges of sea level rise are considered likely (at least 66% probability); however, if a collapse in the marine based sectors of the Antarctic ice sheet were initiated, these projections could be several tenths of a metre higher by late in the century (IPCC 2013). Continued increases in sea level for this location and coastal Victoria in general are projected with *very high confidence*.

In addition to mean sea level rise, impact studies need to consider that extreme coastal sea levels are exacerbated by rising sea levels and are caused by a combination of factors including astronomical tides, storm surges and wind-waves. Along the south coast of Victoria, the majority of storm surges occur in conjunction with the passage of cold fronts during the winter months (e.g. McInnes and Hubbert 2003). Using the method of Hunter (2012), it is possible to compute an allowance based on the mean sea level rise, uncertainty around the rise, and taking into account the nature of extreme sea levels along the Victorian coastline. The Technical Report for the National Climate Change Projections (CSIRO and BoM 2015) provides details on the approach and the cluster report for the Southern Slopes (Grose et al. 2015a) illustrates the application for Victorian coastal areas.

Sea surface temperatures (SSTs) have increased significantly across the globe over recent decades (IPCC 2013). Increases in SSTs pose a significant threat to the marine environment through biological changes in marine species, including local abundance and community structure. For the Victorian coastline, the range of projected SST increases from Portland in western Bass Strait to eastern Bass Strait. It also increases with time and according to the emission scenario considered. For example, in Portland, the SST warming is projected to be 0.3 to 0.8 °C by 2030 with RCP8.5, rising to 1.6 to 3.4 °C by 2090. There is *very high confidence* that sea surface temperatures will continue to rise along the Victorian coastline, with the magnitude of the warming dependent on emission scenarios.
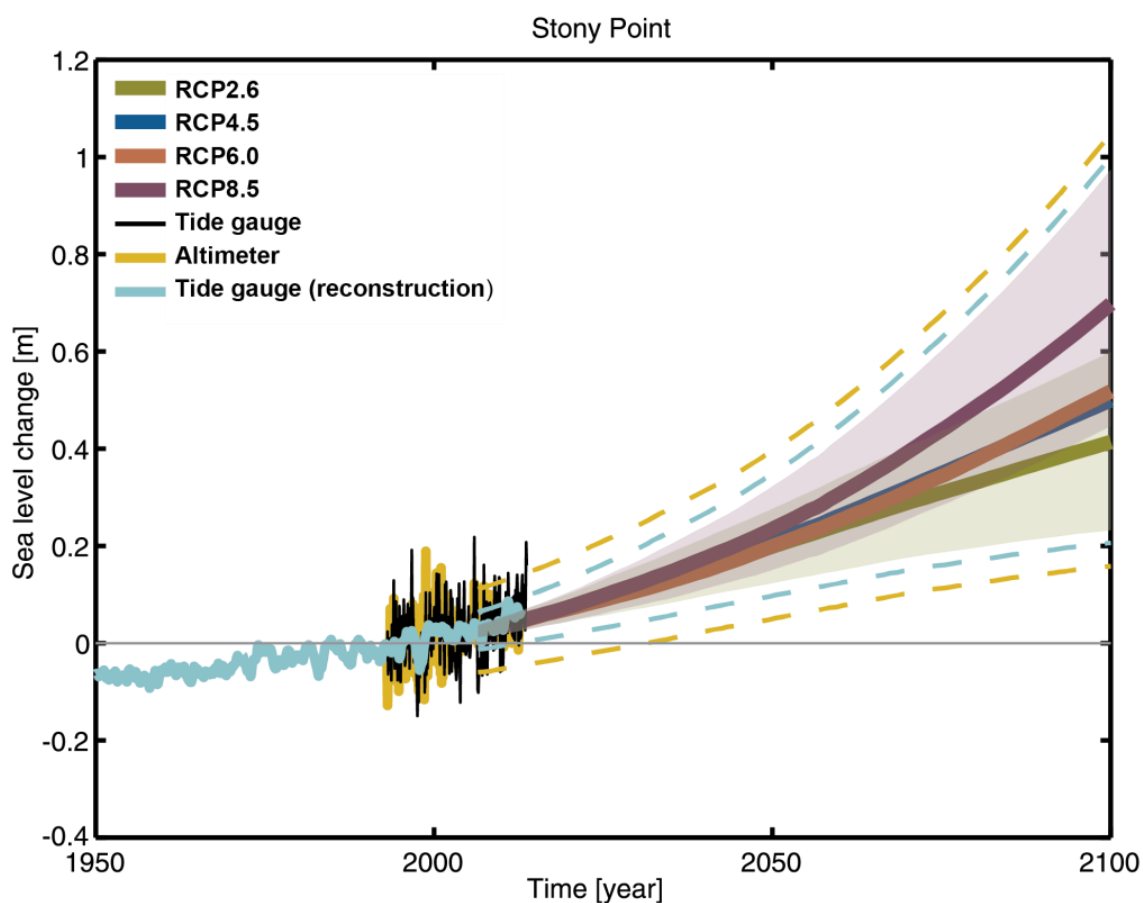
Fig. 30: Observed and projected relative sea level change (metre) relative to 1993–2010 for Stony Point, Victoria. The observed tide gauge sea level records are indicated in black, with the satellite record (since 1993) shown in mustard and the tide gauge reconstruction (which has lower variability) shown in blue. Multi-model mean projections are shown for the RCP8.5 and RCP2.6 scenarios (thick purple and olive lines) as well as RCP4.5 and RCP6.0, with uncertainty ranges shown by the purple and olive shaded regions from 2006–2100. The mustard and blue dashed lines are estimates of inter-annual variability in sea level (i.e. likely uncertainty range for the projections) and indicate that individual monthly averages of sea level can be above or below longer term averages. Note that the ranges of sea level rise should be considered likely (at least 66% probability) and that if a collapse in the marine based sectors of the Antarctic ice sheet were initiated, these projections could be several tenths of a metre higher by late in the century. (Source: Grose et al. 2015a).

Ocean salinity in coastal waters will be affected by changes to rainfall and evaporation and may impact on upwelling and mixing, and potentially nutrient supply. Changes to salinity across the coastal waters of Victoria can also be affected by riverine input. As changes in salinity are related to changes in the hydrological cycle, they are of *low confidence*.

About 30% of the anthropogenic carbon dioxide emitted into the atmosphere over the past 200 years has been absorbed by the oceans (Ciais et al. 2013). As carbon dioxide enters the ocean it reacts with the seawater to cause a decrease in pH and carbonate concentration, collectively known as ocean acidification. Ocean acidification can affect fin and shellfish fisheries, aquaculture, tourism and coastal protection. Along Victorian coastlines, by 2030 pH change is

projected to be another 0.08 units lower relative to 1986-2005; by 2090 this is projected to be up to 0.3 units lower for RCP8.5. These changes together with SST changes will affect all levels of the marine food web, and make it harder for calcifying marine organisms to build their hard shells, potentially affecting the resilience and viability of marine ecosystems. There is *very high confidence* that the ocean will become more acidic, and that the rate of ocean acidification will be proportional to carbon dioxide emissions.

5.   FURTHER INFORMATION

The climate change projections presented in this report are the most comprehensive and broadly based ever produced for the State of Victoria, complementing the report recently released as part of the national climate change projections. They also incorporate state-of-the-art understanding of the complexity of the climate system in this part of the world. These projections provide an excellent basis for impact and adaptation activities.

This has been made possible by advances in modelling and in observations, and also by the research of scientists working over the past decade on many aspects of southeastern Australia climate and associated processes, as part of both the South Eastern Australia Climate Initiative (SEACI) from 2006 to 2012, and the Victorian Climate Initiative (VicCI) since 2013. These regional science programs were established to inform water resource planning and management through improved prediction and understanding of the climate system and its representation by climate models, and to improve understanding of the linkages between climate and water availability. This strategic knowledge provides the basis for improved projections of future climate and associated water availability; in particular, it enhances knowledge of the uncertainties in future projections.

For a regional climate science program such as VicCI it is vital to be in regular communication with related programs at the national and international level. The present report is a clear example, being rooted in the development of national climate change projections delivered in 2015 (CSIRO and BoM, 2015, supported over the years by the Australian Climate Change Science Program (ACCSP), and further supported by phase 5 of the Coupled Model Intercomparison Project (CMIP5) and an increase in international scientific understanding of the global climate system, as presented in the recent reports of the IPCC (IPCC 2013).

A particular aim of VicCI is to encourage the hydrology and climate research communities to collaborate, leading to more comprehensive research outcomes. Climate is clearly the main driver of hydrology, and in turn, the needs of the hydrological community can influence the research focus of the climate community. The nexus between climatology and hydrology provides opportunities for meaningful discussion between research disciplines, leading to better informed water resource planning and management.

REFERENCES

Alexander, L., Wang, X., Wan, H. and Trewin, B. 2011. Significant decline in storminess over southeast Australia since the late 19th century. *Australian Meteorological and. Oceanographic Journal*, 61, 23–30.

Allan, R. and Ansell, T. 2006. A new globally complete monthly historical gridded mean sea level pressure dataset (HadSLP2): 1850–2004. *Journal of Climate*, 19, 5816–5842.

Allen, R. J., Norris, J. R. and Wild, M. 2013. Evaluation of multidecadal variability in CMIP5 surface solar radiation and inferred underestimation of aerosol direct effects over Europe, China, Japan, and India. *Journal of Geophysical Research-Atmospheres*, 118, 6311–6336.

Beard, G., Chandler, E., Watkins, A. and Jones, D. 2011. How does the 2010–11 La Niña compare with past La Niña events. *Bulletin of the Australian Meteorological and Oceanographic Society*, 24, 17–20.

Berry, G., Reeder, M. and Jakob, C. 2011. A global climatology of atmospheric fronts. *Geophysical Research Letters*, 38. L04809

Bhend J., Bathols J. and Hennessy K. 2012. Climate change impacts on snow in Victoria. CAWCR Report. Retrieved from:
http://www.climatechange.vic.gov.au/data/assets/pdf_file/0005/200795/
cawcr_report_on_climate change_and_Victorian_snow_final-dec12_web.pdf

Bhend, J. and Whetton, P. 2015. Evaluation of simulated recent climate change in Australia, *Australian Meteorological and. Oceanographic Journal*, 65, 4–18.

Bradstock, R. 2010. A biogeographic model of fire regimes in Australia: current and future implications. *Global Ecology and Biogeography*, 19, 145–158.

Bureau of Meteorology, 2012. Australia's wettest two-year period on record: 2020–11. *Special Climate Statement No.* 38, National Climate Centre, Bureau of Meteorology.

Cai, W., Borlace, S., Lengaigne, M., Van Rensch, P., Collins, M., Vecchi, G., Timmermann, A., Santoso, A., McPhaden, M., Wu, L., England, M., Wang, G., Guilyardi, E. and Jin, F. 2014. Increasing frequency of extreme El Niño events due to greenhouse warming. *Nature Climate Change,* 4, 111–116.

Cai, W., Van Rensch, P., Cowan, T. and Hendon, H. H. 2011. Teleconnection pathways of ENSO and the IOD and the mechanisms for impacts on Australian rainfall. *Journal of Climate*, 24(15), 3910–3923.

Chiew, F. and McMahon, T. 1991. The Applicability of Morton's and Penman's Evapotranspiration Estimates in Rainfall-Runoff Modeling. *Journal of the American Water Resources Association,* 27, 611–620.

Ciais, P., Sabine, C., Bala, G., Bopp, L., Brovkin, V., Canadell, J., Chhabra, A., Defries, R., Galloway, J., Heimann, M., Jones, C., Le Quéré, C., Myneni, R. B., Piao, S. and Thornton, P. 2013. *Carbon and Other Biogeochemical Cycles.* Contribution of Working Group I to the Fifth Assessment Report of the Intergovernmental Panel on Climate Change. In: Stocker, T. F., D. Qin, G.- K. Plattner, M. Tignor, S.K. Allen, J. Boschung, A. Nauels, Y. Xia, Bex, V. and Midgley, P. M. (eds.) Climate Change 2013: The Physical Science Basis. Cambridge, United Kingdom and New York, NY, USA: Cambridge University Press.

CSIRO. 2010. *Climate Variability and Change in South-Eastern Australia: A Synthesis of Findings from Phase 1 of the South Eastern Australian Climate Initiative (SEACI).* Retrieved from http://www.seaci.org/publications/documents/SEACI-1eports/Phase1_SynthesisReport.pdf

CSIRO. 2012. *Climate and water availability in southeastern Australia: A synthesis of findings from Phase 2 of the South Eastern Australian Climate Initiative (SEACI)*, 41. Retrieved from http://www.seaci.org/publications/documents/SEACI2Reports/SEACI_Phase2_Synthesis Report.pdf

CSIRO and Bureau of Meteorology. 2015. *Climate Change in Australia Information for Australia's Natural Resource Management Regions: Technical Report*. CSIRO and Bureau of Meteorology, Australia, 222 pp. Retrieved from http://www.climatechangeinaustralia.gov.au/

Davis, C. 2013. Towards the development of long term winter records for the Snowy Mountains. *Australian Meteorological and Oceanographic Journal*, 63(2), 303–313.

Dee, D. et al. 2011. The ERA-Interim reanalysis: Configuration and performance of the data assimilation system. *Quarterly Journal of the Royal Meteorological Society*, 137(656), 553–597.

Department of the Environment. 2013. Natural resource management (Online). Commonwealth of Australia: http://www.environment.gov.au/land/nrs/science/ibra

Dittus, A., Karoly, D., Lewis, S. and Alexander, L. 2015. An investigation of some unexpected frost day increases in southern Australia, *Australian Meteorological and Oceanographic Journal,* 64(4), 261–271.

Dowdy, A., Mills, G. and Timbal, B. 2013a. Large-scale diagnostics of extratropical cyclogenesis in eastern Australia. *International Journal of Climatology*, 33(10), 2318–2327.

Dowdy, A., Mills, G., Timbal, B. and Wang, Y. 2013b. Changes in the Risk of Extratropical Cyclones in Eastern Australia. *Journal of Climate*, 26(4), 1403–1417.

Drosdowsky, W. 2005. The latitude of the subtropical ridge over eastern Australia: The L index revisited. *International Journal of Climatology*, 25(10), 1291–1299.

Ekström M., Grose M. and Whetton, P. 2015. An appraisal of downscaling methods used in climate change research. *WIRES Climate Change,* 6(3), 301–319.

England, M., Ummenhofer, C. and Santoso, A. 2006. Interannual rainfall extremes over southwest Western Australia linked to Indian ocean climate variability. *Journal of Climate*, 19, 1948–1969.

Fawcett, R., Trewin, B., Braganza, K, Smalley, R., Jovanovic, B. and Jones, D.A. 2012. On the sensitivity of Australian temperature trends and variability to analysis methods and observation networks. *CAWCR Technical Report No. 50*, Bureau of Meteorology, Melbourne, 66 pp.

Fiddes, S., Pezza, A. and Barras, V. (2015). A new perspective on Australian snow. *Atmospheric Science Letters,* 16(3), 246–252.

Fiddes, S. and Timbal, B. 2016a. Assessment and reconstruction of catchment streamflow trends and variability in response to rainfall across Victoria, Australia. *Climate Research*, Accepted article: DOI: 10.3354/cr01355

Fiddes, S. and Timbal, B. 2016b. Future impacts of climate change on streamflows across Victoria, Australia: making use of statistical downscaling. Submitted to *Climate Research*.

Frederiksen, J., Frederiksen, C., Osbrough, S. and Sisson, J. Changes in Southern Hemisphere rainfall, circulation and weather systems. 19th International Congress on Modelling and Simulation, 2011 Perth, Australia. Modelling and Simulation Society of Australia and New Zealand, 2712–2718.

Gallant, A., Karoly, D. and Gleason, K. 2014. Consistent Trends in a Modified Climate Extremes Index in the United States, Europe, and Australia. *Journal of Climate*, 27, 1379–1394.

Grose, M., Pook, M., McIntosh, P., Risbey, J. and Bindoff, N. 2012. The simulation of cutoff lows in a regional climate model: reliability and future trends. *Climate Dynamics*, 39, 445–459.

Grose, M. et al. 2015a. *Southern Slopes Cluster Report*, Climate Change in Australia Projections for Australia's Natural Resource Management Regions: Cluster Reports, eds. Ekström, M. et al. CSIRO and Bureau of Meteorology, Australia.

Grose, M., Timbal, B., Wilson, L., Bathols, J. and Kent, D. 2015b. The subtropical ridge in CMIP5 models, and implications for projections of rainfall in southeast Australia. *Australian Meteorology and Oceanography Journal,* 65, 90–106.

Grose, M., Risbey, J., Black, M. and Karoly, D. 2015c. Attribution of Exceptional Mean Sea Level Pressure Anomalies South of Australia in August 2014. *Bulletin of the American Meteorological Society*, 96(12), S158–S162.

Guilyardi, E., Wittenberg, A., Fedorov, A., Collins, M., Wang, C., Capotondi, A. and Stockdale, T. 2009. Understanding El Niño in ocean-atmosphere general circulation models: Progress and challenges. *Bulletin American Meteorological Society*, 90, 325–340.

Hasson, A., Mills, G., Timbal, B. and Walsh, K. 2009. Assessing the impact of climate change on extreme fire-weather events over southeastern Australia. *Climate Research*, 39, 159–172.

Hendon, H., Lim, E., Arblaster, J. and Anderson, D. 2014. Causes and predictability of the record wet east Australian spring 2010. *Climate Dynamics*, 42, 1155–1174.

Hendon, H., Thompson, D. and Wheeler, M. 2007. Australian Rainfall and Surface Temperature Variations Associated with the Southern Hemisphere Annular Mode. *Journal of Climate*, 20(11), 2452–2467.

Hennessy, K., Lucas, C., Nicholls, N., Bathols, J., Suppiah, R. and Ricketts, J. 2005. *Climate change impacts on fire weather in southeast Australia.* Melbourne, Australia: Consultancy report for the New South Wales Greenhouse Office, Victorian Department of Sustainability and Environment, Tasmanian Department of Primary Industries, Water and Environment, and the Australian Greenhouse Office. CSIRO Atmospheric Research and Australian Government Bureau of Meteorology, 78 pp. Retrieved from http:// laptop.deh.gov.au/soe/ 2006/publications/drs/pubs/334/lnd/ld_24_climate_change_impacts_on_fire_weather.pdf

Hope, P., Grose, M., Timbal, B., Dowdy, A., Bhend, J., Katzfey, J., Bedin, T. and Whetton, P. 2015a. Seasonal and regional signature of the projected southern Australia rainfall reduction, *Australian Meteorological and. Oceanographic Journal*, 65, 54–71.

Hope, P., Timbal, B., Hendon, H., Ekström, M., Moran, R., Manton, M., Lucas, C., Nguyen, H., Lim, E-P., Luo, J-J., Liu, G., Zhao, M., Fiddes S., Kirono, D., Wilson, L., Potter, N. and Teng, J. 2015. Victorian Climate Initiative: Annual Report 2014–15, *Bureau Research Report No. 5*, Bureau of Meteorology, Melbourne, 128 pp.

Hunter, J. 2012. A simple technique for estimating an allowance for uncertain sea-level rise. *Climatic Change*, 113, 239–252.

Ihara, C., Kushnir, Y. and Cane, M. 2008. Warming trend of the Indian Ocean SST and Indian Ocean dipole from 1880 to 2004. *Journal of Climate,* 21, 2035–2046.

IPCC. 2001. Climate change 2001: the scientific basis. In: Houghton, J. T., Ding, Y., Griggs, D. J., Noguer, M., Van der Linden, P. J., Dai, X., Maskell, K. and Johnson, C. (eds.). Cambridge: Cambridge University Press .

IPCC. 2007. Climate change 2007—the physical science basis: Working group I contribution to the fourth assessment report of the IPCC. In: Solomon, S. (ed.). Cambridge: Cambridge University Press.

IPCC. 2013. Climate Change 2013: The Physical Science Basis. Contribution of Working Group I to the Fifth Assessment Report of the Intergovernmental Panel on Climate Change. In: Stocker, TF., Qin D. Plattner G.-K., Tignor M., Allen SK., Boschung J., Nauels A., Xia Y., Bex V. and Midgley PM. (ed.). IPCC, Geneva, Switzerland.

Jakob, D. 2010. Challenges in developing a high-quality surface wind-speed dataset for Australia. *Australian Meteorological Magazine*, 60, 227–236.

Jones, J., Fogt, R., Widmann, M., Marshall, G., Jones, P. and Visbeck, M. 2009a. Historical SAM Variability. Part I: Century-Length Seasonal Reconstructions. *Journal of Climate*, 22, 5319–5345.

Jones, D. A., Wang, W. and Fawcett, R. 2009b. High quality spatial climate datasets for Australia. *Australian Meteorological and. Oceanographic Journal*, 58, 233–248.

Kalnay, E., Kanamitsu, M., Kistler, R., Collins, W., Deaven, D., Derber, J., Gandin, L., Iredell, M., Saha, S., White, G., Woollen, J., Zhu, Y., Chelliah, M., Ebisuzaki, W., Higgins, W., Janowiak, J., Mo, K., Ropelewski, C., Wang, J., Leetma, A., Reynolds, R., Jenne, R. and Joseph, D. 1996. The NCEP/NCAR 40-year reanalysis project. *Bulletin of the American Meteorological Society*, 77, 437–471.

Kent, D., Kirono, D., Timbal, B. and Chiew, F. 2013. Representation of the Australian sub-tropical ridge in the CMIP3 models. *International Journal of Climatology*, 33, 48–57.

Kirono, D., Jones, R. and Cleugh, H. 2009. Pan-evaporation measurements and Morton-point potential evaporation estimates in Australia: are their trends the same? *International Journal of Climatology,* 29, 711–718.

Leblanc, M., Tweed, S., Van Dijk, A. and Timbal, B. 2012. A review of historic and future hydrological changes in the Murray–Darling Basin. *Global and Planetary Change*, 80–81, 226–246.

Lim, E.-P. and Hendon, H. 2015a. Understanding and predicting the strong Southern Annular Mode and its impact on the record wet east Australian spring 2010. *Climate Dynamics*, 44, 2807–2824.

Lim, E.-P. and Hendon, H. 2015b. Understanding the contrast of Australian springtime rainfall of 1997 and 2002 in the frame of two flavors of El Niño. *Journal of Climate*, 28, 2804–2822,

Lim, E.-P., Hendon, H. and Zhao, M. 2016. Inter-decadal variations in the linkages between ENSO, the IOD and south-eastern Australian springtime rainfall in the past 30 years. Submitted to *Climate Dynamics*.

Lloyd-Hughes, B. and Saunders, M. A. 2002. A drought climatology for Europe. *International Journal of Climatology*, 22, 1571–1592,

Lucas, C. 2010. On developing a historical fire weather dataset for Australia. *Australian Meteorological Magazine,* 60, 1–13.

Lucas, C., Nguyen, H. and Timbal, B. 2012. An observational analysis of Southern Hemisphere tropical expansion. *Journal of Geophysical Research-Atmospheres*, 117.

Lucas, C., Timbal, B. and Nguyen, H. 2014. The expanding tropics: a critical assessment of the observational and modeling studies. *Climate Change*, 5, 89–112.

Marshall, G. 2003. Trends in the Southern Annular Mode from observations and reanalyses. *Journal of Climate*, 16(24), 4134–4143.

Marshall, G. 2007. Half-century seasonal relationships between the Southern Annular Mode and Antarctic temperatures. *International Journal of Climatology*, 27, 1549–1555.

McArthur, A. 1967. Fire behaviour in Eucalypt forests. Leaflet. Forestry Timber Bureau Australia, 35–35.

McBride, J. and Nicholls, N. 1983. Seasonal relationships between Australian rainfall and the Southern Oscillation. *Monthly Weather Review*, 111, 1998–2004.

McGregor, J. and Dix, M. 2008. An updated description of the conformal-cubic atmospheric model. High resolution numerical modelling of the atmosphere and ocean, *Springer*: 51–76.

McInnes, K. and Hubbert, G. 2003. A numerical modelling study of storm surges in Bass Strait. *Australian Meteorological Magazine*, 52, 143–156.

McKee, T., Doesken, N. and Kleist, J. 1993. The relationship of drought frequency and duration to time scales. Proceedings of the 8th Conference on Applied Climatology, American Meteorological Society Boston, MA, 179–183.

McMahon, T., Peel, M., Lowe, L., Srikanthan, R. and McVicar, T. 2013. Estimating actual, potential, reference crop and pan evaporation using standard meteorological data: a pragmatic synthesis. *Hydrology and Earth System Sciences*, 17, 1331–1363.

McVicar, T., Roderick, M., Donohue, R., Li, L., Van Niel, T., Thomas, A., Grieser, J., Jhajharia, D., Himri, Y. and Mahowald, N. 2012. Global review and synthesis of trends in observed terrestrial near-surface wind speeds: Implications for evaporation. *Journal of Hydrology*, 416, 182–205.

Meyers, G., McIntosh, P., Pigot, L. and Pook, M. 2007. The Years of El Niño, La Niña, and Interactions with the Tropical Indian Ocean. *Journal of Climate*, 20(13), 2872–2880. DOI:10.1175/JCLI4152.1

Mills, G. A. 2005. A Re-examination of the Synoptic Mesoscale Meteorology of Ash Wednesday 1983, *Australian Meteorological Magazine*, 54, 35–55.

Murphy, B., Timbal, B., Hendon, H., Ekström, M., Moran, R., Manton, M., Lucas, C., Nguyen, H., Rikus, L., Lim, E-P., Liu, G., Zhao, M., Fiddes S., Grosse, M., Bathols, J., Kirono D. and Teng, J. 2014. Victorian Climate Initiative: Annual Report 2013–14, *CAWCR Technical Report No. 76*, Bureau of Meteorology, Melbourne, 154 pp.

Moise, A., Wilson, L., Grose, M., Whetton, P., Watterson, I., Bhend, J., Bathols, J., Hanson, L., Erwin, T., Bedin, T., Heady, C. and Rafter, T. 2015. Evaluation of CMIP3 and CMIP5 models over the Australian region to inform confidence in projections, *Australian Meteorological and. Oceanographic Journal*, 65, 19–53

Morice, C., Kennedy, J., Rayner, N. and Jones, P. 2012. Quantifying uncertainties in global and regional temperature change using an ensemble of observational estimates: The HadCRUT4 dataset. *Journal of Geophysical Research: Atmospheres* (1984–2012), 117.

Nakićenović, N. and Swart, R. (eds.) 2000. Special Report on Emissions Scenarios. A Special Report of Working Group III of the Intergovernmental Panel on Climate Change, Cambridge, United Kingdom and New York, NY, USA: Cambridge University Press.

Nguyen, H., Evans, A., Lucas, C., Smith, I., and Timbal, B. 2013. The Hadley Circulation in Reanalyses: Climatology, Variability, and Change. *Journal of Climate*, 26(10), 3357–3376.

Nguyen H., Lucas, C. Evans, A., Timbal B. and Hanson, L. 2015. Expansion of the Southern Hemisphere Hadley Cell in response to greenhouse gas forcing. *Journal of Climate*, 28, 8067–8077

Pepler, A., Timbal, B., Rakich, C. and Coutts-Smith, A. 2014. Indian Ocean Dipole Overrides ENSO's Influence on Cool Season Rainfall across the Eastern Seaboard of Australia. *Journal of Climate*, 27(10), 3816–3826.

Pook, M. J., Risbey, J. S. and McIntosh, P. C. 2012. The synoptic climatology of cool-season rainfall in the Central Wheatbelt of Western Australia. *Monthly Weather Review*, 140, 28–43

Power, S. and Colman, R. 2006. Multi-year predictability in a coupled general circulation model. *Climate Dynamics*, 26, 247-272.

Power, S., Delage, F., Chung, C., Kociuba, G. and Keay, K. 2013. Robust twenty-first-century projections of El Niño and related precipitation variability. *Nature*, 502, 541–545.

Power, S., Tseitkin, F., Torok, S., Lavery, B., Dahni, R. and McAvaney, B. 1998. Australian temperature, Australian rainfall and the Southern Oscillation, 1910-1992: coherent variability and recent changes. *Australian Meteorological Magazine*, 47(2), 85–101.

Rayner, N.A., P. Brohan, D.E. Parker, C.K. Folland, J.J. Kennedy, M. Vanicek, T. Ansell and S.F.B. Tett, 2006: Improved analyses of changes and uncertainties in sea surface temperature measured in situ since the mid-nineteenth century: the HadSST2 dataset. *J. Climate*. 19(3) 446–469

Risbey, J., Pook, M., McIntosh, P., Ummenhofer, C. and Meyers, G. 2009a. Characteristics and variability of synoptic features associated with cool season rainfall in southeastern Australia. *International Journal of Climatology*, 29, 1595–1613.

Risbey, J. S., Pook, M. J., McIntosh, P. C., Wheeler, M. C. and Hendon, H. H. 2009b. On the Remote Drivers of Rainfall Variability in Australia. *Monthly Weather Review*, 137(10), 3233–3253.

Saji, N. H., Goswami, B. N., Viayachandran, P. N. and Yamagata, T. 1999. A dipole mode in the tropical Indian Ocean. *Nature*, 401, 360–363.

Sherwood, S. C., Roca, R., Weckwerth, T. M. and Andronova, N. G. 2010. Tropospheric water vapor, convection, and climate. *Reviews of Geophysics*, 48, RG2001.

Simmonds, I. and Keay, K. 2000. Mean southern hemisphere extratropical cyclone behavior in the 40-year NCEP-NCAR reanalysis. *Journal of Climate*, 13(5), 873–885.

Simmonds, I., Keay, K. and Bye, J. 2012. Identification and Climatology of Southern Hemisphere Mobile Fronts in a Modern Reanalysis. *Journal of Climate*, 25, 1945–1962.

Sinclair Knight Merz. 2010. Developing guidelines for the selection of streamflow gauging stations. Malvern, Victoria, Australia: Sinclair Knight Merz Pty Ltd. Retrieved from: http://www.bom.gov.au/water/hrs/papers/SKM2010_Report.pdf

Speer, M. S. 2008. On the late twentieth century decrease in Australian east coast rainfall extremes. *Atmospheric Science Letters*, 9, 160–170.

Sturman, A. P. and Tapper, N. J. 2006. The weather and climate of Australia and New Zealand. 2nd edition. Oxford University Press: South Melbourne.

Taylor, K., Stouffer, R. and Meehl, G. 2012. An overview of CMIP5 and the experiment design. *Bulletin of the American Meteorological Society*, 93, 485–498.

Teng, J., Chiew, F., Vaze, J., Marvanek, S. and Kirono, D. 2012. Estimation of climate change impact on mean annual runoff across continental Australia using Budyko and Fu equations and hydrological models. *Journal of Hydrometeorology*, 13, 1094–1106.

Thompson, D., Solomon, S., Kushner, P., England, M., Grise, K. and Karoly, D. 2011. Signatures of the Antarctic ozone hole in Southern Hemisphere surface climate change. *Nature Geoscience*, 4, 741–749.

Thompson, D. and Wallace, J. 2000. Annular modes in the extratropical circulation. Part I: Month-to-month variability. *Journal of Climate*, 13, 1000–1016.

Timbal, B. and Drosdowsky, W. 2013. The relationship between the decline of Southeastern Australian rainfall and the strengthening of the subtropical ridge. *International Journal of Climatology*, 33(4), 1021–1034.

Timbal, B., Fernandez E. and Z. Li. 2009. Generalization of a statistical downscaling model to provide local climate change projections for Australia. *Environmental Modelling and Software*, 24, 341–358

Timbal, B. and Hendon, H. 2011. The role of tropical modes of variability in the current rainfall deficit across the Murray-Darling basin. *Water Resources Research*, 47(12), W00G09

Timbal, B. et al. 2015a. *Murray Basin Cluster Report,* Climate Change in Australia Projections for Australia's Natural Resource Management Regions: Cluster Reports, eds. Ekström, M. et al. CSIRO and Bureau of Meteorology, Australia

Timbal, B., Griffiths, M. and Tan, K. 2015b. Rainfall and streamflows in the Greater Melbourne catchment area: variability and recent anomalies. *Climate Research*, 63(3), 215–232.

Trewin, B. 2013. A daily homogenized temperature dataset for Australia. *International Journal of Climatology*, 33, 1510–1529.

Troccoli, A., Muller, K., Coppin, P., Davy, R., Russell, C. and Hirsch, A. 2012. Long-term wind speed trends over Australia. *Journal of Climate*, 25, 170–183.

Turner, M., Bari, M., Amirthanathan, G. and Z. Ahmad. 2012. Australian network of hydrologic reference stations - advances in design, development and implementation. *Proceedings of Hydrology and Water Resources Symposium*, 1555–1564. 2012.

Van Vuuren, D., Edmonds, J., Kainuma, M., Riahi, K., Thomson, A., Hibbard, K., Hurtt, G. C., Kram, T., Krey, V. and Lamarque, J.-F. 2011. The representative concentration pathways: an overview. *Climatic Change*, 109, 5–31.

Watterson, I. 1996. Nondimensional measures of climate model performance, *International Journal of Climatology*, 16, 379–391

Watterson, I., Hirst, A. and Rotstayn, L. 2013. A skill score based evaluation of simulated Australian climate. *Australian Meteorological and Oceanographic Journal*, 63, 181–190.

Whetton, P., Hennessy, K., Clarke, J., McInnes, K. and Kent, D. 2012. Use of Representative Climate Futures in impact and adaptation assessment. *Climatic Change*, 115, 433–442.

Zhang, L., Potter, N., Hickel, K., Zhang, Y. and Shao, Q. 2008. Water balance modeling over variable time scales based on the Budyko framework – Model development and testing. *Journal of Hydrology*, 360, 117–131.

APPENDICES

Appendix 1: Observational datasets

Several datasets are used to describe the observed climate of Victoria, its variability and long-term trends and to evaluate its representation in model simulations.

For assessment of rainfall and temperature across Victoria, the observed data are derived from the Australian Water Availability Project (AWAP) (Jones et al. 2009b). This is the current operational gridded dataset used by the Bureau of Meteorology and the data are accessible on-line. The highest resolution available for these gridded observations is a regular grid of 0.05° in latitude and longitude which approximates to a regular grid of 5 by 5 km.

Some global datasets are relied upon to derive global quantities and large-scale indices:

- Surface temperatures are from HadCRUT4, a 5 by 5 degree gridded dataset (Morice et al. 2012), used as a measure of observed global warming;

- Sea Surface Temperatures (SST) are from HadISST, a 1 by 1 degree gridded dataset (Rayner et al. 2006), from which SST indices such as those depicting ENSO variability (Niño 3, 3.4 and 4 indices), Indian Ocean variability (IOD) and the tripole index (Timbal and Hendon 2011), are computed; and

- Mean sea level pressures (MSLP) are from HadSLP2, a 5 by 5 degree gridded dataset (Allan and Ansell 2006), used to derive regional measures of MSLP.

Additional regional or local datasets relied upon are:

- Fire-weather data, based on Bureau of Meteorology local observations of surface parameters combined into a fire-weather index (Lucas 2010);

- Local subtropical ridge (STR) intensity and position, computed both from Bureau of Meteorology local observations of MSLP and from reanalysis data using the method of Drosdowsky (2005);

- The Southern Annular Mode (SAM) index, derived from observed MSLP in locations across the Southern Hemisphere mid-latitudes (Marshall 2003); and

- Streamflow data, derived from the Hydrologic Reference Station (HRS) network compiled by the Bureau of Meteorology (Turner et al. 2012).

Quantities for which observations are lacking are obtained from reanalysis datasets for the current climate. These datasets are derived using a systematic approach whereby all available observations over a historical period are used in a consistent manner to produce a 'complete' climate record. This unchanging analysis framework provides a dynamically consistent estimate of the climate state at each time step. Reanalysis datasets are typically used for climate monitoring purposes. Two main reanalysis datasets are relied upon in this report:

- The 2.5 by 2.5 degree reanalyses prepared jointly by the National Center for Environmental Prediction (NCEP) and the National Center for Atmospheric Research (NCAR), labelled NNR in the report (Kalnay et al. 1996); and

- The 0.75 by 0.75 degree interim reanalyses prepared by the European Centre for Medium-range Weather Forecast (ECMWF), labelled ERA-I in the report (Dee et al. 2011).

Appendix 2: Understanding projection plots
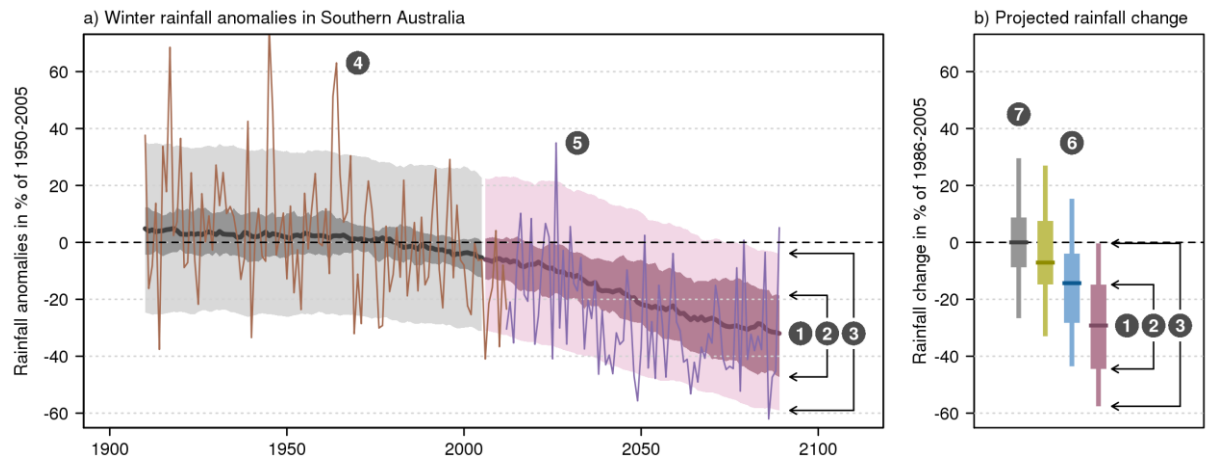
Projections based on climate model results are illustrated using time series (a) and bar plots (b). The model data are expressed as anomalies from a reference climate. For the time series (a), anomalies are calculated as relative to 1950–2005, and for the bar plots (b) anomalies are calculated as the change between 1986–2005 and 2080–2099 (referred to elsewhere as '2090'). The time series plots used a different reference period to the bar plots due to technical reasons in producing visually representative time series plots where simulations of the historical and future time periods are merged into a long series. The graphs can be summarised as follows:

1. The middle (bold) line in both (a) and (b) is the median value of the model simulations (20-year moving average); half the model results fall above and half below this line.

2. The thick bars in (b) and dark shaded areas in (a) show the range (10th to 90th percentile) of model simulations of 20-year average climate.

3. Line segments in (b) and light shaded areas in (a) represent the projected range (10th to 90th percentile) of individual years taking into account year-to-year variability in addition to the long-term response (20-year moving average).

In the time series (a), where available, an observed time series (4) is overlaid to enable comparison between observed variability and simulated model spread. A time series of the future climate from one model is shown to illustrate what a possible future may look like (5). ACCESS1-0 was used for RCP4.5 and 8.5, and BCC-CSM-1 was used for RCP2.6, as ACCESS1-0 output was not available. In both (a) and (b), different RCPs are shown in different colours (6). Throughout this document, green is used for RCP2.6, blue for RCP4.5 and purple for RCP8.5, with grey bars used in bar plots (b) to illustrate the expected range of change due to natural internal climate variability alone (7).

Appendix 3: Evaluation of individual climate models

The entire CMIP5 dataset can be accessed using the global Earth System Grid (ESG) facility (https://www.earthsystemgrid.org/about/overview.htm). Up to 50 global climate models are included in the CMIP5 database. The results presented in this report, unless otherwise indicated, are based on the 36 climate models for which data were suitable and available when the work to deliver the national climate change projections was started. The table below lists the names of these models, the institution and country which developed the model, the model's spatial resolution, whether model results are available for RCP4.5 and RCP8.5 emission pathways and if the model output has additionally been statistically downscaled (SDM). The table also provides useful model performance information which will assist in the selection of appropriate climate models for impact studies, in particular when accessing climate data or using the climate future web tool (www.climatechangeinaustralia.gov.au, see Fig. 17 and text in Section 3.5).

Model	Insitution Name and conutry	Lat. (km)	Lon. (km)	RCP4.5	RCP8.5	SDM	Poor Performance	M-Stat South-Aus	STR evaluation	Tropical evaluation	Stream flow evaluation	RCP8.5 mean warming
ACCESS1-0	CSIRO-BOM, Australia	210	130	X	X	X	1	575	2	1	1	4.63
ACCESS1-.3	CSIRO-BOM, Australia	210	130	X	X	X	2	492	2	1	2	4.58
bcc-csm1-1	BCC, CMA, China	310	310	X	X		0	464	1	1		3.86
bcc-csm1-1-m	BCC, CMA, China	120	120	X	X	X	0	573	2	3	3	3.44
BNU-ESM	BNU, China	310	310	X	X	X	3	388	3	3	3	4.85
CanESM2	CCCMA, Canada	310	310	X	X	X	1	542	2	1	2	4.90
CCSM4	NCAR, USA	130	100	X	X	X	1	519	2		2	3.97
CESM1-BGC	NSF-DOE-NCAR, USA	130	100	X	X		1	518	2	1		3.92
CESM1-CAM5	NSF-DOE-NCAR, USA	130	100	X	X		0	589	2	3		4.70
CMCC-CESM	CMCC, Italy	410	410		X		1	355	3	2		4.25
CMCC-CM	CMCC, Italy	78	78	X	X		0	583	1	2		4.85
CMCC-CMS	CMCC, Italy	210	210	X	X	X	1	471	1	2	2	4.99
CNRM-CM5	CNRM-CERFACS, France	155	155	X	X	X	0	587	1	1	1	3.98
CSIRO-mk3.6	CSIRO-QCCCE, Australia	210	210	X	X	X	2	431	3	3	1	4.67
GFDL-CM3	NOAA, GFDL, USA	275	220	X	X		1	467	2	1		5.17
GFDL-ESM2G	NOAA, GFDL, USA	275	220	X	X	X	3	383	2		3	3.13
GFDL-ESM2M	NOAA, GFDL, USA	275	220	X	X	X	0	458	2	3	1	3.01
GISS-E2-H	NASA/GISS, NY, USA	275	220	X	X		4	473	2	3		3.21
GISS-E2-H-CC	NASA/GISS, NY, USA	110	110	X	X		3	516	2			3.12
GISS-E2-R	NASA/GISS, NY, USA	275	220	X	X		3	543	3	3		2.72
GISS-E2-R-CC	NASA/GISS, NY, USA	110	110	X	X				2			2.76
HadGEM2-CC	MOHC, UK	210	130	X	X	X	0	533	1	2	3	5.30
HadGEM2-ES	MOHC, UK	210	130	X	X		1	556	2	3		5.19
INMCM4	INM, Russia	220	165	X	X		3	455	2	1		3.09
IPSL-CM5A-LR	IPSL, France	410	210	X	X	X	3	395	3	3	1	5.11
IPSL-CM5A-MR	IPSL, France	275	145	X	X	X	3	477	2	2	2	5.05
IPSL-CM5B-LR	IPSL, France	410	210	X	X	X	1	424	3	2	3	3.87
MIROC5	JAMSTEC, Japan	155	155	X	X	X	0	488	2	3	3	3.69
MIROC-ESM	JAMSTEC, Japan	310	310	X	X	X	0	434	3		1	5.35
MIROC-ESM-CHEM	JAMSTEC, Japan	310	310	X	X	X	4	450	3		2	5.60
MPI-ESM-LR	MPI-N, Germany	210	210	X	X	X	1	542	2	3	2	4.01
MPI-ESM-MR	MPI-N, Germany	210	210	X	X	X	1	513	1	3	2	4.02
MRI-CGCM3	MRI, Japan	120	120	X	X	X	1	511	1	1	1	3.84
MRI-ESM1	MRI, Japan	120	120		X				1			
NorESM1-M	NCC, Norway	275	210	X	X	X	1	480	2	2	2	3.62
NorESM1-ME	NCC, Norway	275	210	X	X		1	475	2	2		3.78
Number of models considered in the report				**34**	**36**	**22**	**34**	**34**	**36**	**29**	**22**	**35**

The metrics applied to evaluate the models listed in the table are:

- 'Poor performance' was evaluated in the Technical Report for the National Climate Change Projections (table 5.6.1, p. 76 in CSIRO and BoM, 2015), as the number of times a model scored low (6 to 8 lowest score) on various skill metrics used in that report; here 0 score is indicated in blue and 3+ in red.

- The 'M-statistic' (Watterson 1996) was computed for temperature, rainfall and MSLP for each climate model across the southern part of the Australian continent (reported in table 5.2.2, p. 60 in CSIRO and BoM, 2015). Higher numbers indicate more skilful models; here a score below 460 is indicated in red and above 530 in blue (the mean is 490).

- The 'STR evaluation' reflects the ability of each model to reproduce the observed subtropical ridge (Grose et al. 2015b). Climate models that simulate the subtropical ridge in the correct longitude band are scored as 1 (blue), climate models that simulate the longitudinal band of STR as too wide or shifted are scored as 3 (red), all other models for which a slightly larger longitude band had to be used compare to the observations are scored as 2 (black).

- The 'tropical evaluation' evaluates the ability of the climate models to capture tropical variability in relation to rainfall across southeastern Australia. This assessment was conducted using three metrics: the variability and trends of tropical SSTs and their relationship, on interannual timescales, with rainfall in the region. The models which were always ranked as average or better are given a 1 (blue), the models which were always ranked as average or below are given a 3 (red), all other models are scored as 2 (black), indicating mixed results.

- The 'streamflow evaluation' reflects the ability of statistically downscaled models to reproduce the observed streamflow, via a simple linear relationship. This was assessed (Fiddes and Timbal 2016b) on the mean and variance of the reconstructed streamflow; the seven models with the best score are indicated by a 1 (blue) and the models with the 6 poorest performances are scored as a 3 (red), all other models are scored as 2 (black).

Not all climate models used in this report were evaluated for all statistics; in this case no score is reported. For each column the total numbers of models considered is indicated.

The final column in the table is the global sensitivity of the model measured by the mean global warming obtained in response to the RCP8.5 pathway by the end of the 21st century (2081–2100).

As some models stand out as performing worse on several metrics, and others, in contrast, are consistently performing better, the information provided in this Appendix needs to be considered when accessing climate change projections from the Climate Change in Australia website alongside the information provided with the Climate Future tool (www.climatechangeinaustralia.gov.au).

ABBREVIATIONS

ACORN-SAT	Australian Climate Observations Reference Network – Surface Air Temperature
AWAP	Australian Water Availability Project
BOM	Australian Bureau of Meteorology
CCIA	Climate Change in Australia
CMIP3	Coupled Model Intercomparison Project (Phase 3)
CMIP5	Coupled Model Intercomparison Project (Phase 5)
CSIRO	Commonwealth Scientific and Industrial Research Organisation
EAC	East Australian Current
ENSO	El Niño–Southern Oscillation
FFDI	Forest Fire Danger Index
GCMs	General Circulation Models or Global Climate Models
HC	Hadley Cell/Circulation
IOD	Indian Ocean Dipole
IPO	Inter-decadal Pacific Oscillation
IPCC	Intergovernmental Panel on Climate Change
MB	Murray Basin
MMC	Mean Meridional Circulation
MSLP	Mean Sea Level Pressure
NRM	Natural Resource Management
RCP	Representative Concentration Pathway
SAM	Southern Annular Mode
SEACI	South East Australian Climate Initiative
SPI	Standardised Precipitation Index
SRES	Special Report on Emissions Scenarios
SS	Southern Slopes
SST	Sea Surface Temperature
STR	Subtropical Ridge

GLOSSARY OF TERMS

Adaptation	The process of adjustment to actual or expected climate and its effects Adaptation can be autonomous or planned. *Incremental adaptation* Adaptation actions where the central aim is to maintain the essence and integrity of a system or process at a given scale. *Transformational adaptation* Adaptation that changes the fundamental attributes of a system in response to climate and its effects.
Atmosphere	The gaseous envelope surrounding the Earth. The dry atmosphere consists almost entirely of nitrogen and oxygen, together with a number of trace gases (e.g. argon, helium) and greenhouse gases (e.g. carbon dioxide, methane, nitrous oxide). The atmosphere also contains aerosols and clouds.
Carbon dioxide	A naturally occurring gas, also a by-product of burning fossil fuels from fossil carbon deposits, such as oil, gas and coal, of burning biomass, of land use changes and of industrial processes (e.g. cement production). It is the principal anthropogenic greenhouse gas that affects the Earth's radiative balance.
Climate	The average weather experienced at a site or region over a period of many years, ranging from months to many thousands of years. The relevant measured quantities are most often surface variables such as temperature, rainfall and wind.
Climate change	A change in the state of the climate that can be identified (e.g. by statistical tests) by changes in the mean and/or variability of its properties, and that persists for an extended period of time, typically decades or longer.
Climate projection	A climate projection is the simulated response of the climate system to a scenario of future emission or concentration of greenhouse gases and aerosols generally derived using climate models. Climate projections are distinguished from climate predictions by their dependence on the emission/concentration/radiative forcing scenario used, which in turn is based on assumptions concerning, for example, future socioeconomic and technological developments that may or may not be realised.
Climate scenario	A plausible and often simplified representation of the future climate, based on an internally consistent set of climatological relationships that has been constructed for explicit use in investigating the potential consequences of anthropogenic climate change, often serving as input to impact models.
Climate sensitivity	The effective climate sensitivity (in °C) is an estimate of the global mean surface temperature response to doubled carbon dioxide concentration that is evaluated from model output or observations for evolving non-equilibrium conditions.
Climate variability	Climate variability refers to variations in the mean state and other statistics (such as standard deviations, the occurrence of extremes, etc.) of the climate on all spatial and temporal scales beyond that of individual weather events. Variability may be due to natural internal processes within the climate system (internal variability), or to variations in natural or anthropogenic external forcing (external variability).
CMIP3 and CMIP5	Phases three and five of the Coupled Model Intercomparison Project (CMIP3 and CMIP5), which coordinated and archived climate model simulations based on shared model inputs by modelling groups from around the world. The CMIP3 multi-model dataset includes projections using SRES emission scenarios. The CMIP5 dataset includes projections using the Representative Concentration Pathways.

Confidence	The validity of a finding based on the type, amount, quality, and consistency of evidence (*e.g.* mechanistic understanding, theory, data, models, expert judgment) and on the degree of agreement.
Downscaling	Downscaling is a method that derives local- to regional-scale (10 to 100 km) information from larger-scale models or data analyses. Two main methods exist: dynamical downscaling and empirical/statistical downscaling.
El Niño Southern Oscillation (ENSO)	A fluctuation in global scale tropical and subtropical surface pressure, wind, sea surface temperature, and rainfall, and an exchange of air between the southeast Pacific subtropical high and the Indonesian equatorial low. Often measured by the surface pressure anomaly difference between Tahiti and Darwin or the sea surface temperatures in the central and eastern equatorial Pacific. There are three phases: neutral, El Niño and La Niña. During an El Niño event the prevailing trade winds weaken, reducing upwelling and altering ocean currents such that the eastern tropical surface temperatures warm, further weakening the trade winds. The opposite occurs during a La Niña event.
Emissions scenario	A plausible representation of the future development of emissions of substances that are radiatively active (e.g. greenhouse gases, aerosols) based on a coherent and internally consistent set of assumptions about driving forces (such as demographic and socioeconomic development, technological change) and their key relationships.
Extreme weather	An extreme weather event is an event that is rare at a particular place and time of year. Definitions of rare vary, but an extreme weather event would normally be as rare as or rarer than the 10th or 90th percentile of a probability density function estimated from observations.
Fire weather	Weather conditions conducive to triggering and sustaining wild fires, usually based on a set of indicators and combinations of indicators including temperature, soil moisture, humidity, and wind. Fire weather does not include the presence or absence of fuel load.
Global Climate Model or General Circulation Model (GCM)	A numerical representation of the climate system that is based on the physical, chemical and biological properties of its components, their interactions and feedback processes. The climate system can be represented by models of varying complexity and differ in such aspects as the spatial resolution (size of grid-cells), the extent to which physical, chemical, or biological processes are explicitly represented, or the level at which empirical *parameterisations* are involved.
Greenhouse gas	Greenhouse gases are those gaseous constituents of the atmosphere, both natural and anthropogenic, that absorb and emit radiation at specific wavelengths within the spectrum of terrestrial radiation emitted by the Earth's surface, the atmosphere itself, and by clouds. Water vapour (H_2O), carbon dioxide (CO_2), nitrous oxide (N_2O), methane (CH_4) and ozone (O_3) are the primary greenhouse gases in the Earth's atmosphere.
Hadley Cell/Circulation (HC)	A direct, thermally driven circulation in the atmosphere consisting of poleward flow in the upper troposphere, descending air into the subtropical high-pressure cells, return flow as part of the trade winds near the surface, and with rising air near the equator in the so-called Intertropical Convergence zone.
Indian Ocean Dipole (IOD)	Large–scale mode of interannual variability of sea surface temperature in the Indian Ocean. This pattern manifests through a zonal gradient of tropical sea surface temperature, which in one extreme phase in September to November shows cooling off Sumatra and warming off Somalia in the west, combined with anomalous easterlies along the equator.
Murray Basin cluster	The Murray Basin cluster encompasses the Murray Basin region of Victoria and part of NSW and S.A (see Fig. 1 and Timbal et al. 2015a).
Murray Basin region	The Murray Basin region of Victoria comprises the CMAs of Victoria encompassed by the larger Murray Basin cluster, north of the Great Dividing

	Range (GDR). The CMAs include the Mallee, Wimmera, North Central, Goulburn Broken and North East region; (see Fig. 1).
Percentile	A percentile is a value on a scale of one hundred that indicates the percentage of the dataset values that is equal to or below it. The percentile is often used to estimate the extremes of a distribution. For example, the 90th (or 10th) percentile may be used to refer to the threshold for the upper (or lower) extremes.
Radiative forcing	Radiative forcing is the change in the net, downward minus upward, radiative flux (expressed in $W\ m^{-2}$) at the tropopause or top of atmosphere due to a change in an external driver of climate change, such as, for example, a change in the concentration of carbon dioxide or the output of the Sun.
Reanalysis	Reanalysis is the method of data assimilation which aims to assimilate all available historical observational data spanning an extended period, using a single consistent assimilation (or 'analysis') scheme throughout, providing a complete climatology for that historical period.
Representative Concentration Pathways (RCPs)	Scenarios that include time series of emissions and concentrations of the full suite of greenhouse gases and aerosols and chemically active gases, as well as land use/ cover. The word representative signifies that each RCP provides only one of many possible scenarios that would lead to the specific radiative forcing characteristics.
Return period	An estimate of the average time interval between occurrences of an event (e.g. flood or extreme rainfall) of a defined size or intensity.
Risk	The potential for consequences where something of value is at stake and where the outcome is uncertain. Risk is often represented as a probability of occurrence of hazardous events or trends multiplied by the consequences if these events occur.
Risk assessment	The qualitative and/or quantitative scientific estimation of risks.
Risk management	The plans, actions, or policies implemented to reduce the likelihood and/or consequences of risks or to respond to consequences.
South-East region	South-East region of Victoria is the southeast of the GDR, which includes the West and East Gippsland CMA regions (see Fig. 1).
Southern Annular Mode (SAM)	The leading mode of variability of Southern Hemisphere geopotential height, which is associated with shifts in the latitude of the mid-latitude jet.
Southern Slope cluster	The Southern Slopes cluster encompasses both the South-West and South-East regions of Victoria and part of New South Wales and South Australia as well as Tasmania (see Fig. 1 and Grose et al. 2015a).
South-West region	South-West region of Victoria is the southwest of the GDR which includes the Glenelg-Hopkins, Corangamite and Port Philip and Westernport CMA regions (see Fig. 1).
SRES scenarios	SRES scenarios are emissions scenarios developed by Nakićenović and Swart (2000) and used, among others, as a basis for some of the climate projections shown in chapters 9 to 11 of IPCC (2001) and chapters 10 and 11 of IPCC (2007).
Uncertainty	A state of incomplete knowledge that can result from a lack of information or from disagreement about what is known or even knowable. It may have many types of sources, from imprecision in the data to ambiguously defined concepts or terminology, or uncertain projections of human behaviour. Uncertainty can therefore be represented by quantitative measures (e.g. a probability density function) or by qualitative statements (e.g. reflecting the judgment of a team of experts).
Walker circulation	An east-west circulation of the atmosphere above the tropical Pacific, with air rising above warmer ocean regions (normally in the west, called the warm pool), and descending over the cooler ocean areas (normally in the east). Its strength fluctuates with that of the Southern Oscillation.